AD-A092 318 AIR FORCE INST OF TECH WRIGHT-PATTERSON AFB OH F/G 17/9
DIGITAL DOPPLER RADIAL VELOCITY DATA COMPARED OBJECTIVELY WITH --ETC(U
MAY 80 T F BEAVER
UNCLASSIFIED AFIT-CI-80-11T NL

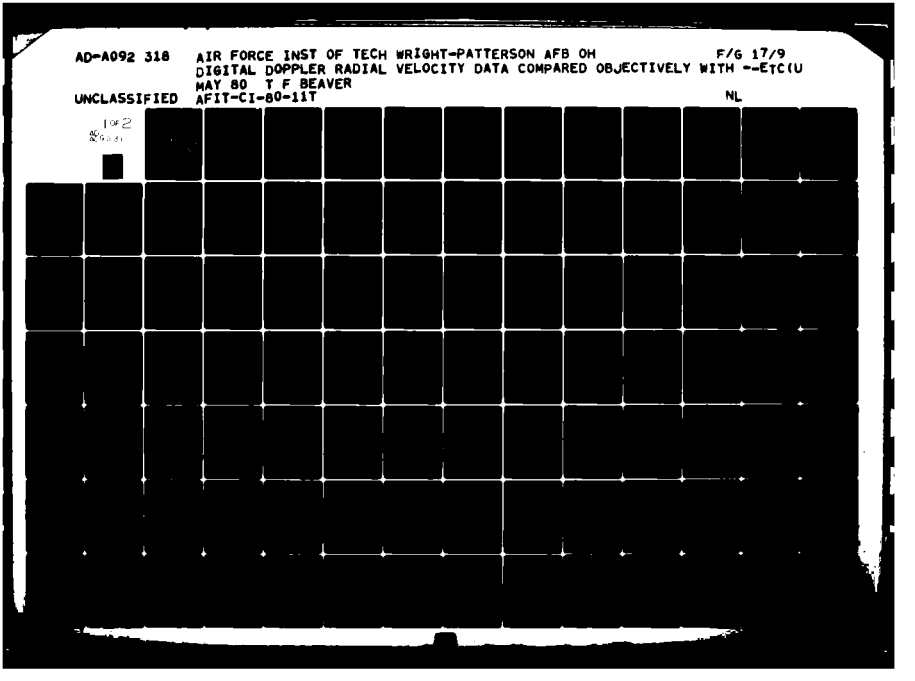

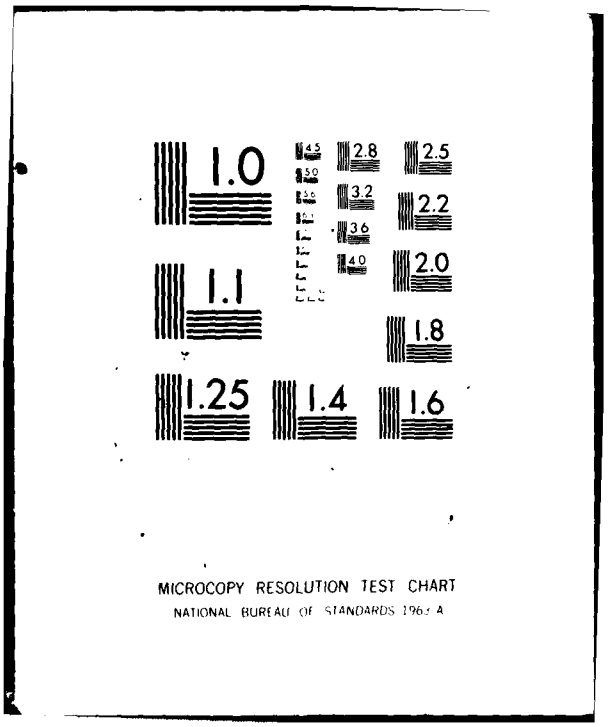
1.0
1.1
1.25
1.4
1.6
1.8
2.0
2.2
2.5
2.8
3.2
3.6
4.0
4.5
5.0
5.6
MICROCOPY RESOLUTION TEST CHART
NATIONAL BUREAU OF STANDARDS 1963 A

UNCLASS

SECURITY CLASSIFICATION OF THIS PAGE (When Data Entered)

REPORT DOCUMENTATION PAGE

READ INSTRUCTIONS BEFORE COMPLETING FORM

1. REPORT NUMBER: 80-11T	2. GOVT ACCESSION NO.: AD-A092318
3. RECIPIENT'S CATALOG NUMBER:	
4. TITLE (and Subtitle): Digital Doppler Radial Velocity Data Compared Objectively with Digital Reflectivity Radar Data.	5. TYPE OF REPORT & PERIOD COVERED: THESIS/DISSERTATION
	6. PERFORMING ORG. REPORT NUMBER:
7. AUTHOR(s): Thomas Foster Beaver, Capt USAF	8. CONTRACT OR GRANT NUMBER(s):
9. PERFORMING ORGANIZATION NAME AND ADDRESS: AFIT STUDENT AT: Texas A&M University	10. PROGRAM ELEMENT, PROJECT, TASK AREA & WORK UNIT NUMBERS:
11. CONTROLLING OFFICE NAME AND ADDRESS: AFIT/NR, WPAFB OH 45433	12. REPORT DATE: May 1980
	13. NUMBER OF PAGES: 110
14. MONITORING AGENCY NAME & ADDRESS (if different from Controlling Office)	15. SECURITY CLASS. (of this report): UNCLASS
	15a. DECLASSIFICATION DOWNGRADING SCHEDULE:

LEVEL II

16. DISTRIBUTION STATEMENT (of this Report)

APPROVED FOR PUBLIC RELEASE; DISTRIBUTION UNLIMITED

DTIC ELECTE DEC 2 1980 S D C

17. DISTRIBUTION STATEMENT (of the abstract entered in Block 20, if different from Report)

18. SUPPLEMENTARY NOTES

APPROVED FOR PUBLIC RELEASE: IAW AFR 190-17

FREDRIC C. LYNCH, Major, USAF
Director of Public Affairs

Air Force Institute of Technology (ATC)
Wright-Patterson AFB, OH 45433

19. KEY WORDS (Continue on reverse side if necessary and identify by block number)

20. ABSTRACT (Continue on reverse side if necessary and identify by block number)

ATTACHED

DD FORM 1 JAN 73 1473 EDITION OF 1 NOV 65 IS OBSOLETE

UNCLASS

SECURITY CLASSIFICATION OF THIS PAGE (When Data Entered)

ABSTRACT

Digital Doppler Radial Velocity Data

Compared Objectively with

Digital Reflectivity Radar Data

Thomas Foster Beaver

Captain, United States Air Force

1980

110 Pages

M. S. Degree Texas A&M University

An investigation was conducted to determine the feasibility of objectively analyzing digital Doppler radial velocity data at constant altitudes. Data were supplied by the National Severe Storms Laboratory (NSSL) at Norman, Oklahoma. The study area was a 96 km by 116 km box surrounding the Chickasha, Oklahoma, synoptic network. A computer program, initially developed by Greene (1971), modified by Pittman (1976), Sieland (1977), and others was used as the basis for this computer program development. This research demonstrated that mesocyclones could be located using constant altitude radial velocity maps (CAVM) on a 2-km horizontal and a 1-km vertical grid scale without correcting for storm motion. However a 1-km horizontal and vertical grid scale was found to be 'optimum' for location and study of mesocyclones. Constant altitude velocity maps (CAVM) were then compared with constant altitude reflectivity maps (CAZM). This comparison, using two different storms, demonstrated that CAVM analysis was superior to CAZM analysis for detection of severe storm areas.

DIGITAL DOPPLER RADIAL VELOCITY DATA COMPARED OBJECTIVELY WITH DIGITAL REFLECTIVITY RADAR DATA

A Thesis

by

THOMAS FOSTER BEAVER

Submitted to the Graduate College of
Texas A&M University
in partial fulfillment of the requirement for the degree of

MASTER OF SCIENCE

May 1980

Major Subject: Meteorology

DIGITAL DOPPLER RADIAL VELOCITY DATA COMPARED OBJECTIVELY WITH DIGITAL REFLECTIVITY RADAR DATA

A Thesis

by

THOMAS FOSTER BEAVER

Approved as to style and content by:

Dr. George L. Huebner, Jr.
(Chairman of Committee)

Dr. Vance E. Moyer
(Member)

Dr. Glen N. Williams
(Member)

Dr. Kenneth C. Brundidge
(Head of Department)

May 1980

80-11

AFIT RESEARCH ASSESSMENT

The purpose of this questionnaire is to ascertain the value and/or contribution of research accomplished by students or faculty of the Air Force Institute of Technology (ATC). It would be greatly appreciated if you would complete the following questionnaire and return it to:

AFIT/NR
Wright-Patterson AFB OH 45433

Research Title: Digital Doppler Radial Velocity Data Compared Objectively with Digital Reflectivity Radar Data

Author: Capt Thomas Foster Beaver

Research Assessment Questions:

1. Did this research contribute to a current Air Force project?

a. Yes b. No

2. Do you believe this research topic is significant enough that it would have been researched (or contracted) by your organization or another agency if AFIT had not?

a. Yes b. No

3. The benefits of AFIT research can often be expressed by the equivalent value that your agency achieved/received by virtue of AFIT performing the research. Can you estimate what this research would have cost if it had been accomplished under contract or if it had been done in-house in terms of manpower and/or dollars?

a. Man-years _____. b. $_____

4. Often it is not possible to attach equivalent dollar values to research, although the results of the research may, in fact, be important. Whether or not you were able to establish an equivalent value for this research (3 above), what is your estimate of its significance?

a. Highly Significant b. Significant c. Slightly Significant d. Of No Significance

5. AFIT welcomes any further comments you may have on the above questions, or any additional details concerning the current application, future potential, or other value of this research. Please use the back of this questionnaire for your statement(s).

NAME GRADE POSITION

ORGANIZATION LOCATION

USAF SCN 75-20B

ABSTRACT

Digital Doppler Radial Velocity Data Compared Objectively with Digital Reflectivity Radar Data. (May 1980)

Thomas Foster Beaver, B.S., Grove City College, Pennsylvania

Chairman of Advisory Committee: Dr. G. L. Huebner, Jr.

An investigation was conducted to determine the feasibility of objectively analyzing digital Doppler radial velocity data at constant altitudes. Data were supplied by the National Severe Storms Laboratory (NSSL) at Norman, Oklahoma. The study area was a 96 km by 116 km box surrounding the Chickasha, Oklahoma, synoptic network. A computer program, initially developed by Greene (1971), modified by Pittman (1976), Sieland (1977), and others was used as the basis for this computer program development. This research demonstrated that mesocyclones could be located using constant altitude radial velocity maps (CAVM) on a 2-km horizontal and a 1-km vertical grid scale without correcting for storm motion. However a 1-km horizontal and vertical grid scale was found to be 'optimum' for location and study of mesocyclones. Constant altitude velocity maps (CAVM) were then compared with constant altitude reflectivity maps (CAZM). This comparison, using two different storms, demonstrated that CAVM analysis was superior to CAZM analysis for the detection of severe storm areas.

ACKNOWLEDGEMENTS

The author's graduate program was sponsored and financed by the Air Force Institute of Technology, United States Air Force.

I wish to express my appreciation and gratitude to the following individuals who have made this endeavor possible:

To my committee members, Dr. George L. Huebner, my chairman, for his guidance and encouragement during the research phase of this study, and for his advice in the preparation of this manuscript. To Dr. Vance E. Moyer, for serving on my committee and for his invaluable assistance in the preparation of this manuscript, and to Dr. Glen Williams, for reviewing this manuscript.

To Captain Dan McMorrow, for his help, advice, and encouragement during all phases of this research. Dr. E. Kessler and his staff at NSSL, particularly D. Burgess, W. Bumgarner, and R. Brown, for supplying the data, taking time to answer questions, and encouraging my research. Also to Captain Dave Howell and Mr. Keith Knight, for 'unpacking' the data, and for their support, and to Mr. Sid Theis, for his computer programming expertise and assistance with many computer problems.

To my wife, Roxee, and my children for their sacrifices, love, and support. My parents, Mr. and Mrs. Bernard F. Beaver for their love and support, and to Captain Gary Sickler, for his philosophy.

Finally, to Mrs. Elaine Erwin, Joyce Landin, and my wife for their fine typing assistance.

Funds for this research were provided by NOAA grant #NA 79RAD00019.

DEDICATION

To my wonderful family, Roxee, my wife, for her encouragement, faith, patience, and devotion; children, Tara and Broc, for understanding, and Amy, for her smile.

TABLE OF CONTENTS

	Page
ABSTRACT	iii
ACKNOWLEDGEMENTS	iv
DEDICATION	vi
LIST OF FIGURES	viii
1. INTRODUCTION	1
2. BACKGROUND	3
3. OBJECTIVES	8
4. THE RADARS USED	9
5. DATA	15
6. RESULTS	23
a. May 1, 1977 Mesocyclone	24
b. May 20, 1977 Mesocyclone	57
7. CONCLUSIONS	78
8. RECOMMENDATIONS	81
REFERENCES	83
APPENDIX A	87
APPENDIX B	89
VITA	110

LIST OF FIGURES

Figure		Page
1	(Top) Horizontal Single Doppler radar mesocyclone signature of a stationary nondivergent Rankine combined vortex. (Bottom) Velocity profile along the X-Y axis	5
2	Timing sequence for normal (a) and expanded (b) data collection modes	13
3	Area outlined is the 96 km by 116 km box over which the data were analyzed	16
4	1-km CAZM, 1740-1743 CDT, 1 May 1977 (2-km grid), WSR-57 data	26
5	4-km CAZM, 1740-1743 CDT, 1 May 1977 (2-km grid), WSR-57 data	27
6	8-km CAZM, 1740-1743 CDT, 1 May 1977 (2-km grid), WSR-57 data	28
7	10-km CAZM, 1740-1743 CDT, 1 May 1977 (2-km grid), WSR-57 data	29
8	1-km CAVM, 1742-1748 CDT, 1 May 1977 (2-km grid), Doppler data	31
9	3-km CAVM, 1742-1748 CDT, 1 May 1977 (2-km grid), Doppler data	32
10	4-km CAVM, 1742-1748 CDT, 1 May 1977 (2-km grid), Doppler data	33
11	[illegible]m CAZM, 1750-1753 CDT, 1 May 1977 (2-km grid), [illegible]-57 data	35
12	8-km CAZM, 1750-1753 CDT, 1 May 1977 (2-km grid), WSR-57 data	36
13	3-km CAZM, 1800-1804 CDT, 1 May 1977 (2-km grid), WSR-57 data	37
14	3-km CAVM, 1805-1812 CDT, 1 May 1977 (2-km grid), Doppler data	38

Figure		Page
15	4-km CAVM, 1805-1812 CDT, 1 May 1977 (2-km grid), Doppler data	40
16	5-km CAVM, 1805-1812 CDT, 1 May 1977 (2-km grid), Doppler data	41
17	3-km CAVM, 1724-1730 CDT, 1 May 1977 (1-km grid), Doppler data	43
18	4-km CAVM, 1724-1730 CDT, 1 May 1977 (1-km grid), Doppler data	44
19	3-km CAVM, 1742-1746 CDT, 1 May 1977 (1-km grid), Doppler data	45
20	4-km CAVM, 1742-1746 CDT, 1 May 1977 (1-km grid), Doppler data	46
21	3-km CAVM, 1805-1812 CDT, 1 May 1977 (1-km grid), Doppler data	47
22	4-km CAVM, 1805-1812 CDT, 1 May 1977 (1-km grid), Doppler data	48
23	5-km CAVM, 1805-1812 CDT, 1 May 1977 (1-km grid), Doppler data	49
24	1-km CAZM, 1742-1746 CDT, 1 May 1977 (1-km grid), Doppler data	51
25	3-km CAZM, 1742-1746 CDT, 1 May 1977 (1-km grid), Doppler data	52
26	4-km CAZM, 1742-1746 CDT, 1 May 1977 (1-km grid), Doppler data	53
27	1-km CAZM, 1805-1812 CDT, 1 May 1977 (1-km grid), Doppler data	54
28	3-km CAZM, 1805-1812 CDT, 1 May 1977 (1-km grid), Doppler data	55
29	5-km CAZM, 1805-1812 CDT, 1 May 1977 (1-km grid), Doppler data	56

Figure		Page
30	7-km CAVM, 1627-1631 CDT, 20 May 1977 (1-km grid), Doppler data	58
31	10-km CAZM, 1627-1631 CDT, 20 May 1977 (1-km grid), Doppler data	60
32	1-km CAVM, 1634-1640 CDT, 20 May 1977 (1-km grid), Doppler data	61
33	5-km CAVM, 1634-1640 CDT, 20 May 1977 (1-km grid), Doppler data	62
34	7-km CAVM, 1634-1640 CDT, 20 May 1977 (1-km grid), Doppler data	63
35	2-km CAZM, 1634-1640 CDT, 20 May 1977 (1-km grid), Doppler data	64
36	5-km CAZM, 1634-1640 CDT, 20 May 1977 (1-km grid), Doppler data	65
37	7-km CAZM, 1634-1640 CDT, 20 May 1977 (1-km grid), Doppler data	66
38	11-km CAZM, 1634-1640 CDT, 20 May 1977 (1-km grid), Doppler data	67
39	1-km CAVM, 1640-1643 CDT, 20 May 1977 (1-km grid), Doppler data	69
40	2-km CAVM, 1640-1643 CDT, 20 May 1977 (1-km grid), Doppler data	70
41	3-km CAVM, 1640-1643 CDT, 20 May 1977 (1-km grid), Doppler data	71
42	4-km CAVM, 1640-1643 CDT, 20 May 1977 (1-km grid), Doppler data	72
43	5-km CAVM, 1640-1643 CDT, 20 May 1977 (1-km grid), Doppler data	73
44	2-km CAZM, 1640-1643 CDT, 20 May 1977 (1-km grid), Doppler data	74

Figure		Page
45	2-km CAVM, 1640-1643 CDT, 20 May 1977 (2-km grid), Doppler data	75
46	2-km CAZM, 1640-1643 CDT, 20 May 1977 (2-km grid), Doppler data	77

1. INTRODUCTION

Since the very first radar-detected storm was observed on February 20, 1941, by a 10-cm wavelength radar, weather radar has advanced to become the meteorologists' best tool for severe storm detection. Before the development of digitizing units, called Digital Video Integrator Processors, radar echoes could be analyzed only subjectively with the analysis dependent totally on operator skill, training, experience, and motivation (Muench, 1976). Digitized radar data have increased tremendously the utility of radar data. Data now can be transmitted rapidly via teletype, archived on digital tape or disc for later research, or processed directly by computer to track storms and forecast movement by extrapolation (Muench, 1976). Substantial research has been done with archived digital data to define and identify severe weather cells. Greene (1971) developed a computer program to plot digital radar data at constant altitudes that he labelled Constant Altitude Reflectivity Maps (CAZM). These CAZM's were corrected for radar beam bending by assuming a 4/3 Earth curvature as the beam refraction. He discovered that this type of analysis resulted in a very detailed three-dimensional picture of the storm. Later researchers such as Vogel (1973), Pittman (1976), Sieland (1977), and others continued research on CAZM analysis, each refining and improving the computer

---

The citations on this and following pages follow the style of the Journal of Applied Meteorology.

program. Each researcher also tried to develop other techniques that would use less computer time yet would still be as accurate as the CAZM. Although new techniques were developed, none could compare with the detail of the CAZM for post storm research.

Numerous studies have been accomplished and techniques developed to detect and identify severe cells by conventional reflectivity data; none of them is conclusive. Whiton (1971) prepared an excellent reference combining many severe thunderstorm studies into one report. More recently, Lemon (1977) updated Whiton's report with new information and identification techniques. Some of the numerous diagnostic reflectivity characteristics include: hook echoes (Figure 6 shape), V notch, echo protrusions, fingers or scalloped echo edge, weak echo regions (WER), and bounded weak echo regions (BWER), to mention but a few. True, these are all indicators of probable severe weather; but, by the time they are detected, if they are detected, the severe weather is occurring. It seems that reflectivity signatures alone cannot conclusively locate severe weather, especially not tornadoes. By 1970, researchers began using Doppler radar as a possible severe weather detection tool.

2. BACKGROUND

Doppler radar is defined as that 'class of radar sets which measures the shift in microwave frequency caused by moving targets' (Battan, 1973). Doppler radar, then, adds the detection of movement or rotation within the storm itself that is not possible with conventional, non-coherent radars. It must be realized that the measured Doppler velocity is really the component of velocity along the radar radial. Since the moving targets are water drops, the measured velocity is actually the radial precipitation particle velocity, more commonly referred to as radial velocity. Doppler research studies have indicated that significant improvements are possible in forecasting storm dangers associated with tornadoes, damaging winds, and turbulence (Donaldson et al., 1975b).

Early displays of radial velocities were denoted as plan shear indicators (PSI). Armstrong and Donaldson (1969) labelled their display as PSI because of its capability to detect and locate regions of strong wind shear from the characteristic arc pattern for stationary targets. PSI, indicating radial shear as gaps or bunching in the arcs, is difficult to interpret, while tangential shear, namely a vortex, is indicated by wrinkles in the arcs. (See Armstrong and Donaldson, 1969, for more detail on PSI.) More recent displays are labelled as multimoment displays (MMD) (Burgess et al., 1976). Burgess describes this display as a field of arrows with arrow length proportional to the log of received

power (reflectivity), arrow direction proportional to radial velocity, and arrow head width proportional to the Doppler Spectrum also called spectrum width. This display is unique in that it relates all three Doppler moments at the same time, but it also can be very easily misinterpreted. It must be remembered that displayed velocities are radial components of motion and should not be interpreted as streamlines. Also the spectrum width, velocity difference, indicated by the arrowhead size is only interpreted up to 34 m s^{-1} with differences greater than this ignored; therefore, arrow direction must be used to correctly interpret large velocity differences. (See Burgess et al., 1976 for more detail and displays.) Both of these displays reveal evidence of cyclonic vortices associated with severe weather, especially tornadoes.

Well before Doppler radar observations of severe storms, a cyclonic vortex was known to be associated with tornadoes. As early as 1949, Brooks identified the so-called tornado cyclone, and in 1963 Fujita labelled it a mesocyclone (Lemon et al., 1977). The flow in such a mesocyclone has been described by Lemon et al. as 'most closely resembling that of a Rankine combined vortex... characterized essentially by two flow regimes' (Fig. 1). The vortex core is treated as a solidly rotating body, the diameter of this core being the diameter of a mesocyclone detected by a single Doppler radar. The center line through the core is the azimuth along which the radial velocities are perpendicular to the beam, i.e., zero component of radial velocity. At a radius perpendicular

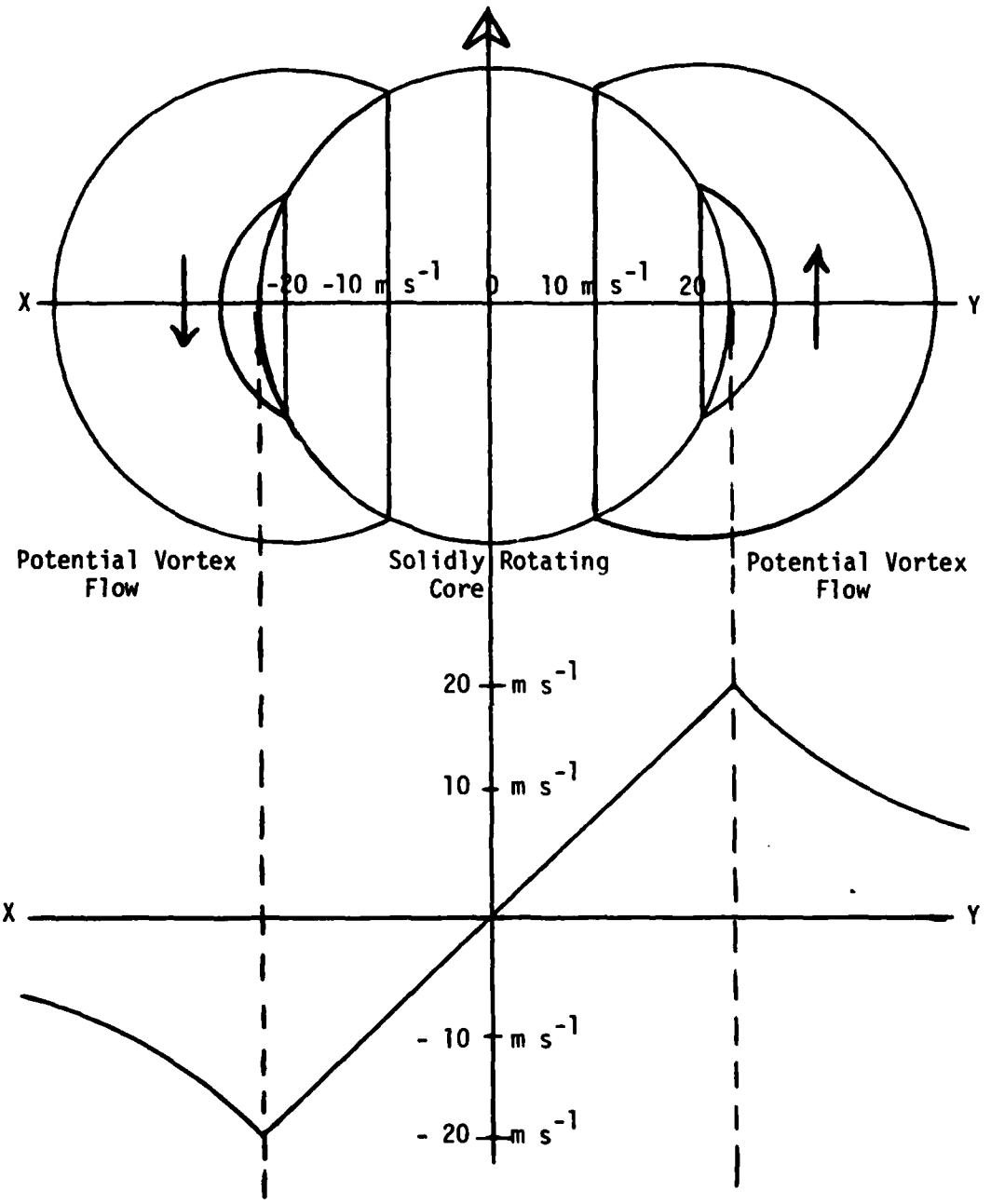

FIG. 1. (Top) Horizontal single Doppler radar mesocyclone signature of a stationary non-divergent Rankine combined vortex. (Bottom) Velocity profile along the X-Y axis. (After Lemon et al., 1977).

to the zero radial velocity azimuth, on the right of the solidly rotating core, there is a closed area of maximum positive radial velocities. The positive sign indicates a radial component away from the radar. On the left side of the core there is an area of maximum negative radial velocities. The negative sign indicates a radial component toward the radar. It is assumed that the radar is east of this approaching vortex, and therefore a mesocyclone (cyclonic vortex) that is east of the radar would have negative and positive components in reverse of those described above. The second flow regime is the area outside this solidly rotating core, and is referred to as the potential vortex flow. Potential vortex flow is generally at least twice the core diameter (Lemon et al., 1972).

Early Doppler researchers realized that the only velocity component measurable by a single Doppler radar was the radial velocity component. Therefore, they suggested that at least three radars, measuring the same volume from three different locations, were necessary for the unambiguous definition of the vector wind field within the volume (Donaldson, 1970). However, initial research with single Doppler radars suggested that a vortex could be identified by the radial velocity field of a single Doppler radar. Using the concept of a Rankine combined vortex, Donaldson (1970) described in detail how a vortex signature could be identified by a single Doppler radar. The objective criteria described by

Donaldson have since been used as guidelines for identifying mesocyclones. He described three primary criteria for a mesocyclone: 1) the vortex must be encompassed by a moderately narrow range of azimuth angles, 2) it must extend through a height comparable to its diameter, and 3) it must be persistent. Very encouraging results have been documented by using these criteria for mesocyclone detection.

Statistics covering 5 yr of early mesocyclone detection at the National Severe Storms Laboratory (NSSL) (1970-1975) showed that approximately 1/10 (37) of all the storms sampled had confirmed mesocyclones (Lemon et al., 1977). Of these 37 confirmed mesocyclones, 23 (62%) were associated with tornadoes and were detected on the average 36 min before the tornado. In addition, 35 (95%) produced enough surface damage to qualify the storm as severe. Also during this period, no tornado was reported that was not preceded by a mesocyclone. Since this time, interest and research in Doppler weather radar have increased immensely. The mesocyclone has been found to be a definite key to the prediction of severe weather phenomena, especially tornadoes. Although occassional small, but still damaging, tornadoes have occurred without prior mesocyclone detection (NOAA, 1979), the diagnosis of the mesocyclone has significantly improved the probability of detection, lowered the false alarm rate, and bettered the critical success index of severe weather forecasts (Donaldson et al., 1975a).

3. OBJECTIVES

The intent of this study was twofold. The first objective was to determine if it was feasible to detect mesocyclones by using constant altitude mapping of radial velocities. This was done by designing a computer program similar to that developed by Greene (1971) and modified by Pittman (1976), Sieland (1977), and others. Previous studies used conventional radar and therefore had only reflectivity values to use as a measuring device for the detection of severe weather echoes. Although this research includes reflectivity values, the principal emphasis is on the use of radial velocities to locate severe weather by identifying mesocyclones. The constant altitude maps (CAZM) designed by Greene (1971) are used in the detection of mesocyclones by radial velocity and therefore are now labelled constant altitude velocity maps (CAVM). By realizing that the average mesocyclone is approximately 5.7 km in diameter and extends vertically approximately 7.5 km (Lemon et al., 1977), the 2-km grid scale and 5000 ft vertical increment used previously have been adjusted to more 'optimum' scales for the detection of mesocyclones. The second objective was to compare reflectivity data and radial velocity data during the same time frame, at constant altitudes, for a better understanding of the severe weather echo.

4. THE RADARS USED

The Norman Digital Doppler radar is one of several Doppler radars operated by NSSL. Some general characteristics of this radar are shown in Table 1. As earlier noted, the primary advantage of Doppler radar is that it adds the extra dimension of particle

Table 1. Norman Doppler Radar Characteristics (from Ray et al., 1977).

General	
Wavelength (cm)	10.52
Beamwidth (deg)	0.81
Pulse Length (m)	150
Number of Range Gates	762
Maximum Unambiguous Velocity (m s^{-1})	$\pm$34.2
Velocity Resolution (m s^{-1})	1
Intensity Resolution (dB)	1.3
Normal Mode	
Pulse Repetition Frequency (s^{-1})	1300
Maximum Unambiguous Range (km)	115
Range Increment (m)	150
Expanded Mode	
Pulse Repetition Frequency (s^{-1})	325
Reflectivity Maximum Unambiguous Range (km)	460
Velocity Maximum Unambiguous Range (km)	115
Reflectivity Range Increment (m)	600
Velocity Range Increment (m)	150

motion to the intensity measurement of conventional radars. However, this added dimension of radial velocity is also a limiting factor when designing a Doppler radar. As explained by Battan (1973), in order to measure the Doppler shift frequency (f), it is necessary to obtain measurements of phase (ϕ) over a frequency of at least 2f. Recall that the pulse-repetition frequency (PRF) is the rate at which pulses are transmitted; then it is realized that the maximum Doppler shift frequency detected is

$$f_{max} = \frac{PRF}{2} . \tag{1}$$

Since the Doppler shift frequency also can be written as

$$f = \frac{2V}{\lambda} \tag{2}$$

for V equal to the radial velocity, the maximum unambiguous Doppler Velocity can be written as

$$V_{max} = (PRF) \frac{\lambda}{4} . \tag{3}$$

Likewise the maximum unambiguous range (r_{max}) is

$$r_{max} = 1/2 \left(\frac{c}{PRF}\right) \tag{4}$$

for c equal to the speed of propagation of electromagnetic radiation ($c = 2.998 \times 10^8$ m s^{-1}).

By substituting (4) into (3), we express the maximum unambiguous radial velocity as a function of maximum range,

$$V_{max} = \frac{\lambda}{8} \frac{c}{r_{max}} . \qquad (5)$$

In this format it is clear that there must be a compromise between V_{max} and r_{max} if they are to be measured unambiguously.

For the detection of mesocyclones it is desirable to be able to measure large radial velocities unambiguously. However, from (5), this would mean a short range of detection, since c and λ are constant. But, it also is desirable to be able to detect mesocyclones at long distances. Therefore, both maximum range and maximum velocity must be compromised to an acceptable mean. In this case, the Norman Doppler has been compromised to maximum unambiguous radial velocities of $\pm$ 34.2 m s^{-1} with a maximum unambiguous range of 115 km in the normal mode. Data also are collected occasionally in the expanded mode.

The expanded mode of collection has reflectivity gates every 600 m instead of every 150 m thereby yielding a maximum reflectivity range of 460 km. Nevertheless, the radial velocity gate spacing remains at 150-m intervals and the maximum radial velocity range at 115 km. For radial velocities, each 115-km increment out to 460 km is called a trip. The recorded radial velocity at any given gate is assumed to come from the trip that had the maximum reflectivity. For example if the maximum reflectivity is measured at 250 km, when in expanded mode, then the radial velocity for the corresponding gate is assumed to be the radial velocity component of the water drops at 250 km. The radial velocity would then come

from the third trip (Bumgarner, 1979). In this way mesocyclones, and/or radial velocities, are measurable out to 460 km; however, we cannot be certain which trip these velocities are from and therefore they are not as dependable as unambiguous velocities within 115 km when collected in the normal mode. Figure 2, taken from Ray et al., 1977, shows a diagram of normal and expanded velocity modes.

A third mode of collection, called high PRF is also available; however, no data from the high PRF mode were used in this research. The normal and expanded modes of collection are taken into account when the data are converted from 7-track to 9-track magnetic tapes, discussed in Appendix A.

Another point to note about the Norman Doppler radar is its beamwidth (0.81°). In general a beamwidth is defined as twice the angle between the direction of the maximum power and the direction at which the power is half the maximum power, i.e., the so called half-power point (Battan, 1973). The solid angle, beamwidth, between the half-power points contains approximately 80% of the total power. It is obvious that the smaller the beamwidth the finer the resolution. This is especially critical in the detection of mesocyclones, which, as noted, have an average diameter of approximately 5.7 km and are detected by a single Doppler radar as azimuthally separated velocity peaks of opposite sign (Lemon et al., 1977). Beamwidths of conventional radars are not nearly as critical as those for Doppler radars. For example, the Norman WSR-57 radar,

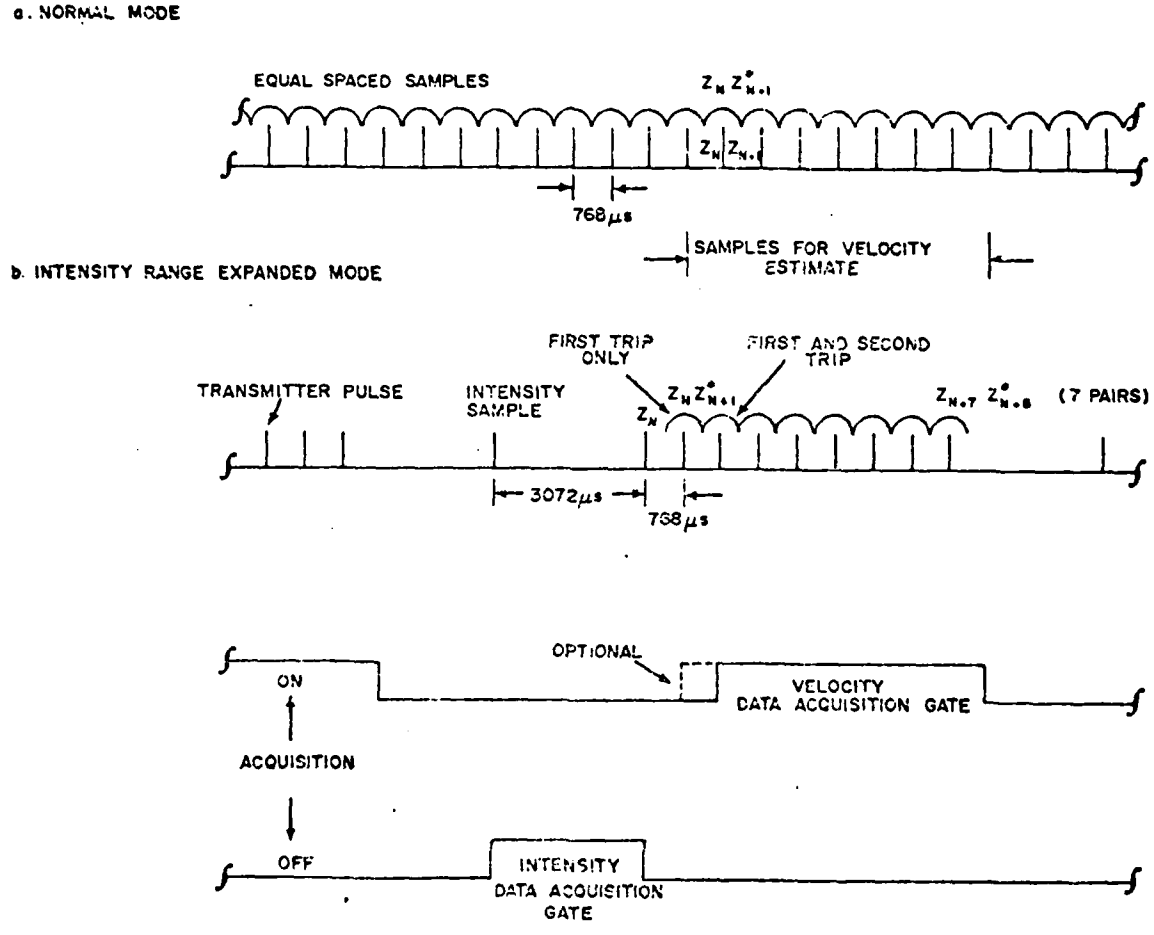

FIG. 2. Timing sequence for normal (a) and expanded (b) data collection modes. (After Ray et al., 1977)

used initially in this research to compare CAZM's to Doppler CAZM's and CAVM's, has a beamwidth of 2°. The Norman Doppler then, has a resolution 2 1/2 times better than the WSR-57. Other general characteristics of the WSR-57 radar include a 10.4-cm wavelength, a PRF of only 164 s^{-1}, and a maximum range of 200 km. Further characteristics and details of the WSR-57 processing technique are described by Pittman (1976) and Sieland (1977).

5. DATA

Data for this research were collected over the Chickasha, Oklahoma, synoptic network (Fig. 3) and were supplied by NSSL at Norman, Oklahoma, on magnetic tapes. These tapes were prepared from the Norman digital Doppler radar and the Norman WSR-57 digital radar during the 1977 severe storm season, and in connection with the Joint Doppler Operational Project (JDOP). The tapes received were 7-track and contained 'raw' data without correction. The WSR-57 tape was processed by using a program developed by Pittman and Sieland. But, the Doppler tapes had to be 'unpacked' and loaded onto 9-track magnetic tapes in Fortran (see Appendix A).

Once corrected to Fortran on 9-track tapes, this author developed a program to convert the arrays of reflectivity and radial velocity in spherical coordinates to arrays in cylindrical coordinates. Finally the arrays were converted to rectangular arrays, objectively contoured by Conrec, and plotted by the Versatec plotter. The conversion to cylindrical and rectangular coordinates was primarily the same as that described by Sieland (1977) and employed a linear quadratic interpolation scheme. However, instead of using 5000-ft increments as Sieland did, this author converted to 1-km height increments for even finer vertical detail, and also to keep all units consistent. Also, it was felt that Sieland's so-called surface map was misleading since it only used data along one tilt angle with no correction for beam bending. Therefore this

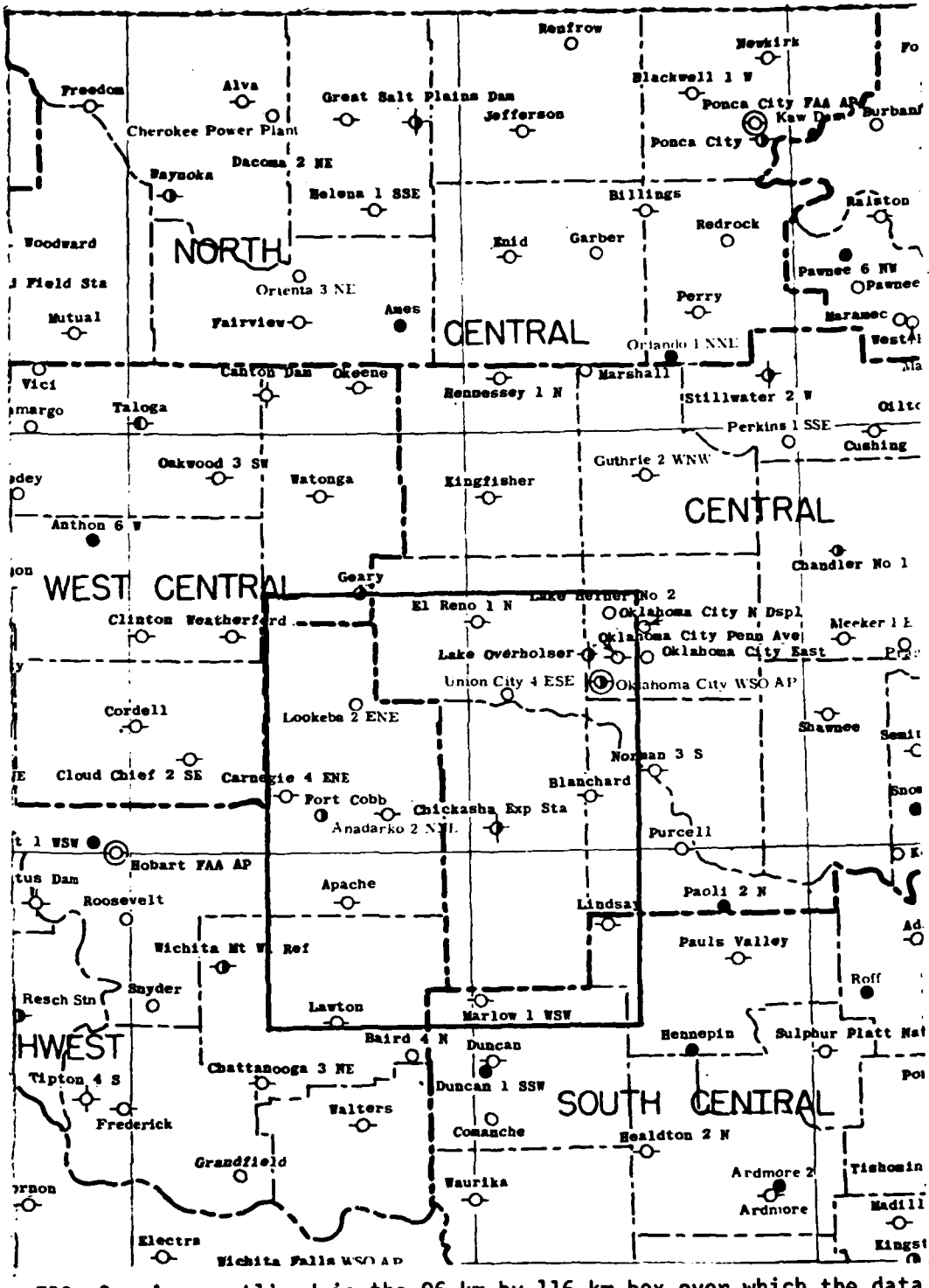

FIG. 3. Area outlined is the 96 km by 116 km box over which the data were analyzed.

author opted not to plot a single elevation angle map but rather to plot the lowest available constant-height interpolated map. This lowest available map is a function of the lowest tilt angle and the horizontal distance to the data of interest. For example, if we use the equation from the program

$$\tan^{-1} \phi = \frac{H}{X} - \frac{X}{RP2}, \tag{1}$$

where ϕ is the tile angle, H is the vertical height of the constant-altitude cylindrical array (km), X is the horizontal distance of interest (km), and RP2 is 2 times the 4/3 Earth curvature correction (km) (Greene, 1971). The solution of (1) for H is

$$H = (\tan^{-1} \phi + \frac{X}{RP2}) X. \tag{2}$$

Then let us assume that

$$\phi = 0.2°$$

$$X = 95 \text{ km}$$

$$RP2 = 16990.173 \text{ km (constant)}.$$

We find that H equals 0.863 km. Therefore, the lowest available map would be approximately 0.9 km with no data available beyond 95 km. Likewise this equation is used to determine the closest data available at the highest constant-altitude mapping by using the highest tilt angle.

After conversion to a rectangular array, each map is stored on a disc file and then used by the 'Conrec' program for an objectively contoured map. Details of the Conrec procedure are documented

by Neyland (1978). This author's plotting procedure includes some revisions to Neyland's procedure, as is noted in Appendix B.

The main area of change going from conventional data to Doppler data involved converting the enormous amount of data, 762 gates along each radial versus 200 gates, with not only reflectivity data but also radial velocity and spectrum widths, into accurate values without losing or over-smoothing the data. Initially, data were processed using every sixth gate (900 m). This procedure was tried because it was comparable to earlier research using 1-km spherical array points as the basis for conversion to cylindrical and rectangular coordinates. Also this appeared to be the most direct way to process the data without significant modification to previous programs. Secondly, a slightly more sophisticated approach was attempted by searching for the closest 150-m gate to each kilometer point along the radial, and using that gate in the spherical array. Although both these procedures produced seemingly accurate results, comparable to conventional data schemes, only approximately 15% of the data along each radial were being used. In order to use more of the available data, a linear averaging technique was designed. This technique averaged data across the seven 150-m gates closest to each kilometer. However, inclusion of practically all the data still was not satisfactory, since the averaged value could easily be biased by values on either side of the kilometer point. Biased values would then give false images of the actual reflectivity or radial velocity patterns. Finally it was determined that the most

accurate averaging technique would be to use a radius-of-influence average along each radial.

Radius-of-influence averaging is similar to Gaussian normalization. A 450-m radius-of-influence was selected. This radius allows practically all the data to be used without any overlapping of data points. A minimum of six or a maximum of seven gates are used in this averaging technique. Each gate is weighted according to its distance from the kilometer point. A gate at the kilometer point has a weighting value of one, while a gate 450 m from the kilometer point has a weighting value of 0.05. The value of reflectivity, or radial velocity, at each point is multiplied by the weighting value of that gate. Then the weighted sum of the six or seven gates is divided by the sum of the weights to determine the value for the kilometer point. To attain even greater accuracy, a consideration was given to the use of a radius-of-influence averaging across the radials. However, from simple trigonometry it is realized immediately that a 450-m separation of 1-deg radials occurs only out to approximately 26 km. Since the primary area of interest for this research deals with areas much farther away than 26 km, it was not feasible to add averaging across radials.

The next major change involved a correction for folding of radial velocities. Folding is assumed to occur when the gate-to-gate difference of radial velocity is greater than 34 m s^{-1} (Burgess et al., 1976). Recall from Table 1 that the maximum unambiguous velocity is $\pm$34.2 m s^{-1}; however, the maximum velocity recorded

is $\pm$34 m s^{-1}. Then, if the actual radial component is -40 m s^{-1} (toward the radar), it would not be recorded as -40 m s^{-1} but rather as a lesser positive value. This recording of velocities greater than $\pm$34 m s^{-1} as lesser numbers of opposite sign is called folding. To find the actual velocity, prior to averaging, requires that the folded velocity be corrected. Initially it is assumed that the very first gate is not a folded value. This is normally a good assumption unless there happens to be a tornado, or mesocyclone, directly over the first gate. If the absolute difference of gate 1 minus gate 2 is less than 34, no folding has occurred. Gate 3 is then subtracted from gate 2, and so forth, until an absolute difference greater than or equal to 34 is found. Now assume that gate 590 has an unfolded value of -32 m s^{-1} and gate 591 a value of +28 m s^{-1}. The absolute difference (/-32-(+28)/) is 60; therefore, gate 591 is a folded value. The actual value of gate 591 is found by multiplying 2 times the maximum unambiguous velocity using the algebraic sign of the unfolded gate, namely gate 590, and then adding the folded value.

$$2(V_{max}) + \text{Folded Velocity} = \text{Actual Velocity}$$

$$2(-34) + 28 = -40$$

Negative 40 m s^{-1} is then the actual value of gate 591, and this value is used in the radius-of-influence averaging. Gate 590 is then kept as the gate to compare with gate 592, and so forth, until no further folding occurs (see Appendix B). All gates along each radial are checked and corrected for folding prior to any radius-of-

influence averaging. Some implied assumptions, due to the limited maximum unambiguous velocity, are that the radial component of velocity will not be greater than ± 68 m s^{-1}, and, that the maximum gate-to-gate shear will not exceed 34 m s^{-1}.

The final adjustment was necessary due to the antenna rotation. Initially, it was assumed that the antenna would be in record mode only when rotating in a clockwise direction. This assumption was soon misproven. In order to get as much information as possible on a mesocyclone in a short period of time, the operators at NSSL, at times, recorded data both clockwise and counterclockwise over a small number of azimuth angles (sector scanning). By doing this, data were not always collected at 1° increments. Therefore numerous checks had to be added to the computer program in an attempt to cover all data collections, including different directions and rates of rotation. Due to the variable azimuth separations, it was decided to use azimuths at approximately 1° separations. Checks were added to compare two azimuths at a time, find the one closest to the predetermined integer azimuth, compare this closest azimuth to the next read azimuth to finally locate the closest azimuth to the integer value. This way when different tilts are used for the cylindrical averaging conversion, the compared azimuth angles will be at least within a few tenths of a degree to each other. Nevertheless, there are some exceptions. Occasionally an azimuth may have been determined to be inaccurate during the conversion from 7-track to 9-track and was therefore noted as a 999 azimuth and

omitted. Also, an integer value azimuth may be skipped, in rare cases. In these instances, instead of averaging in false zero values, the missing azimuths are assigned values exactly the same as the previously processed azimuth. This technique results in much better averaging than would accrue from use of a false zero value in the middle of an echo. (See Appendix B for further details of the actual computer program used in this research.)

6. RESULTS

The primary emphasis of this research was to determine if it was feasible to detect mesocyclones by using constant altitude mappings of radial velocities (CAVM). If this was feasible, what horizontal and vertical scales provided 'optimum' detection over a relatively large area, approximately 50 km by 50 km? How do constant altitude reflectivity maps (CAZM) compare with CAVMs for severe weather features?

Two severe storms were chosen for this research. On May 1, 1977, at 1810 CDT (02/0110 GMT), NSSL identified a weak mesocyclone along the 252° radial at 62 km with a diameter of 3.3 km (Burgess, et al., 1977). No tornadoes were observed although large hail was reported between 1815 CDT and 1850 CDT, thereby calling for classification as severe. The second storm that was analyzed was detected on May 20, 1977, along the 262° radial at 95 km with a diameter of 3.3 km at 1641 CDT (2341 GMT). This storm met the criteria for a strong mesocyclone and was, in fact, identified as a tornado vortex signature (TVS). Brown and Lemon, 1976, describe a TVS as:

(1) An area of azimuthal shear of at least 15 to 20 m s^{-1} over an azimuthal range of 1° or less (approximately 1 beamwidth).

(2) A cyclonic signature with peak Doppler velocity values of opposite sign.

(3) Anomalous shear region of not more than approximately 1-km range extent.

(4) A shear region at least a few kilometers in vertical extent.

(5) A persistent anomalous shear region at the same general heights for approximately 10 min or more.

Since these two storms occupy the two limits of the mesocyclone spectrum, it was felt they would make good test cases for this research.

a. May 1, 1977 Mesocyclone

Available radar data on this day include sets from both the WSR-57 and the Norman Doppler. Because WSR-57 data had been successfully analyzed by previous researchers, these data were processed initially and used as a check for the new Doppler processing scheme. The WSR-57 radar data were processed on the 96 km by 116 km Chickasha grid with 2-km horizontal spacings and 1-km vertical intervals. This produced CAZM's similar to those produced by Sieland (1977). Processing of data began 30 min prior to the report of the mesocyclone since Doppler velocity profiles have been shown to be able to detect mesocyclones at mid-levels approximately 30 min to 1 h prior to surface disturbances (Lemon et al., 1977). The Norman Doppler data were then processed over the same grid area and the same horizontal and vertical scales. Although the recording times and the antenna locations of the two radars were not exactly the same, they were close enough to use as a check to ensure accuracy of the new processing scheme.

In all of the figures dealing with this case, CAZM isopleths of reflectivity start with 15 dBZ and are incremented every 10 dBZ. Also, all maps have a line with a point marked on it indicating the location of the mesocyclone (262° at 62 km). The first sequence of data, recorded from 1740 CDT to 1743 CDT by WSR-57 radar, shows a maximum core of 45 dBZ vertically stacked from 1 km through 9 km, then decreasing to 35 dBZ at 10 km (Figs. 4 to 7). Doppler radar CAZM's collected between 1742 CDT and 1748 CDT indicated patterns very much like those from the WSR-57 radar data. This assured that the new processing scheme, with its numerous checks and radius-of-influence averaging, was processing the Doppler data accurately. While the WSR-57 data were collected to a maximum tilt angle of 13°, the Doppler radar data, up to the time of mesocyclone, were collected only to a maximum tilt angle of 5.1°. Therefore, the highest available CAZM and CAVM analyses of Doppler data were only to 5 km, whereas WSR-57 CAZM's could be processed to higher altitudes. Note that Figs. 4 through 7 indicate no obvious severe weather features other than a high reflectivity core.

Constant altitude velocity maps (CAVM) were processed with the same grid criteria. Isopleths of radial velocity, isodops, were analyzed in meters per second at 5-m s^{-1} intervals. In the following figures, dashed lines indicate radial components toward the radar (negative), while solid lines represent radial component flow away from the radar (positive). The zero line (0-m s^{-1} isodop) represents zero radial component or all flow perpendicular to the beam. Storm

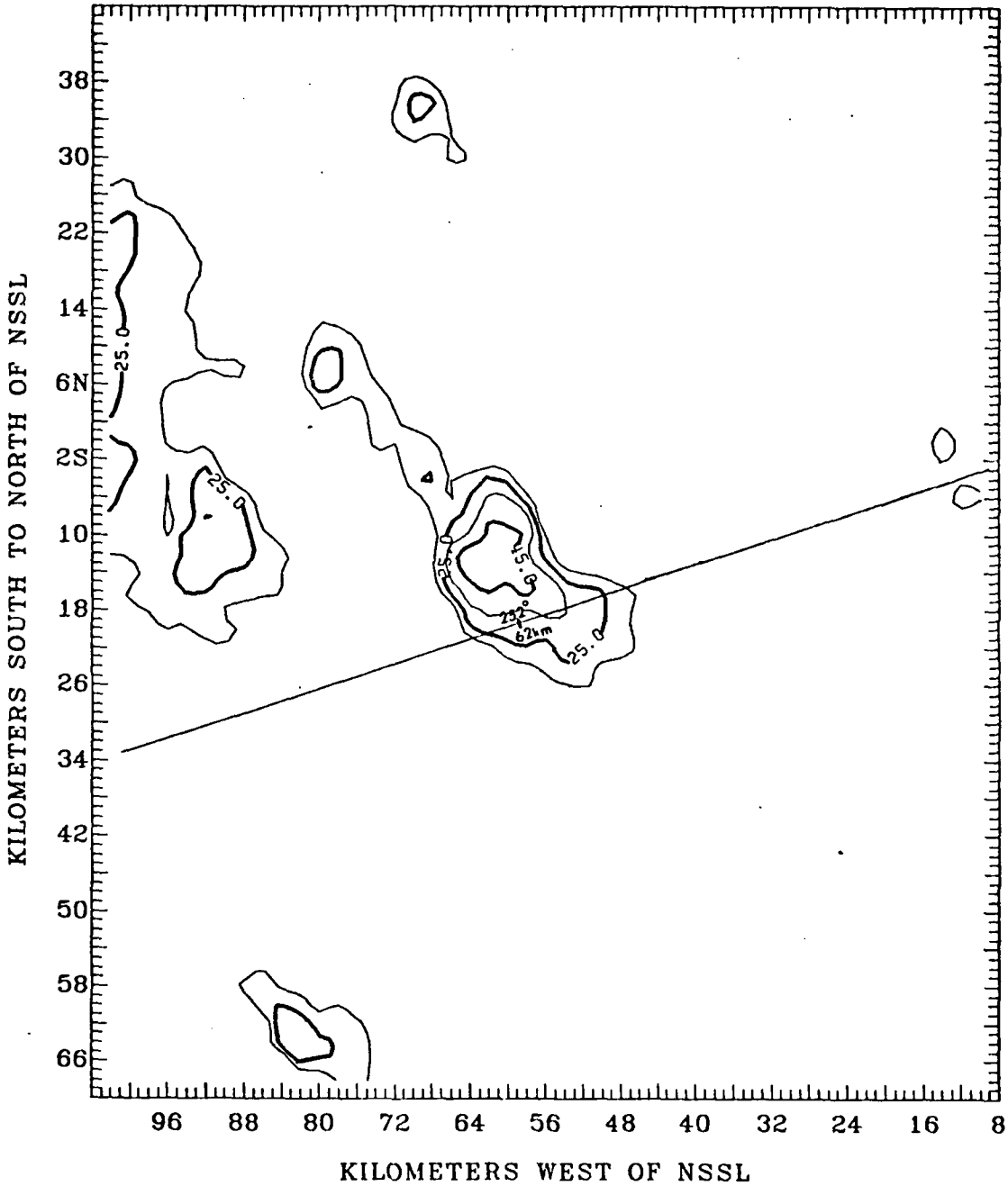

FIG. 4. 1-km CAZM, 1740-1743 CDT, 1 May 1977 (2-km grid), WSR-57 data.

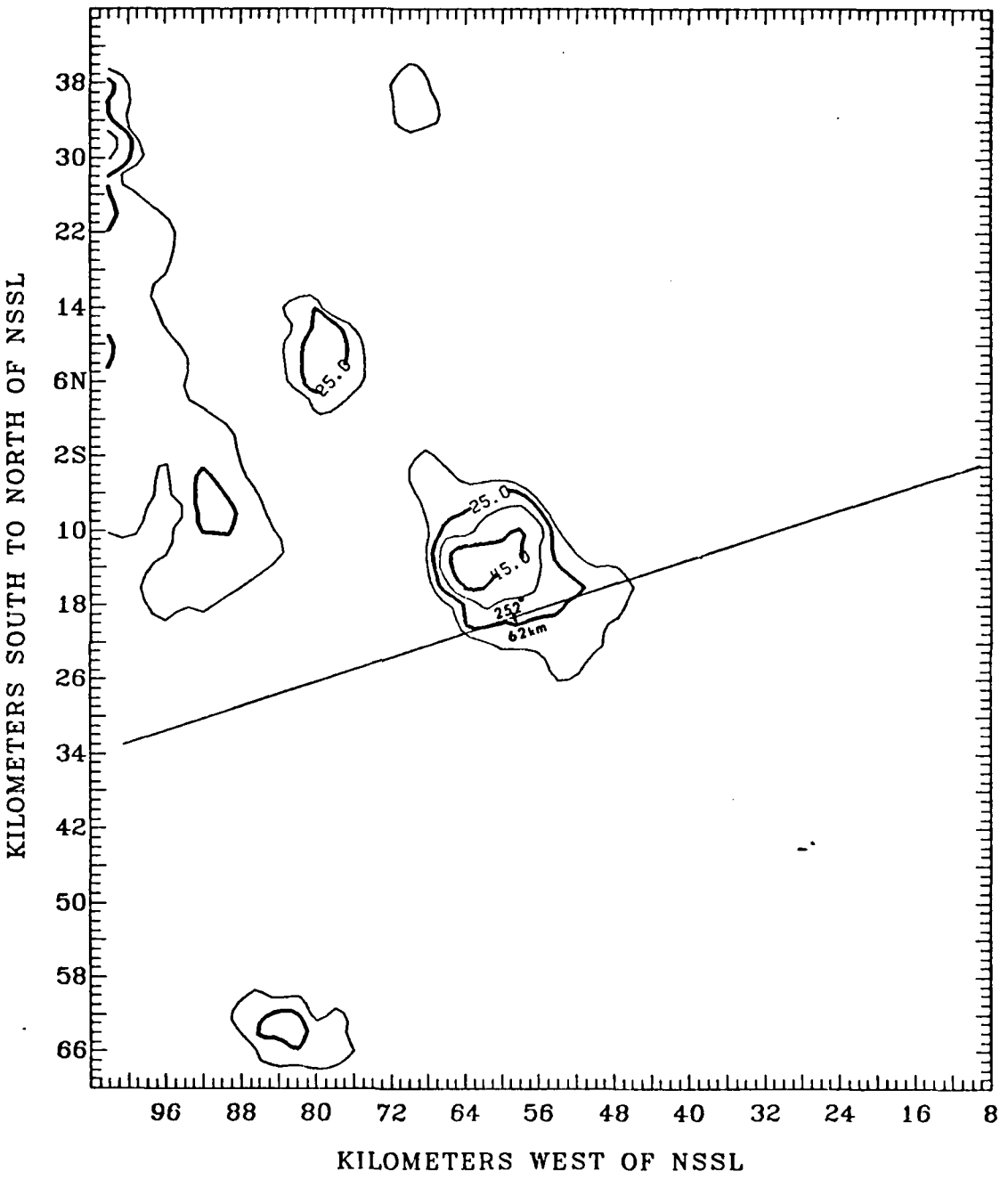

FIG. 5. 4-km CAZM, 1740-1743 CDT, 1 May 1977 (2-km grid), WSR-57 data.

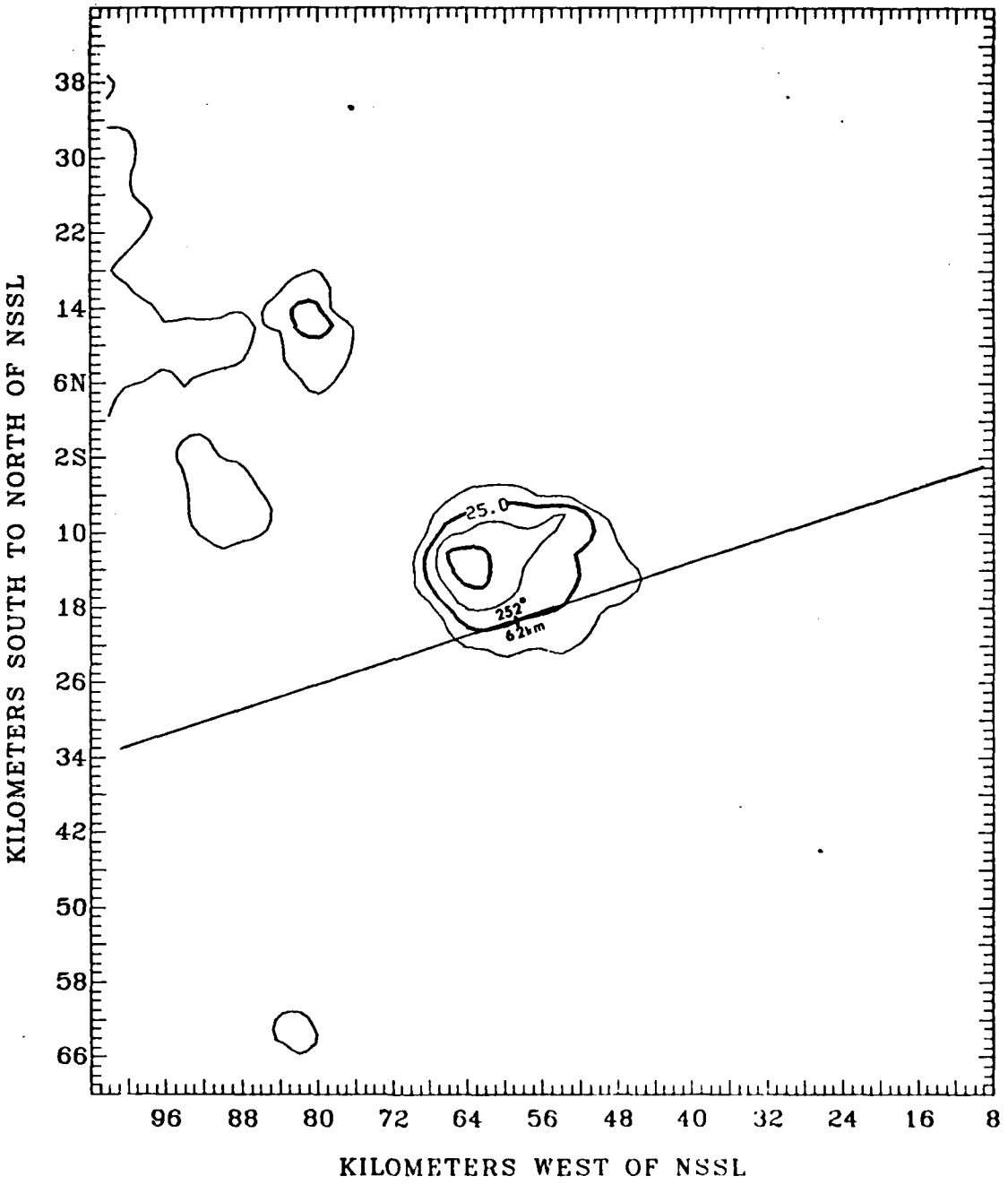

FIG. 6. 8-km CAZM, 1740-1743 CDT, 1 May 1977 (2-km grid), WSR-57 data.

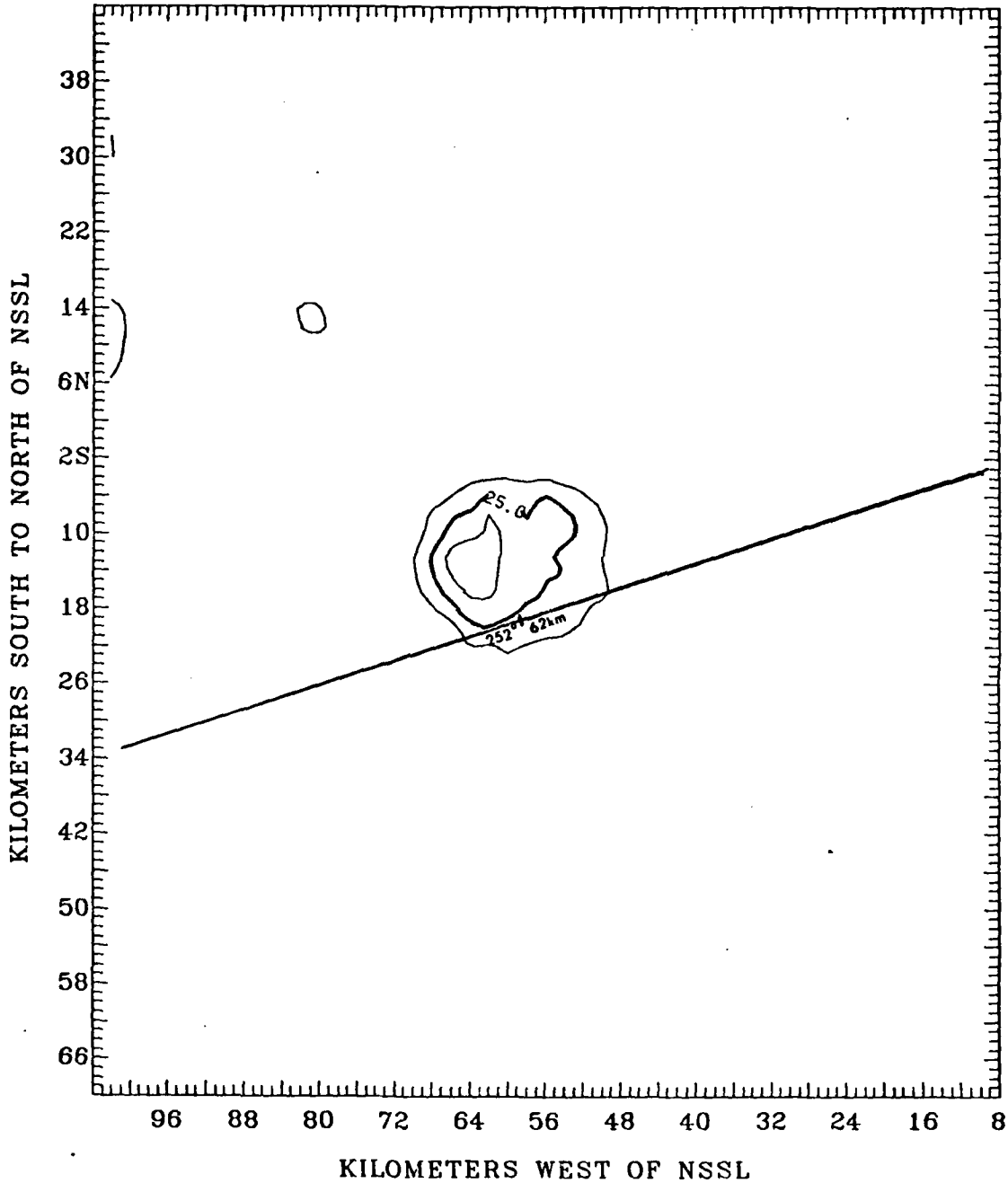

FIG. 7. 10-km CAZM, 1740-1743 CDT, 1 May 1977 (2-km grid), WSR-57 data.

motion was not removed from the data. Therefore it is natural for radial velocities west of the radar to have higher negative components than positive. These components can be balanced closely by accounting for cell motion; this was tested. However, accounting for individual cell motion resulted in inaccurate values over the remainder of grid box and, in fact, even indicated 'false' mesocyclone and convergent areas. The method tested was a cosine function correction assuming one movement for the entire grid box. In addition numerous cosine function corrections were tested for a small area surrounding the mesocyclone center. These also resulted in 'false' isodops, especially near the edge of the corrected area. It was determined that, although storm motion correction would tend to balance the negative and positive components for a small area, no single solution could be accurate for the entire grid box. Likewise, since storm motion correction would not change the location of the vortex, but only balance the components, it was deemed inadvisable to use storm motion correction.

The first series of CAVM analyses is for the time period of 1742 CDT to 1748 CDT. Figure 8 shows the 1-km CAVM. Both the 1-km and 2-km heights indicated little more than the 0-m s^{-1} isodops, i.e., few components toward or away from the radar greater than 5 m s^{-1}. However at 3 km and 4 km a definite area of convergence is noted (Figs. 9 and 10). Although neither the reflectivity nor radial velocity analyses at this time indicate any definitive

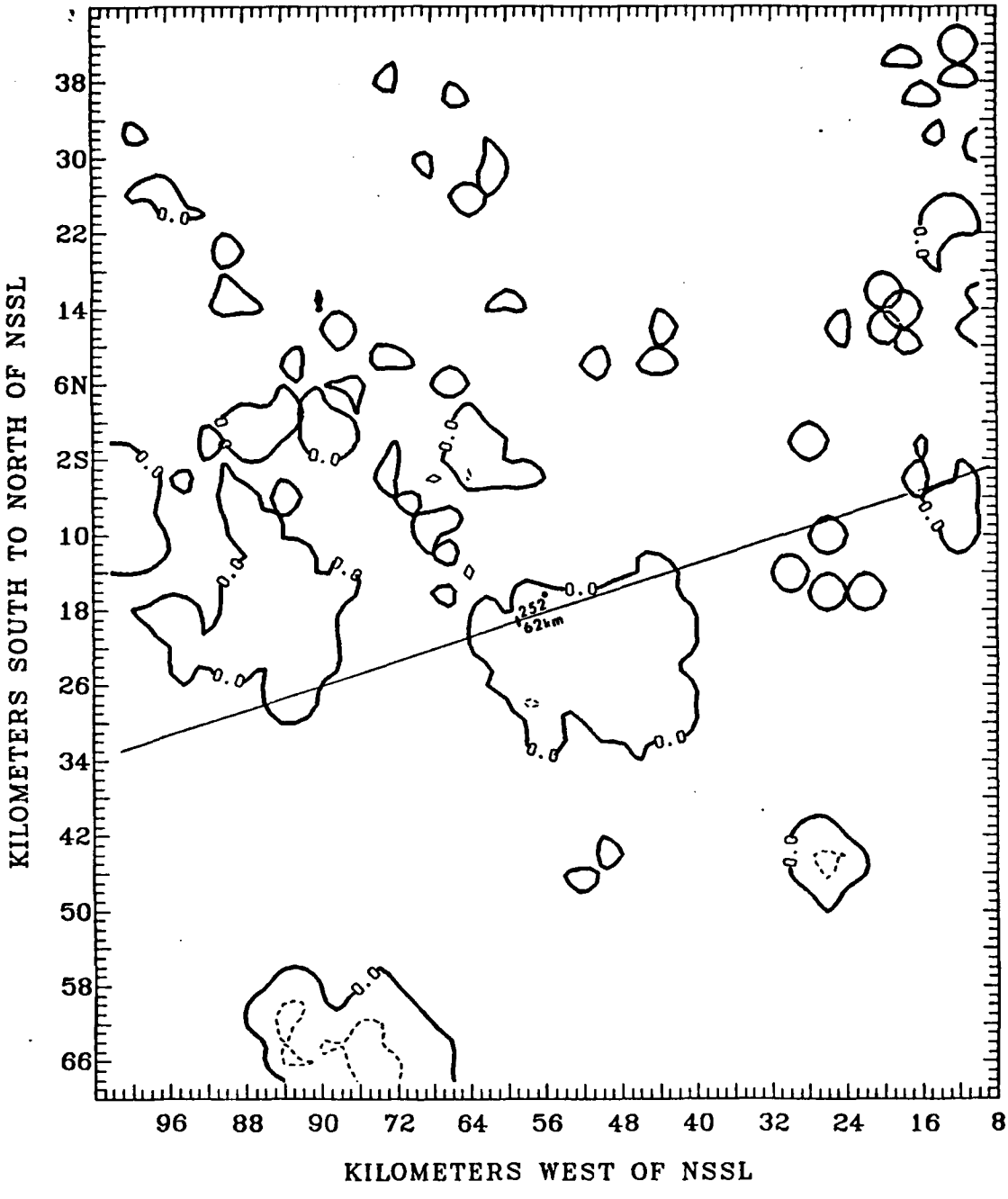

FIG. 8. 1-km CAVM, 1742-1748 CDT, 1 May 1977 (2-km grid), Doppler data.

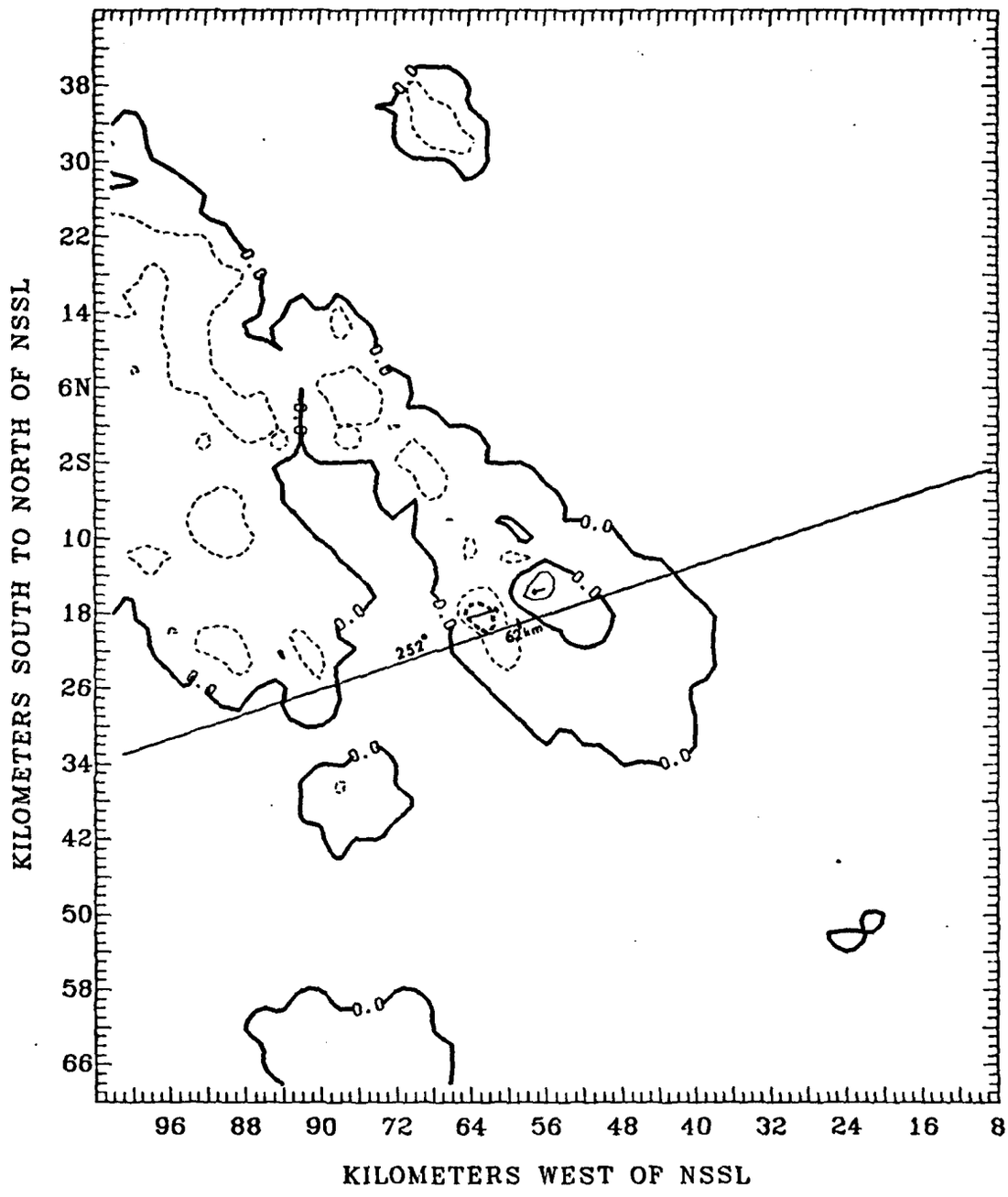

FIG. 9. 3-km CAVM, 1742-1748 CDT, 1 May 1977 (2-km grid), Doppler data.

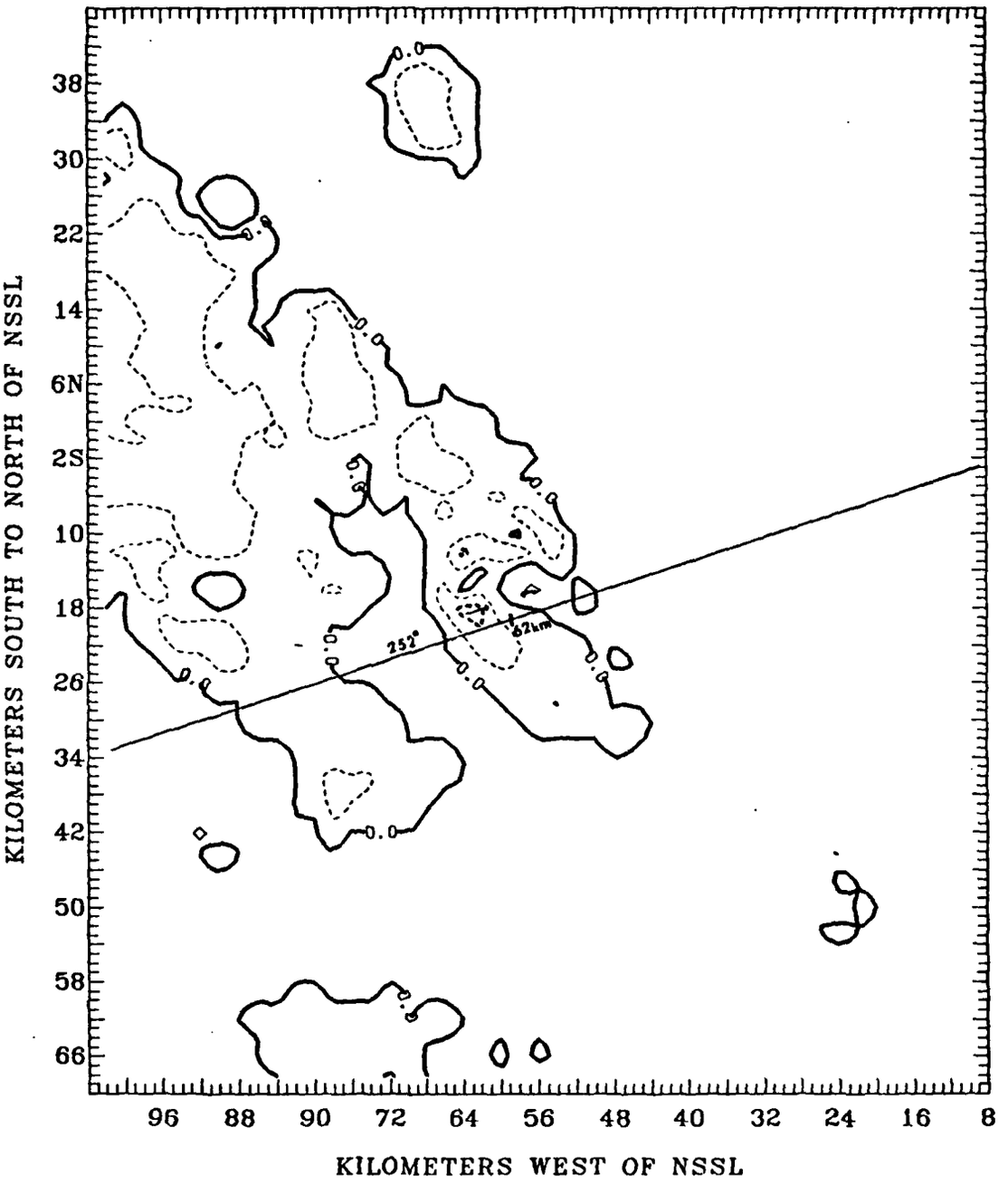

FIG. 10. 4-km CAVM, 1742-1748 CDT, 1 May 1977 (2-km grid), Doppler data.

severe weather features, at least the CAVM analysis indicates the probable severe weather area.

Between 1750 CDT and 1805 CDT two more sequences of WSR-57 radar data were recorded, but no Doppler radar data were collected. The 1750-1753 CDT sequence shows a slight southeast movement had occurred of the 45-dBZ core, which now extends only to 6 km (Fig. 11). Figure 12, 8-km CAZM, indicates an indentation of the 25-dBZ and 35-dBZ isopleths which might be interpreted as the beginning of a weak echo region (WER). By 1800 CDT the 45-dBZ core has elongated, and again a very slight east-southeast movement is detected at all levels. The 45-dBZ core split into two distinct cells at the 2-, 3- (Fig. 13), and again at 10-km heights. (For further details on the aspects of this splitting storm see Bluestein and Sohl, 1979.) *During this 15-min time period the reflectivity data indicated* that the storm moved east-southeast such that the largest 45-dBZ core of the 3-km CAZM (Fig. 13) is located directly within the area of convergence noted on the 3-km CAVM at 1748 CDT (Fig. 9). Still, the only reflectivity feature of severe weather is the intensity of the core and the indication of a split.

The second series of Doppler radar data was recorded between 1805 CDT and 1812 CDT. Again the lowest CAVM's indicated nothing more than the 0-m s^{-1} isodops, whereas the 3-km CAVM (Fig. 14) indicates that the -5 m s^{-1} field has shifted to the southeast and the 0-m s^{-1} isodop is parallel to the 252° azimuth at 62 km, but

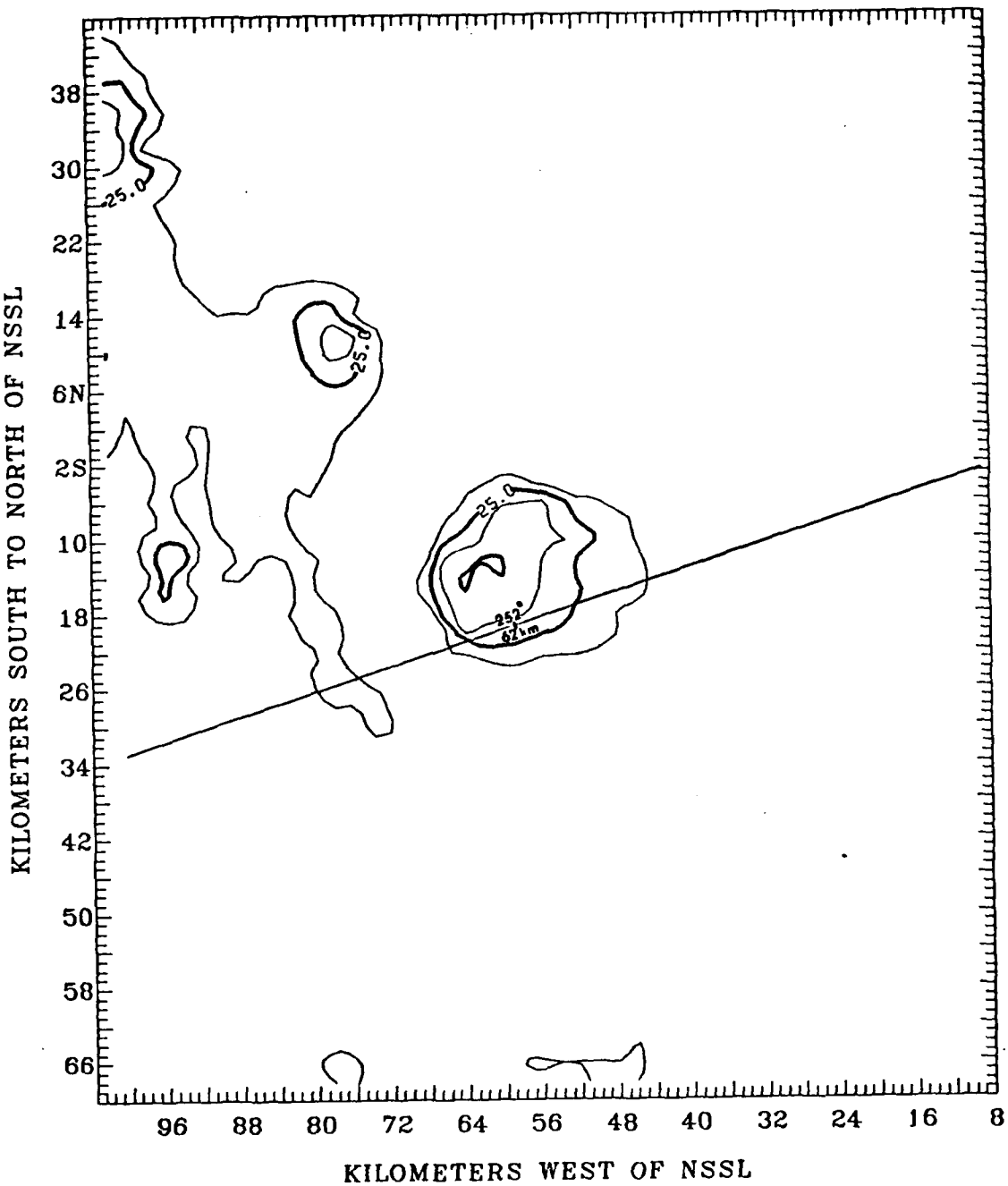

FIG. 11. 6-km CAZM, 1750-1753 CDT, 1 May 1977 (2-km grid), WSR-57 data.

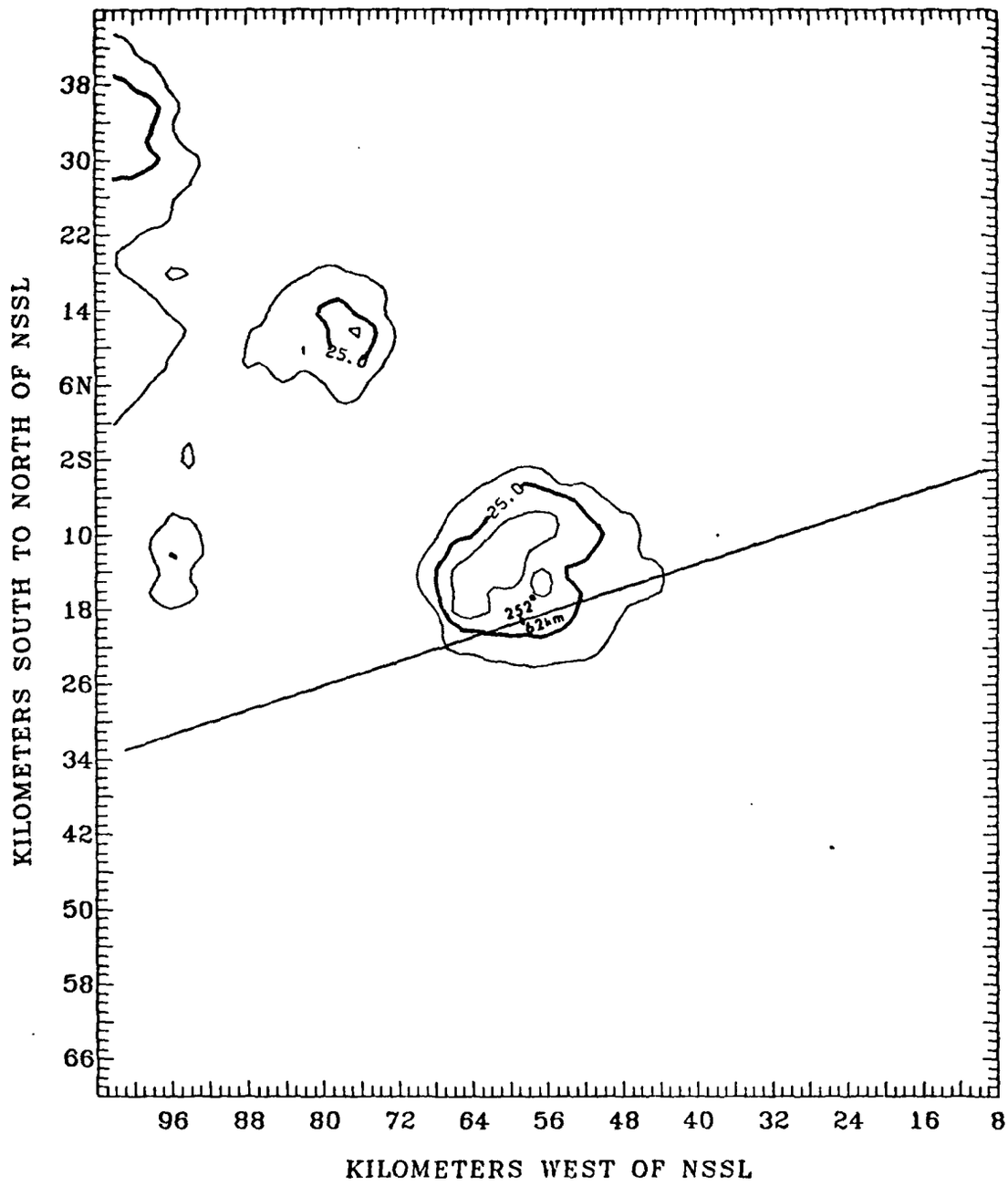

FIG. 12. 8-km CAZM, 1750-1753 CDT, 1 May 1977 (2-km grid), WSR-57 data.

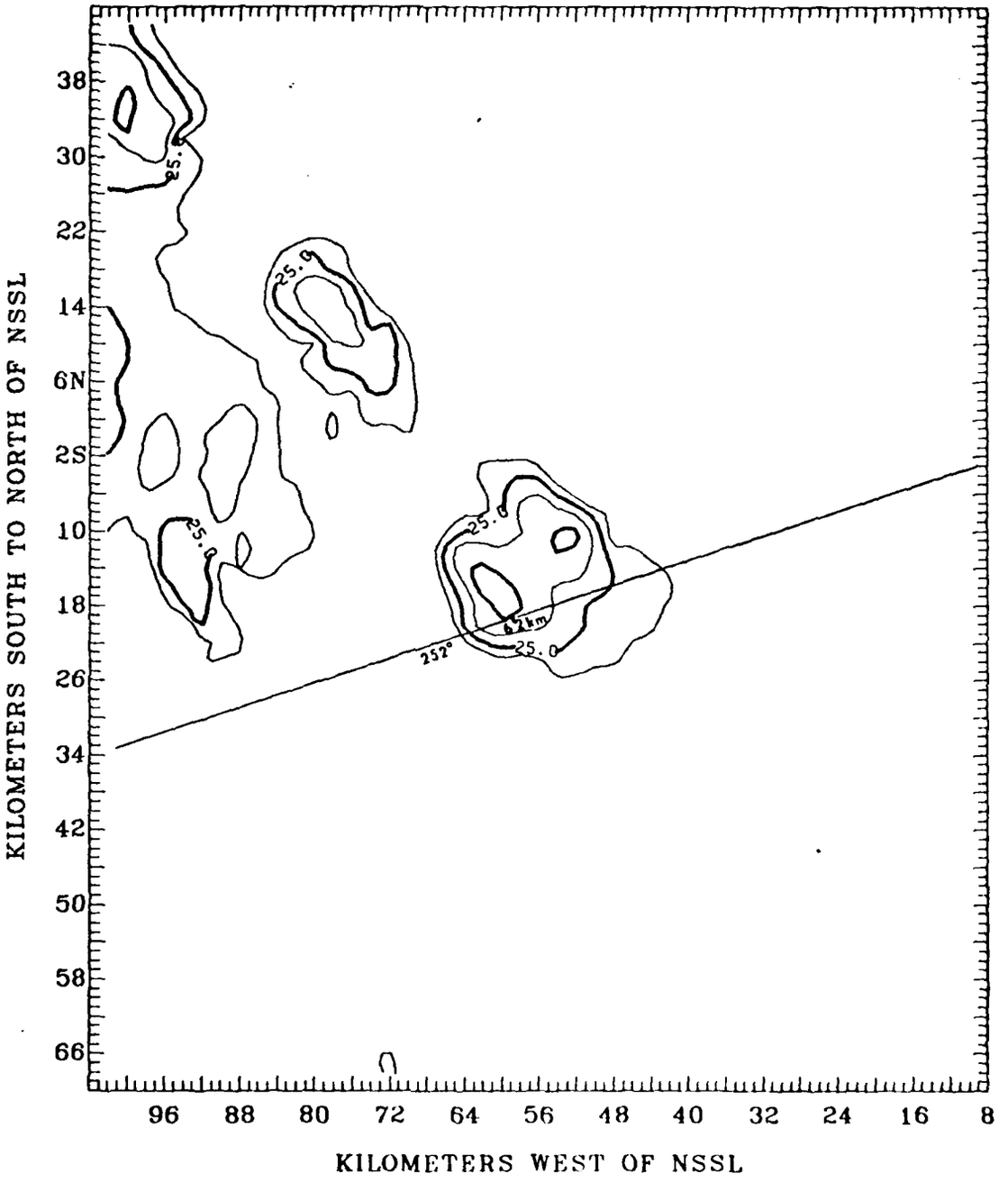

FIG. 13. 3-km CAZM, 1800-1804 CDT, 1 May 1977 (2-km grid), WSR-57 data.

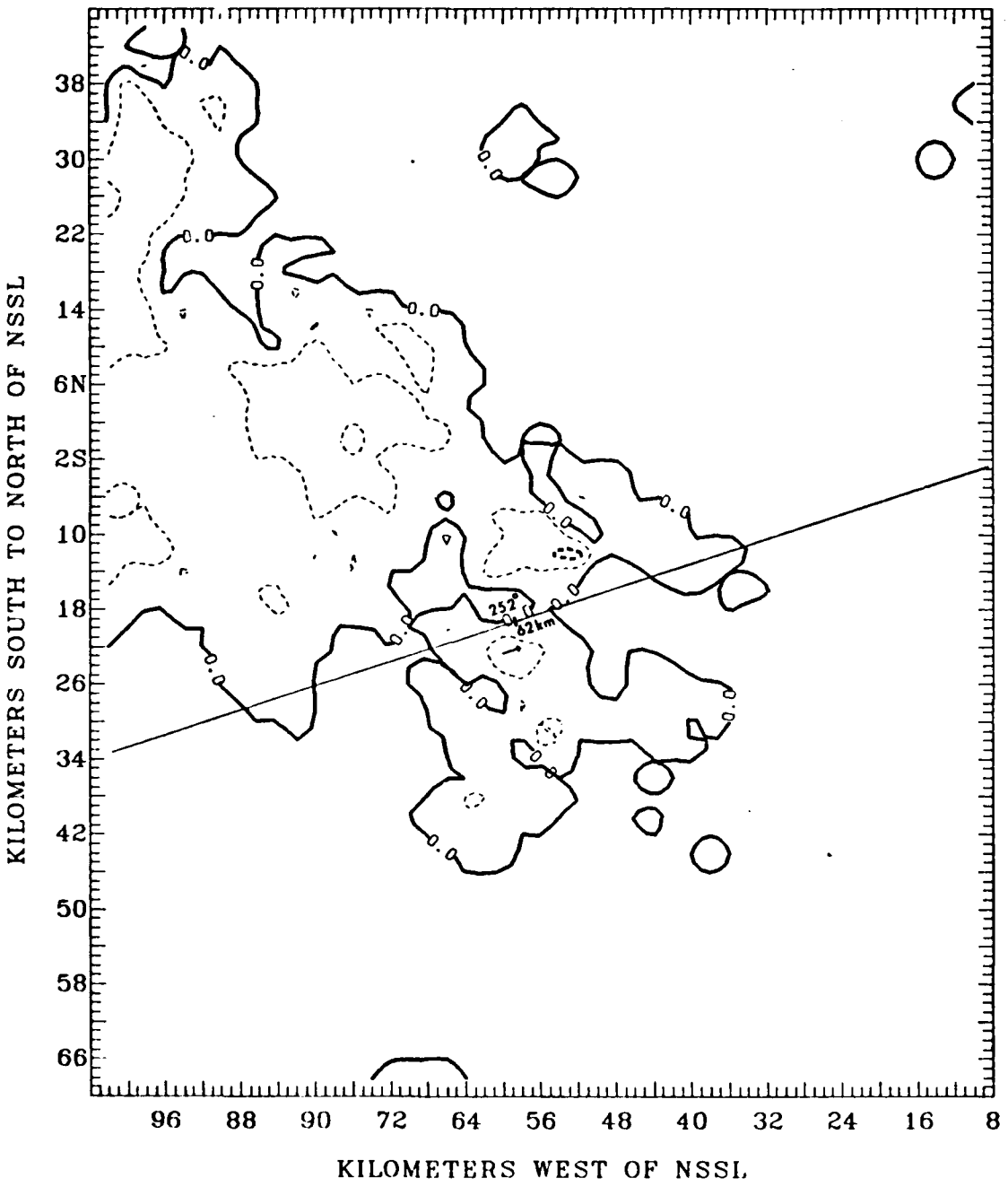

FIG. 14. 3-km CAVM, 1805-1812 CDT, 1 May 1977 (2-km grid), Doppler data.

no positive area of at least 5 m s^{-1} is indicated. Recall from Figure 1 that a mesocyclone must have negative and positive isodops on either side of an azimuth with the 0-m s^{-1} isodop parallel to the azimuth. Figures 15 and 16 then indicate suspected cyclonic rotation at 4 km and 5 km, but still no 5-m s^{-1} isodop is detected. Since this was a weak mesocyclone having a diameter of 3.3 km, and storm motion was not accounted for, it seems likely that the cyclonic vortex may not be detectable on a 2-km horizontal grid. Nevertheless, an area of convergence, which now suspiciously resembles cyclonic flow, was noted as early as 22 min before mesocyclone detection.

With this grid scale, the 1-km vertical spacing proved sufficient to detect sustained cyclonic flow through a vertical height at least as great as its horizontal diameter. On the other hand, with a vertical grid spacing of 1.5 km (approximately 5000 ft as in previous research), the presumed cyclonic rotation was detectable only at 3 km and 4.5 km and therefore was not able to detect this small mesocyclone. The 1-km vertical interval therefore was selected as the 'optimum' vertical scale. Only suspected cyclonic flow could be inferred on the 2-km horizontal grid, which was felt to be inadequate. Therefore, an adjustment was made to use a 1-km horizontal grid spacing over an area of 49 km by 59 km, or half of the 2-km grid box, and nearly centered on the mesocyclone area.

The following results were obtained from processing Doppler radar data only on the new 1-km horizontal and vertical scales.

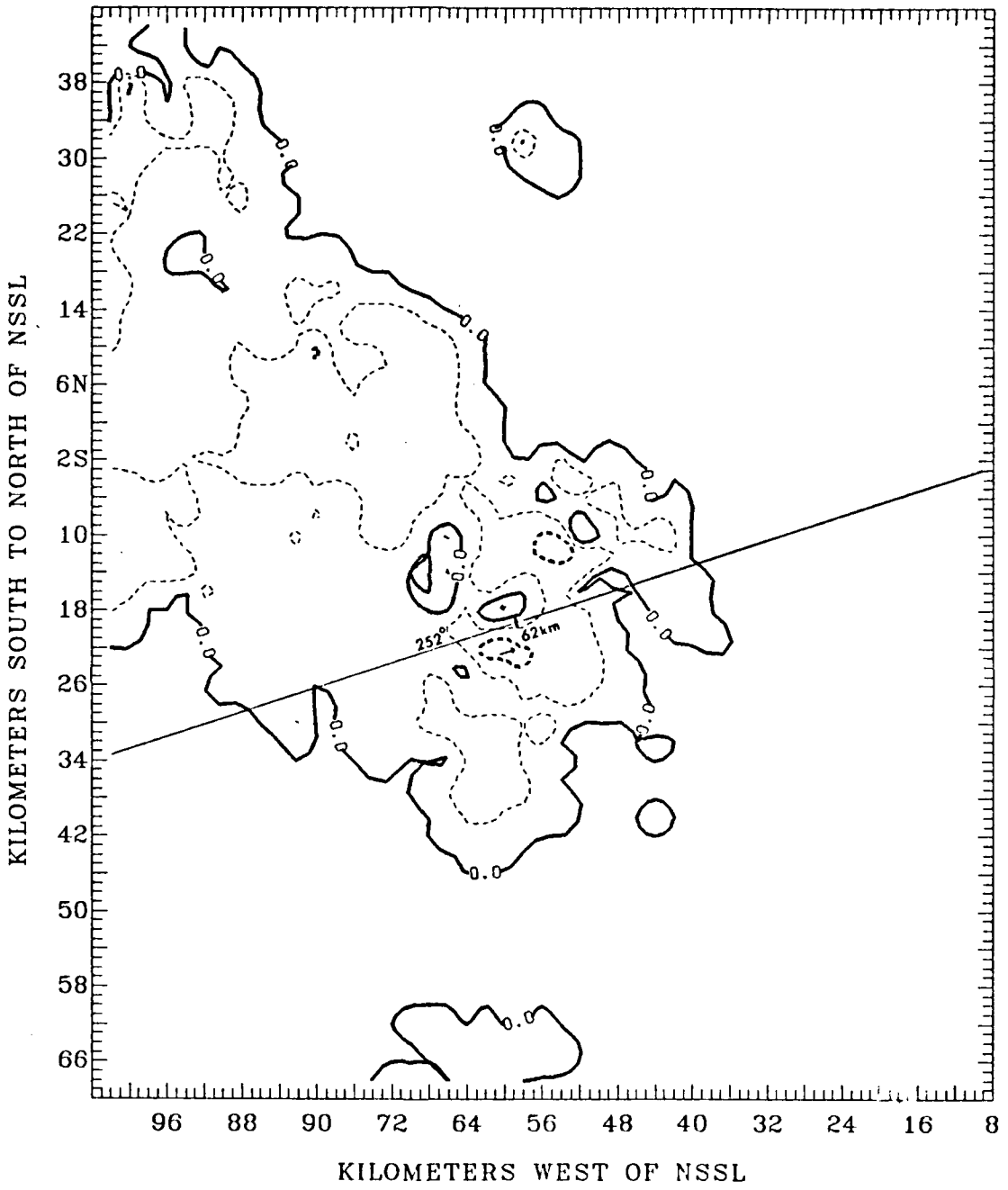

FIG. 15. 4-km CAVM, 1805-1812 CDT, 1 May 1977 (2-km grid), Doppler data.

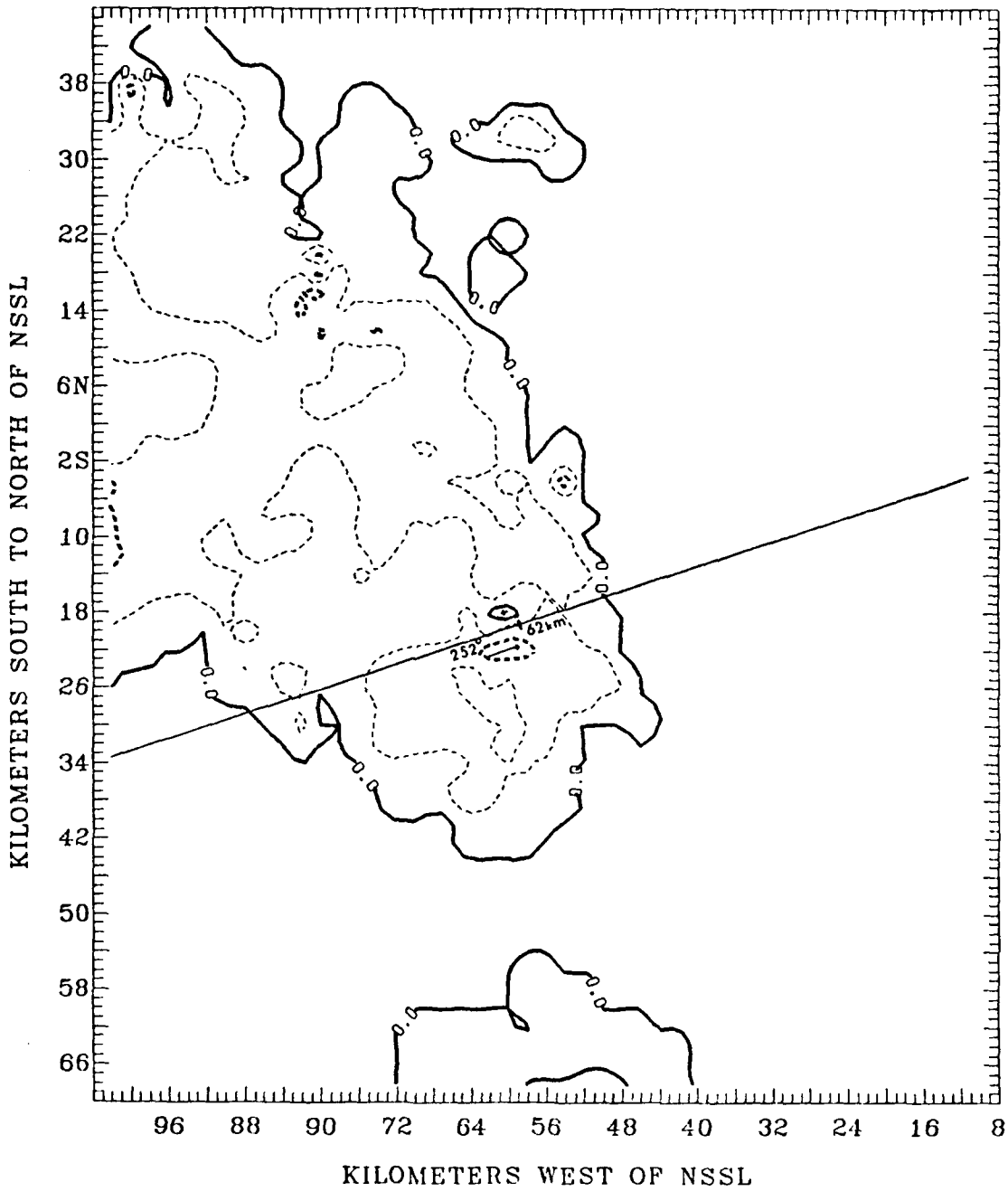

FIG. 16. 5-km CAVM, 1805-1812 CDT, 1 May 1977 (2-km grid), Doppler data.

As early as 1730 CDT, from a collection made from 1724 CDT to 1730 CDT, an area of convergence was detected at 3-km and 4-km heights, approximately 4-km north-northwest of the future mesocyclone site (Figs. 17 and 18). Figures 19 and 20 are for the same time as Figs. 9 and 10 but now on a 1-km horizontal grid. The convergence area is much more obvious. From comparison of Figs. 21-23 with Figs. 14-16, the cyclonic flow is highly suspected but still there are no positive isodops. Figures 21-23 do, however, indicate a radial component of at least 10 m s^{-1} at 3 km not detected by the 2-km grid and also a 15-m s^{-1} isodop at 4 km that was not detected. Since there were still no positive isodops, a special 450-m grid scheme was used to process a small area of data around the mesocyclone for this time sequence. The analysis was output as numerical values for each 450-m point and did in fact show an area of positive values within the 0-m s^{-1} isodop at all three levels. At 3 km, the maximum positive values were 4 m s^{-1}, while at 4 km and 5 km, a maximum value of 5 m s^{-1} was found but only at two consecutive gates and therefore was not indicated on a 1-km grid spacing. It was determined that the 450-m grid spacing would result in excellent detailed mappings of an individual mesocyclone. However, the limited 450-m grid box was considered too small for the initial location of mesocyclones over a sufficiently large area. It also is possible to decrease the isodop interval which was tested but negative isodop bunching results. Therefore the 1-km horizontal

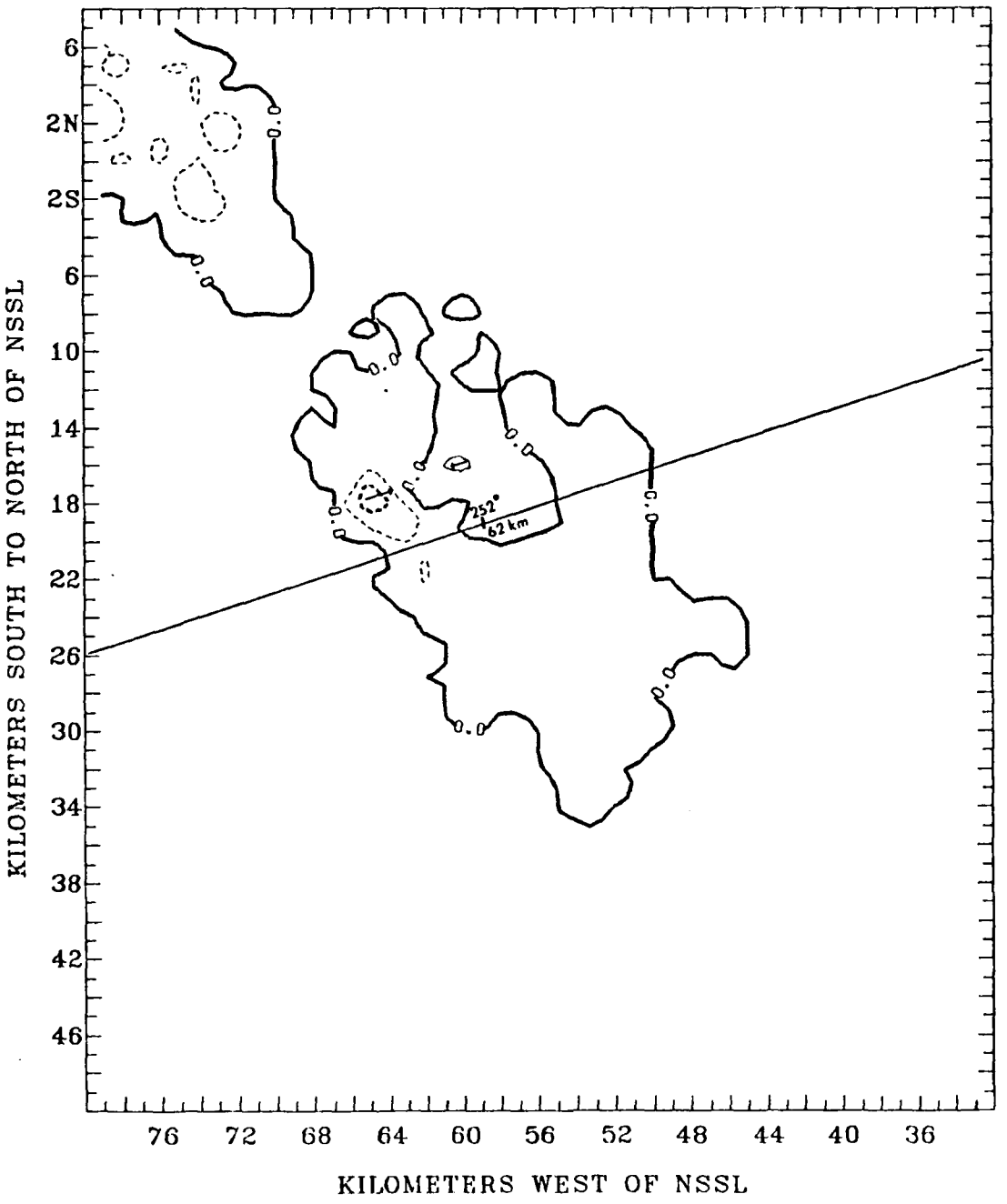

FIG. 17. 3-km CAVM, 1724-1730 CDT, 1 May 1977 (1-km grid), Doppler data.

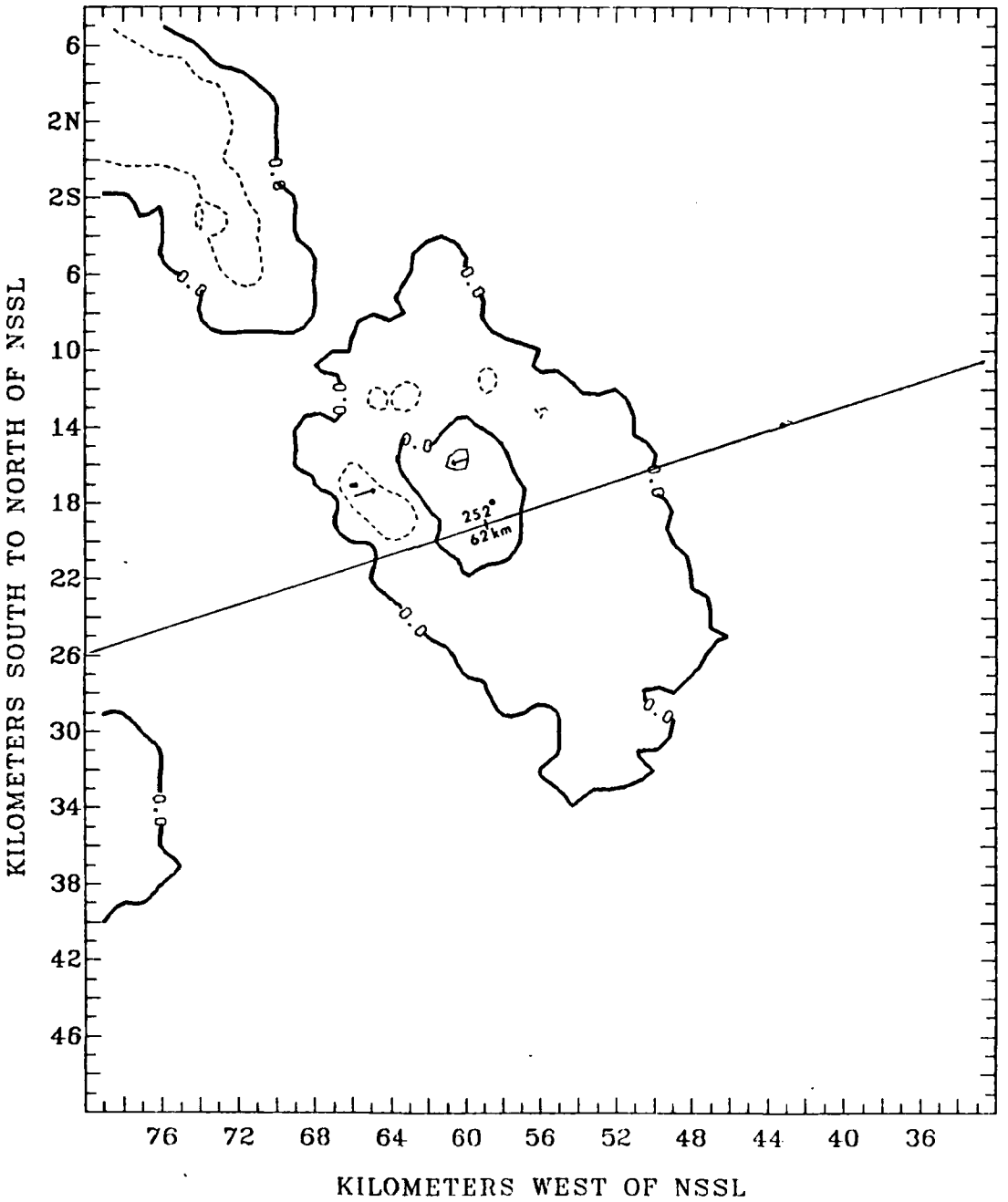

FIG. 18. 4-km CAVM, 1724-1730 CDT, 1 May 1977 (1-km grid), Doppler data.

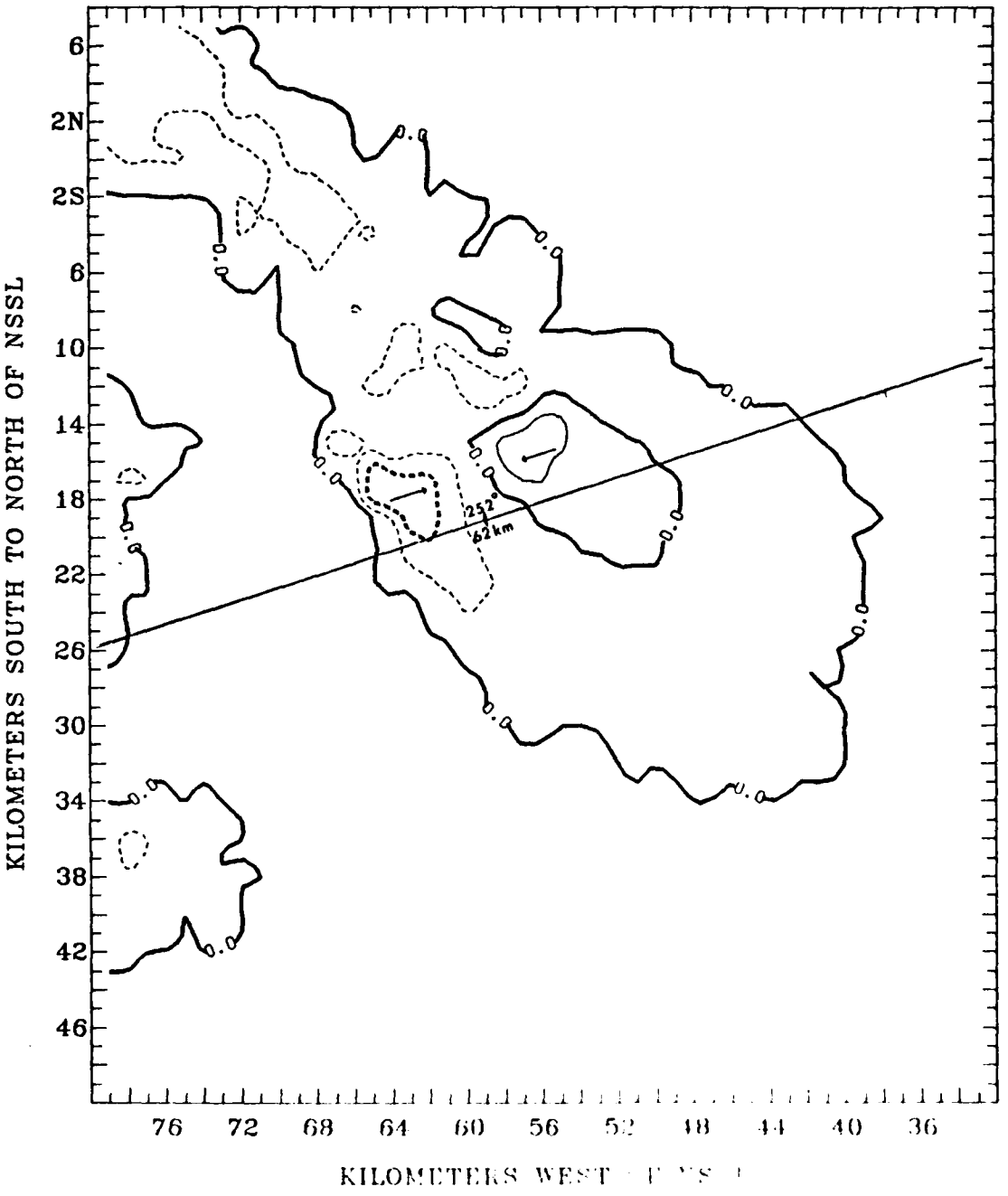

FIG. 19. 3-km CAVM, 1742-1746 CDT, 1 May 1977 (1-km grid), Doppler data.

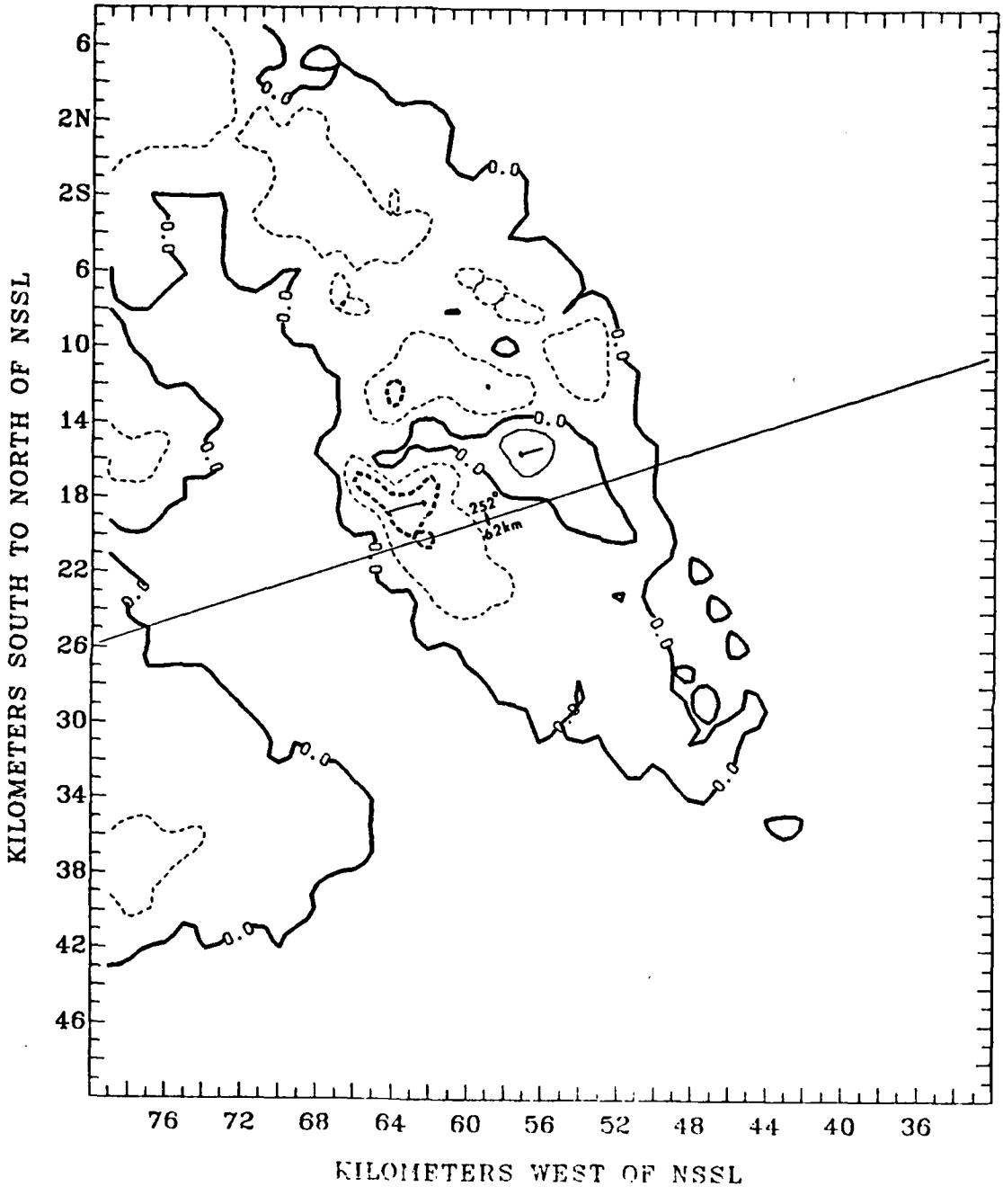

FIG. 20. 4-km CAVM, 1742-1746 CDT, 1 May 1977 (1-km grid), Doppler data.

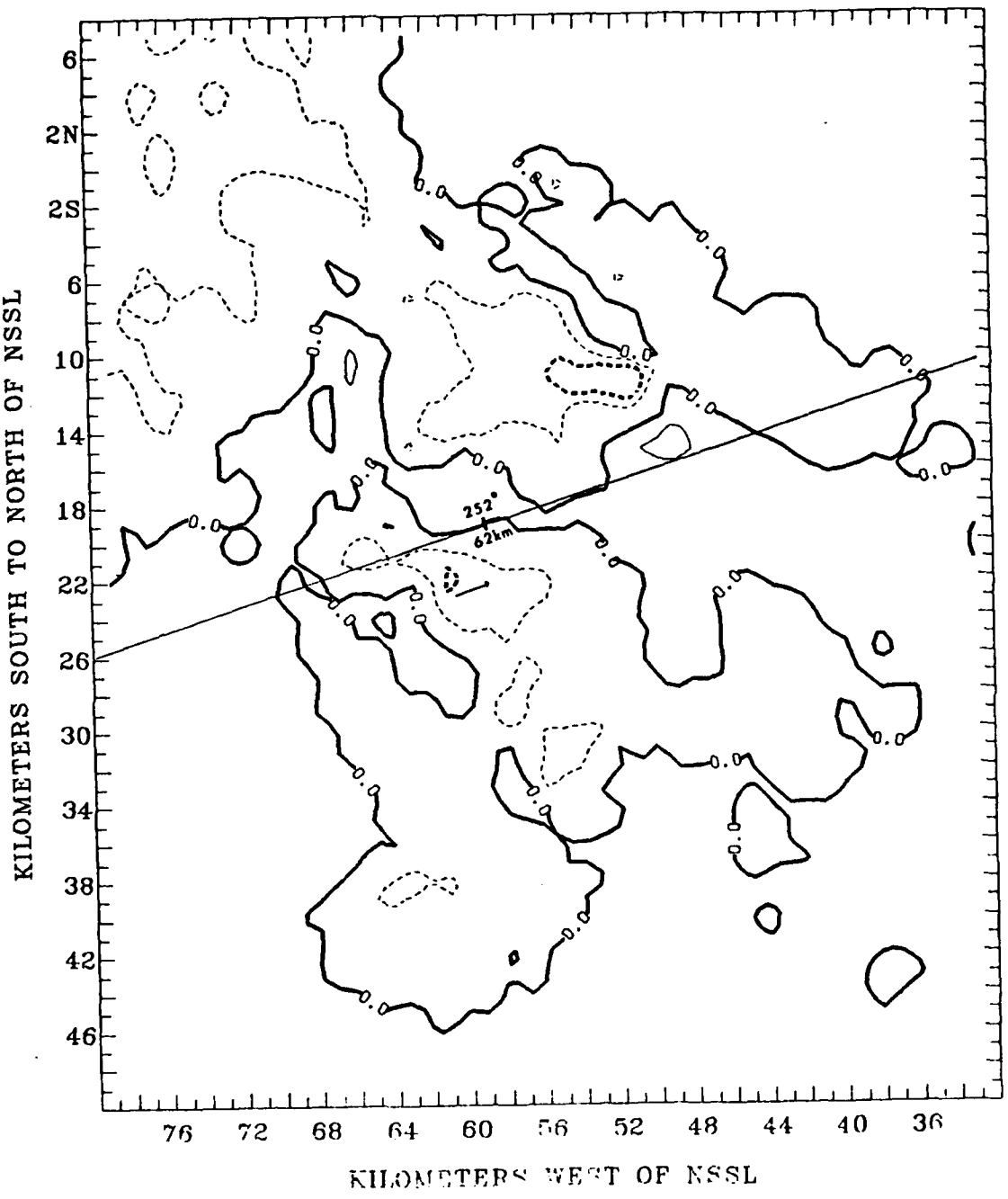

FIG. 21. 3-km CAVM, 1805-1812 CDT, 1 May 1977 (1-km grid), Doppler data.

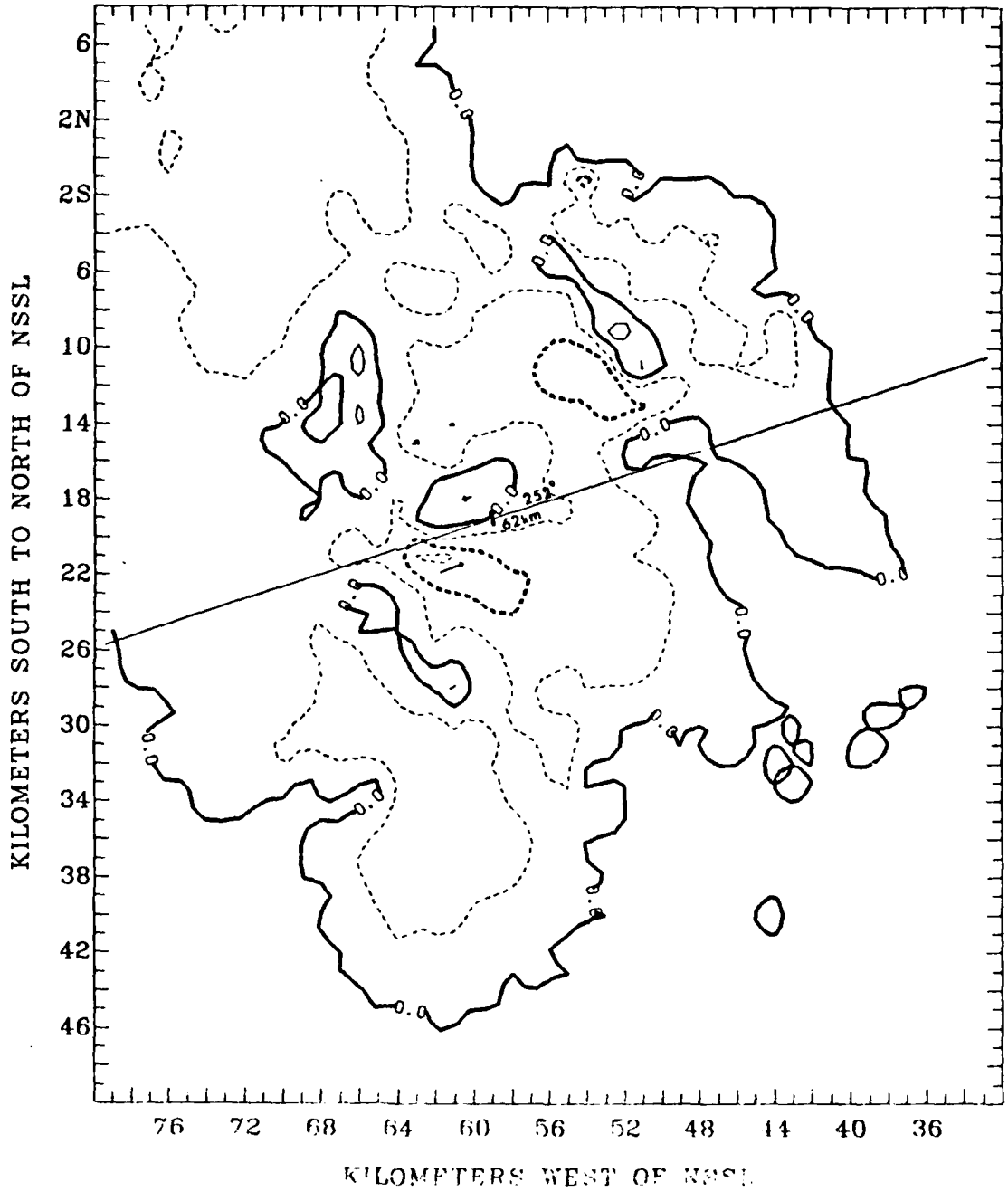

FIG. 22. 4-km CAVM, 1805-1812 CDT, 1 May 1977 (1-km grid), Doppler data.

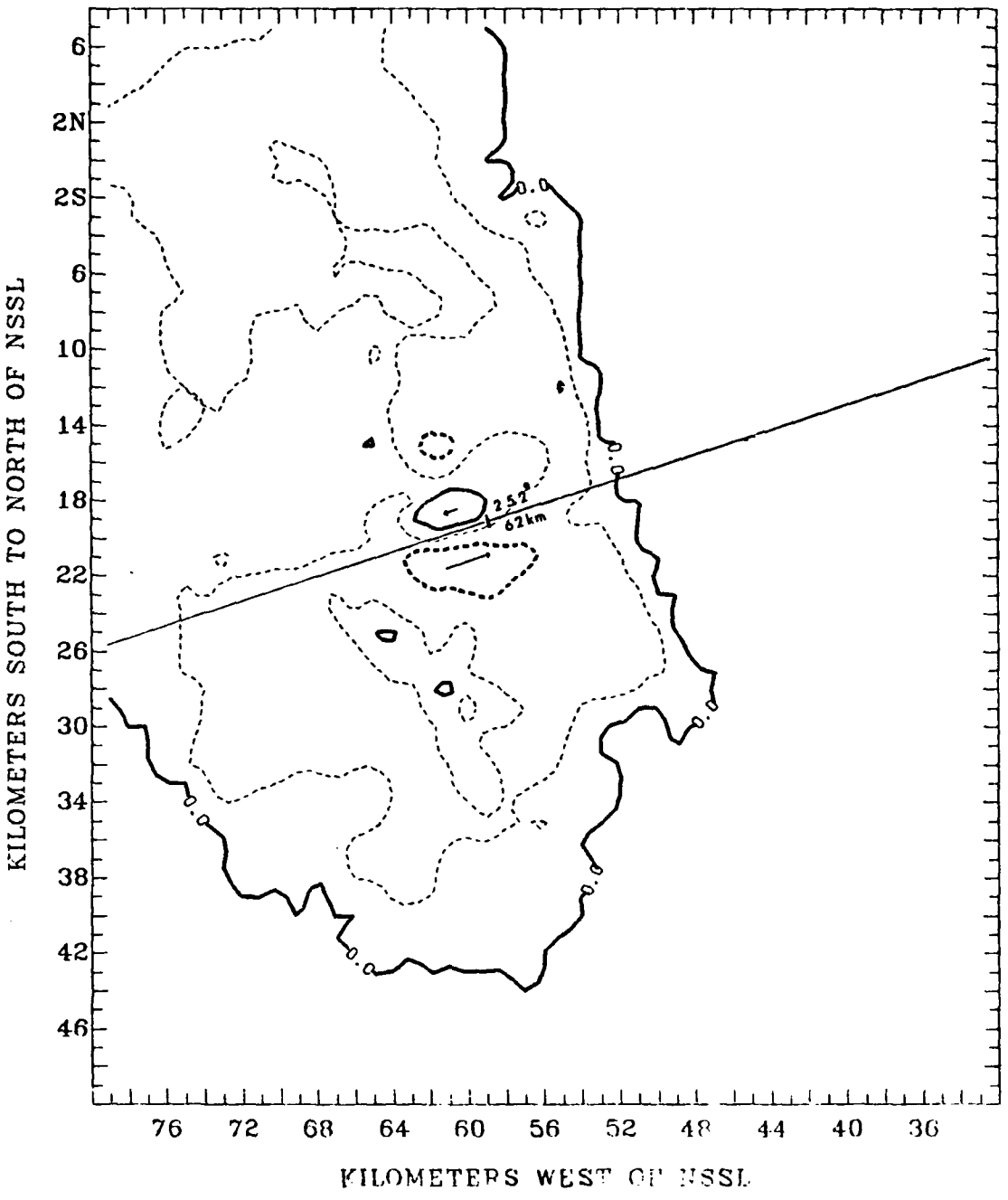

FIG. 23. 5-km CAVM, 1805-1812 CDT, 1 May 1977 (1-km grid), Doppler data.

and vertical grid spacings with 5 m s^{-1} interval isodops were accepted as the 'optimum' scales.

This 1-km horizontal grid also resulted in much more detailed CAZM analyses. The 1-km CAZM, Fig. 24 compared to Fig. 4, indicates a maximum core of 55 dBZ and a sharp indentation of the 45-dBZ isopleth just north of the future mesocyclone location. This WER is directly under the area of convergence noted in Figs. 19 and 20. This also was indicated on the 2-km CAZM but was not as sharp. The 3-km CAZM indicates this WER as filling still more while the 55-dBZ core is larger with an eastward growth. At this time a WER is seen to the northeast of the core (Fig. 25). At 4 km, the southern WER has disappeared and the region northeast of the core is persistent (Fig. 26). Even with greater detail, it is difficult to forecast where the maximum activity will develop while using only the reflectivity values. Then, at the time of mesocyclone detection, the 55-dBZ core on the 1-km CAZM is located with its southern edge at the mesocyclone location (Fig. 27). The 45-dBZ isopleth has split. While the southern cell is stacked vertically, the northern core tilts rapidly eastward (Fig. 28) and disappears at 5 km. The 55-dBZ core increases in size with height and elongates, thereby indicating a westward tilt with height (Fig. 29).

In this case the mesocyclone never reached the surface, and no tornadoes were reported. Why some mesocyclones propagate to the surface while others remain aloft is still a major question that must be studied. A much more detailed analysis was evident with

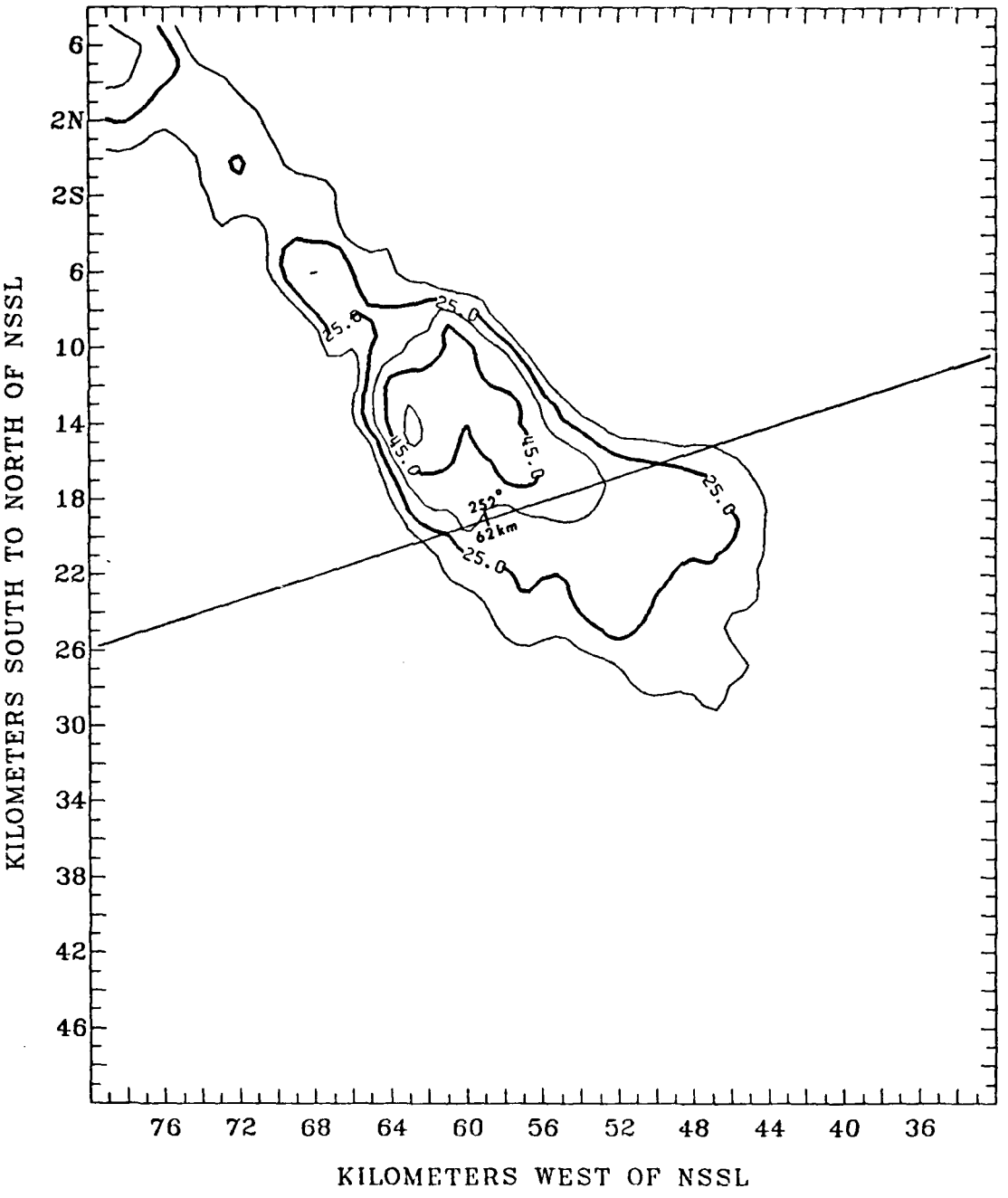

FIG. 24. 1-km CAZM, 1742-1746 CDT, 1 May 1977 (1-km grid), Doppler data.

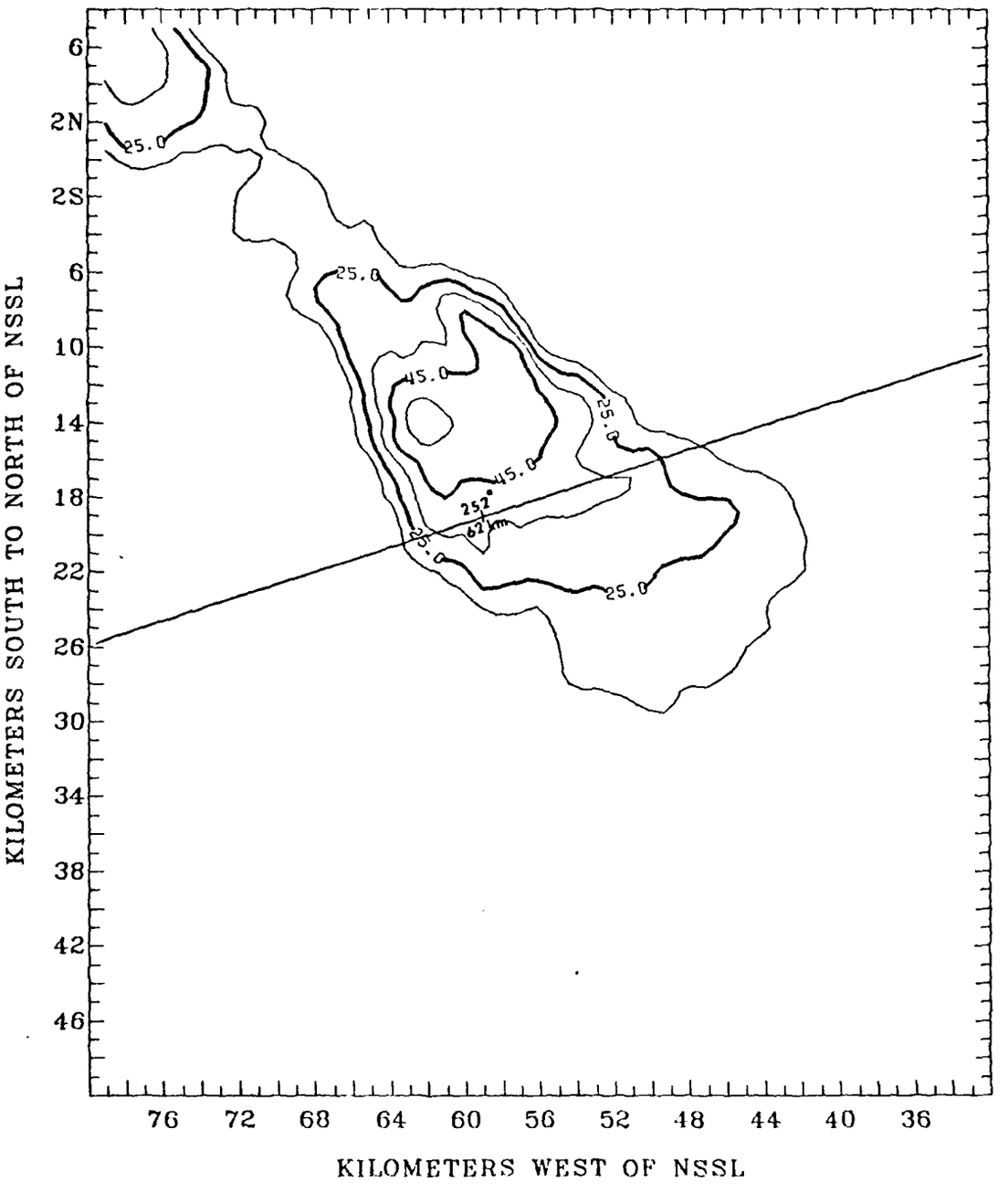

FIG. 25. 3-km CAZM, 1742-1746 CDT, 1 May 1977 (1-km grid), Doppler data.

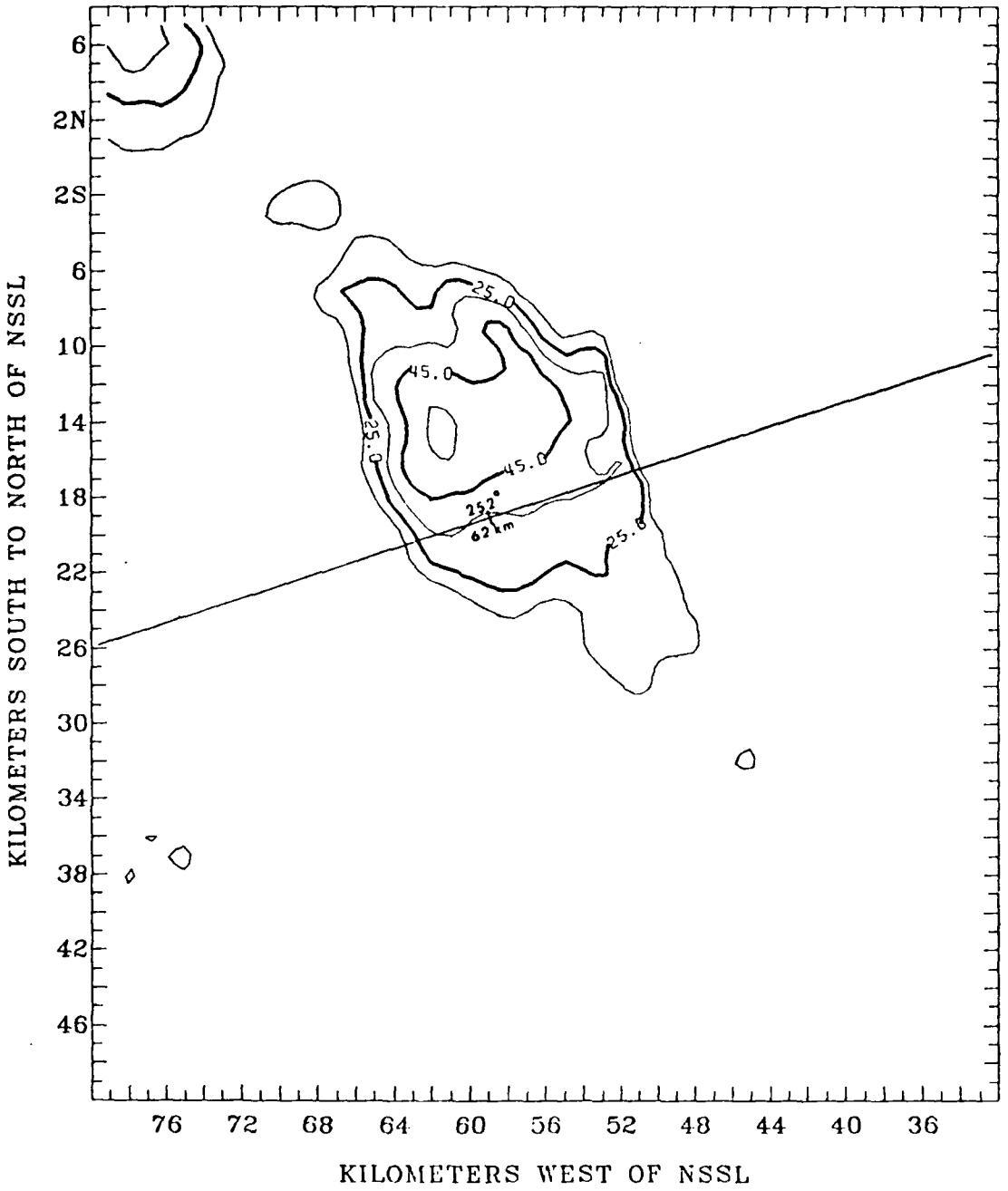

FIG. 26. 4-km CAZM, 1974-1976 CDT, 1 May 1977 (1-km grid), Doppler data.

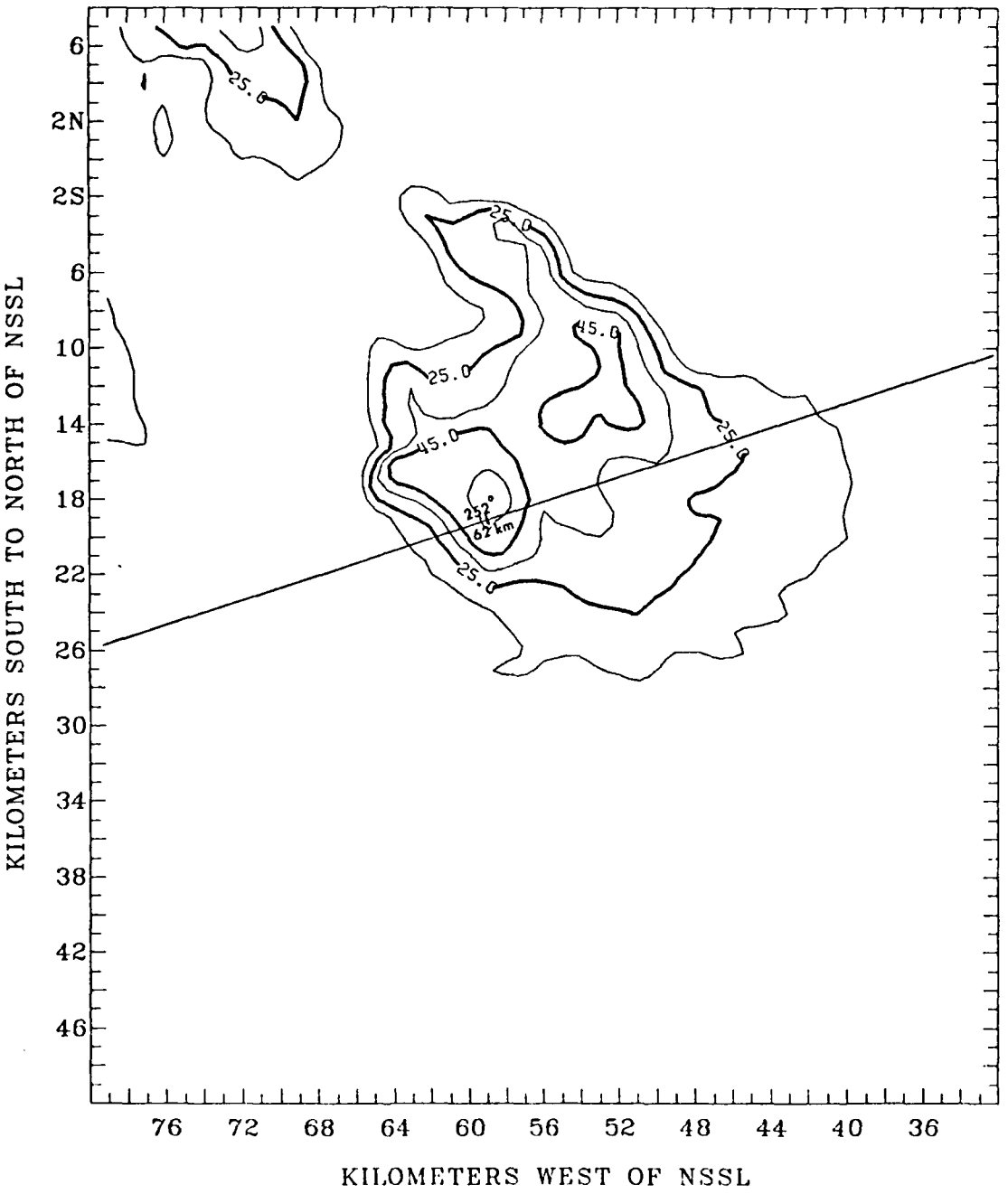

FIG. 27. 1-km CAZM, 1805-1812 CDT, 1 May 1977 (1-km grid), Doppler data.

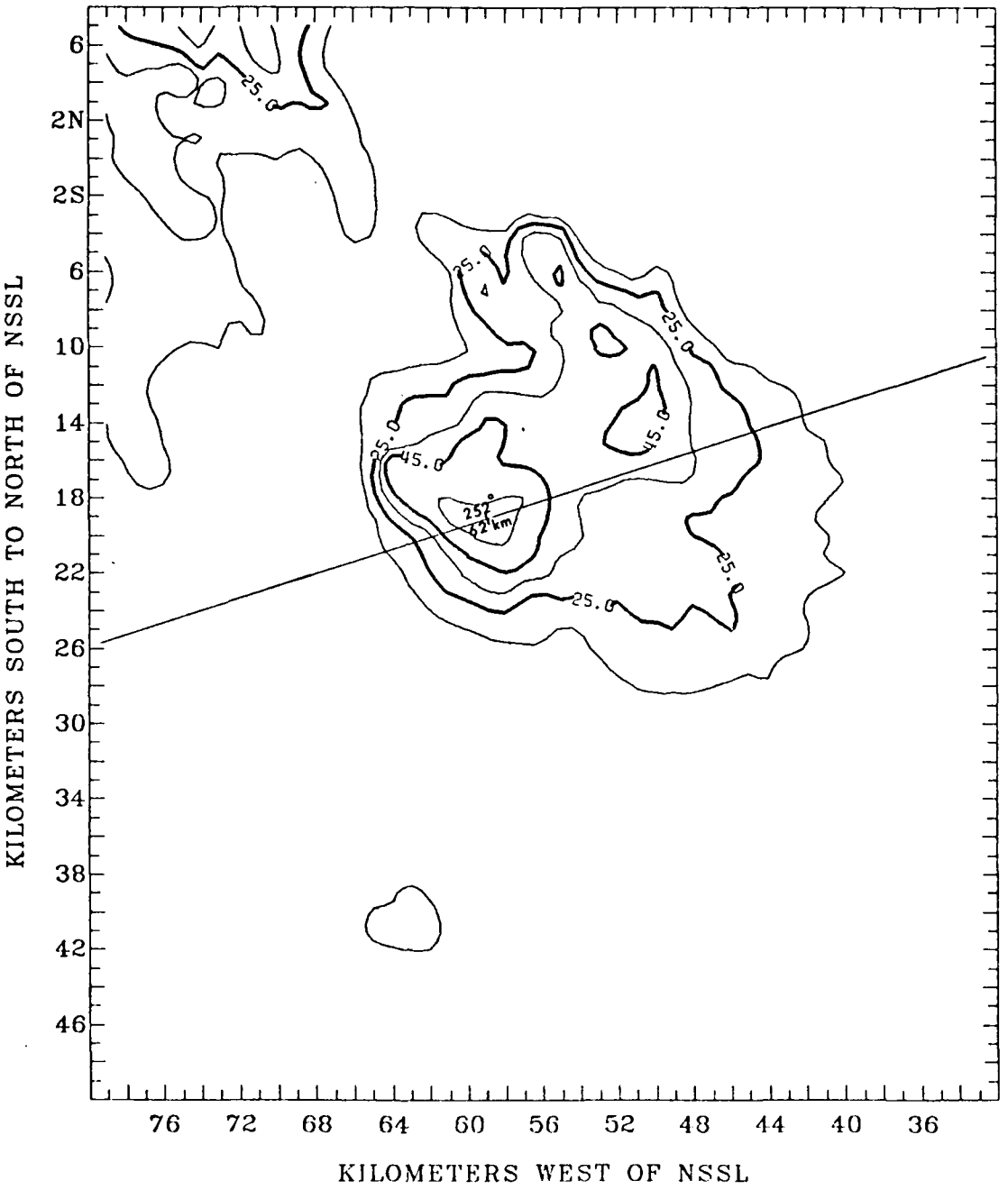

FIG. 28. 3-km CAZM, 1805-1812 CDT, 1 May 1977 (1-km grid), Doppler data.

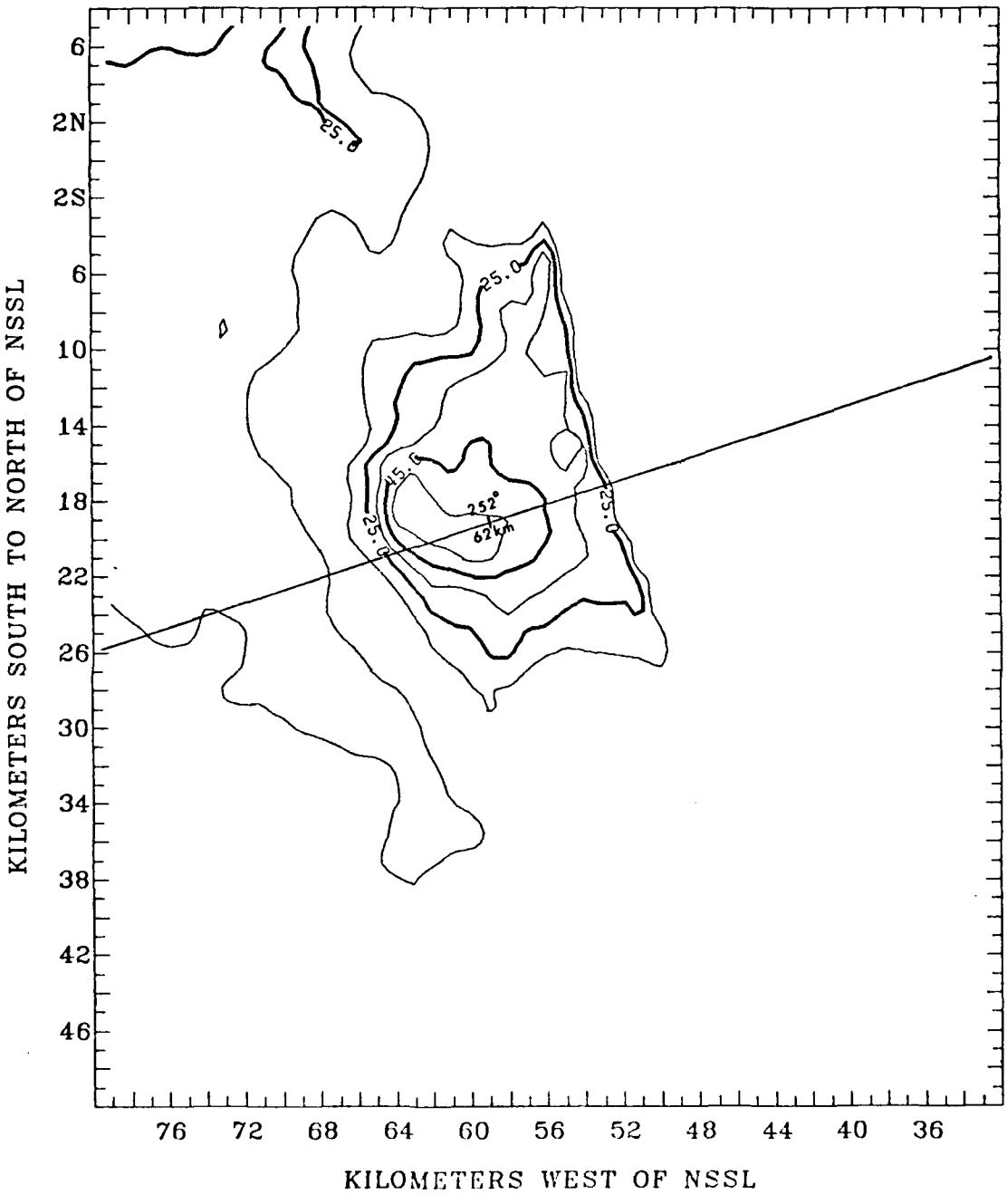

FIG. 29. 5-km CAZM, 1805-1812 CDT, 1 May 1977 (1-km grid), Doppler data.

the 1-km scale, thus indicating many features that were not readily evident on the 2-km scale, yet still covering a sufficiently large area of 49 km by 59 km. Likewise CAVM analyses seem to indicate probable areas of severe weather much more readily than CAZM analyses.

b. May 20, 1977 Mesocyclone

Since the 1-km horizontal and vertical scales were found to be 'optimum' for the May 1, 1977, mesocyclone, these scales were used for the May 20, 1977, analysis. As in the previous figures, isopleths of reflectivity begin at 15 dBZ with 10-dBZ increments, and isodops are processed at 5 m s^{-1} intervals. The line indicates the azimuth and distance of the mesocyclone (252° at 95 km). The earliest data processed were obtained from 1627 CDT until 1631 CDT. During this time period data were collected beginning with the 3.9° tilt angle, thus restricting the lowest possible map level to 7 km, with data processed out to only 95 km (Fig. 30). Therefore, the 0-m s^{-1} isodop of Fig. 30 is not the back edge of the storm but only the edge of available data for the 7-km CAVM. CAVM's were analyzed up to 12 km, and they all indicated strong negative component flow with no hint of any cyclonic rotation. It is felt that, at these heights, the upper-level winds dominate the flow pattern and that any mesocyclone formation features would have been indicated at lower levels. In addition, CAZM analysis indicated no significant severe weather features at these heights. It was suspected that a WER or BWER would be detected. However, none was

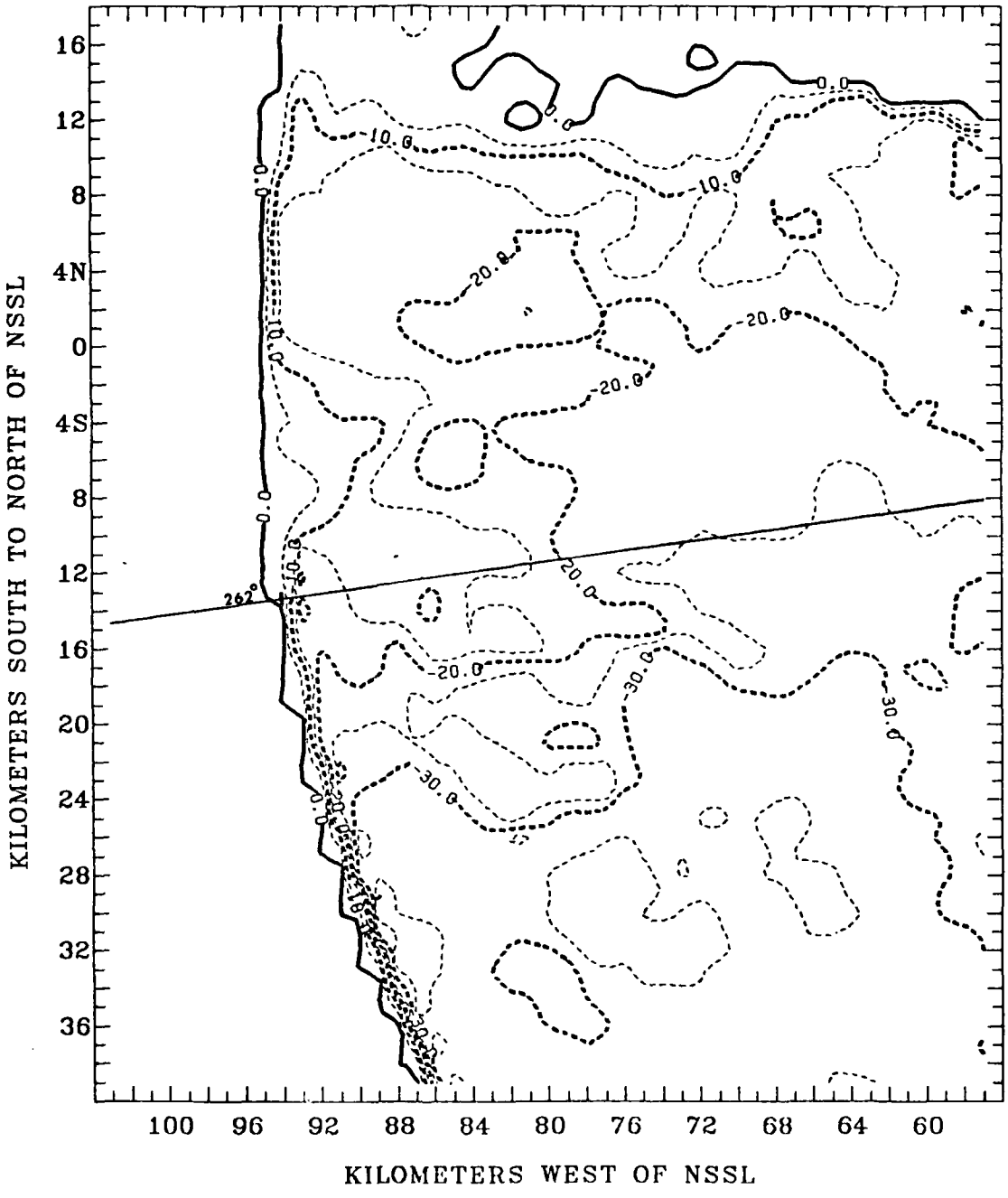

FIG. 30. 7-km CAVM, 1627-1631 CDT, 20 May 1977 (1-km grid), Doppler data.

found. Figure 31 represents the typical type of reflectivity analysis for this time period. The 45-dBZ core was stacked from 8 km through 11 km as the strongest area of reflectivity.

One of the best sequences of data was collected between 1634 CDT and 1640 CDT, when tilt angles were recorded from 0.2° through 10.8° at approximately 0.5° increments. The analyses for this time sequence consist of maps from 1- to 11-km heights. A very broad area of cyclonic circulation is indicated from 1- to 5-km heights (Figs. 32 to 33) with suspected cyclonic flow up to 7-km (Fig. 34). By 8 km the upper-level winds again dominate and no 0-m s^{-1} isodop or positive isodops are indicated. This tends to support the analysis of the earlier series of data from which it was inferred that the upper-level winds dominated the 7- to 12-km CAVM's. The reflectivity analyses show the 45-dBZ area to have propagated well northward, and on the 2-km CAZM there is a suspicious appendage to the 45-dBZ isopleth (Fig. 35). On the 3-km CAZM, a small 55-dBZ core was found 5 km northwest of the future mesocyclone point. This 55-dBZ core was found to expand and extend vertically to the 5-km CAZM (Fig. 36). Then at 7 km (Fig. 37), the 45-dBZ core splits and extends through the 11-km CAZM, while decreasing in size with height (Fig. 38). Again, no WER or BWER was obvious.

Finally, during the reported mesocyclone sequence, data were collected between 1640 CDT and 1643 CDT from 0.2° through 5.8° tilt angles. The previously-noted cyclonic rotation area decreased drastically in size while increasing in intensity. At this point

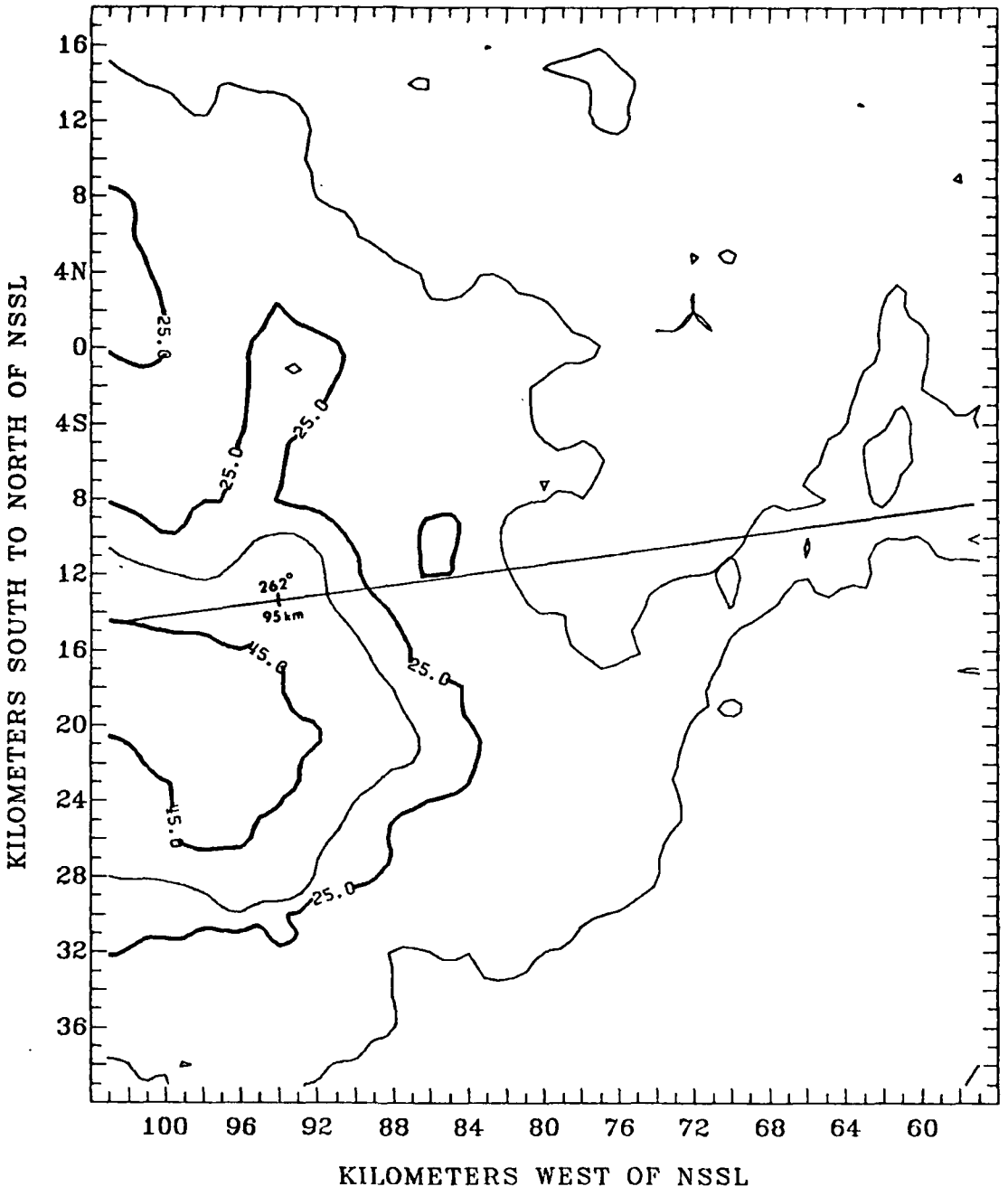

FIG. 31. 10-km CAZM, 1627-1631 CDT, 20 May 1977 (1-km grid), Doppler data.

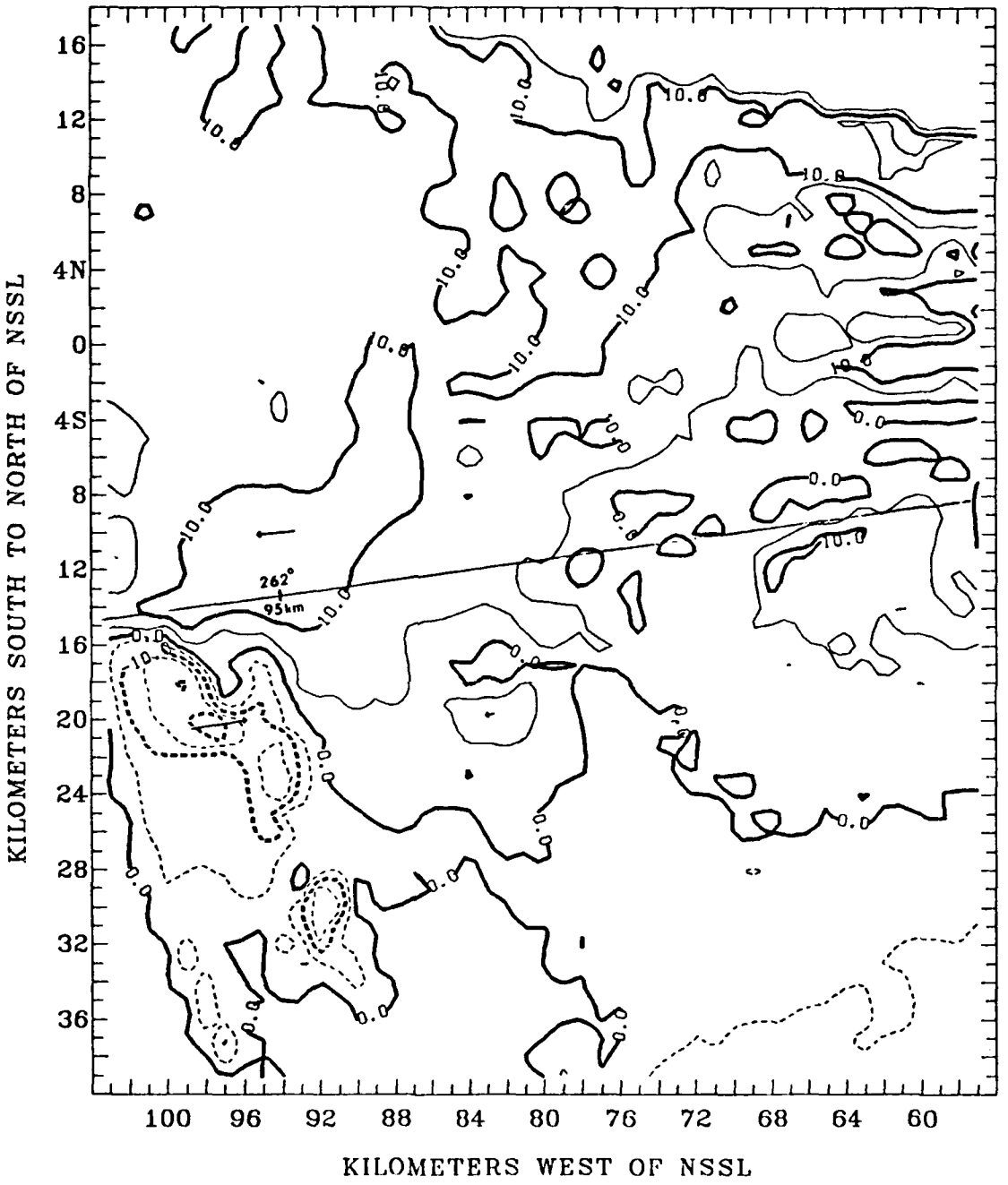

FIG. 32. 1-km CAVM, 1634-1640 CDT, 20 May 1977 (1-km grid), Doppler data.

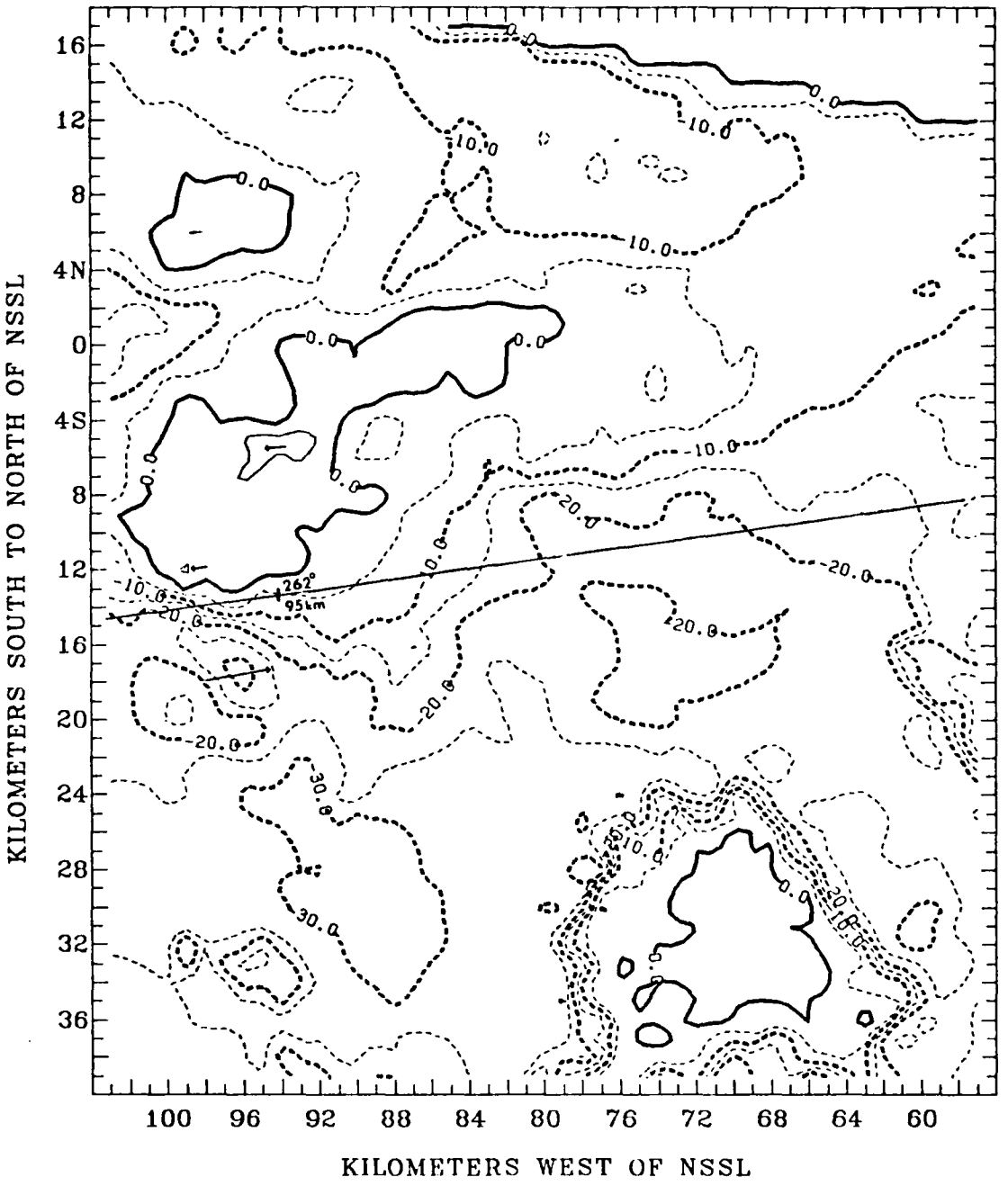

FIG. 33. 5-km CAVM, 1634-1640 CDT, 20 May 1977 (1-km grid), Doppler data.

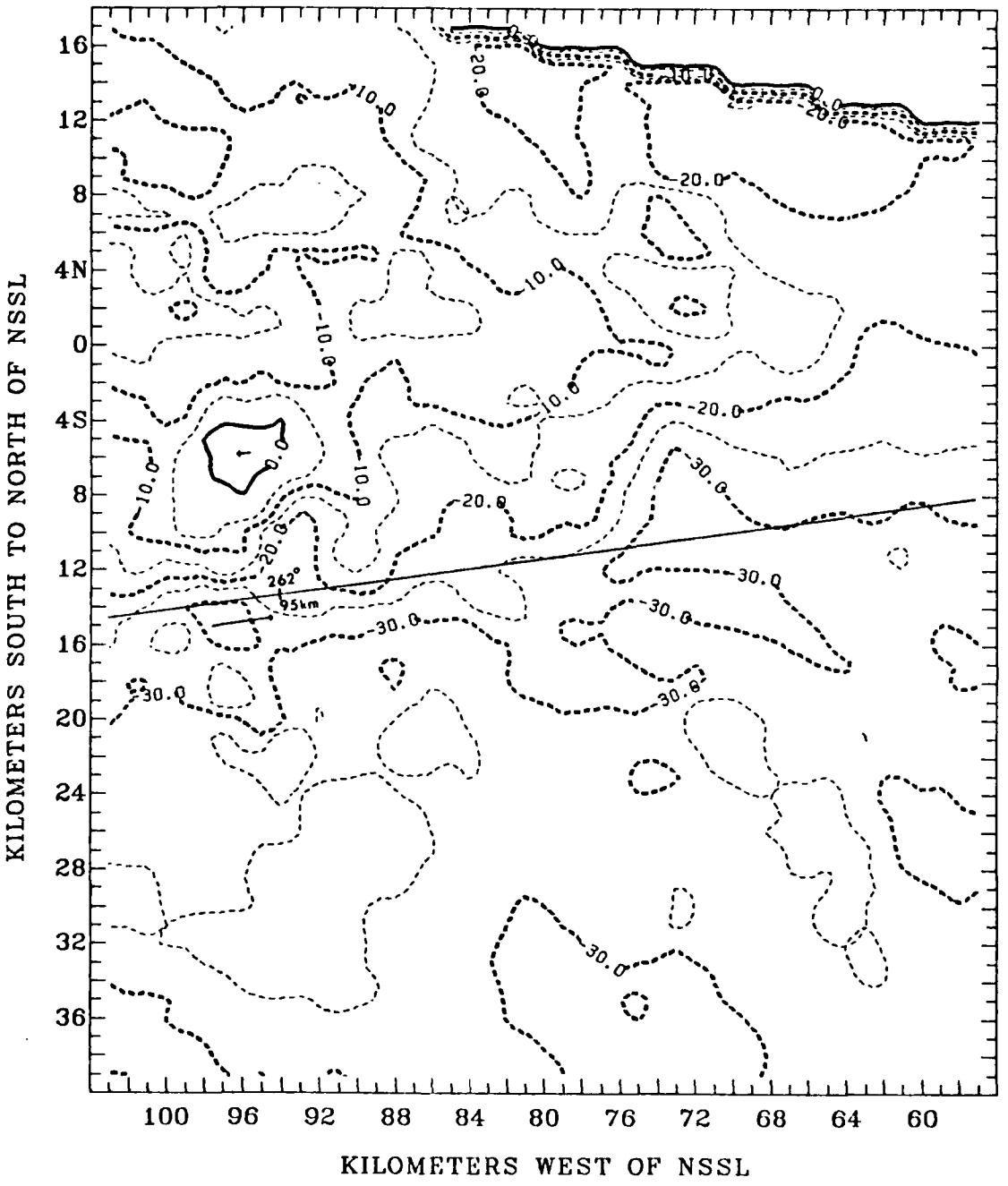

FIG. 34. 7-km CAVM, 1634-1640 CDT, 20 May 1977 (1-km grid), Doppler data.

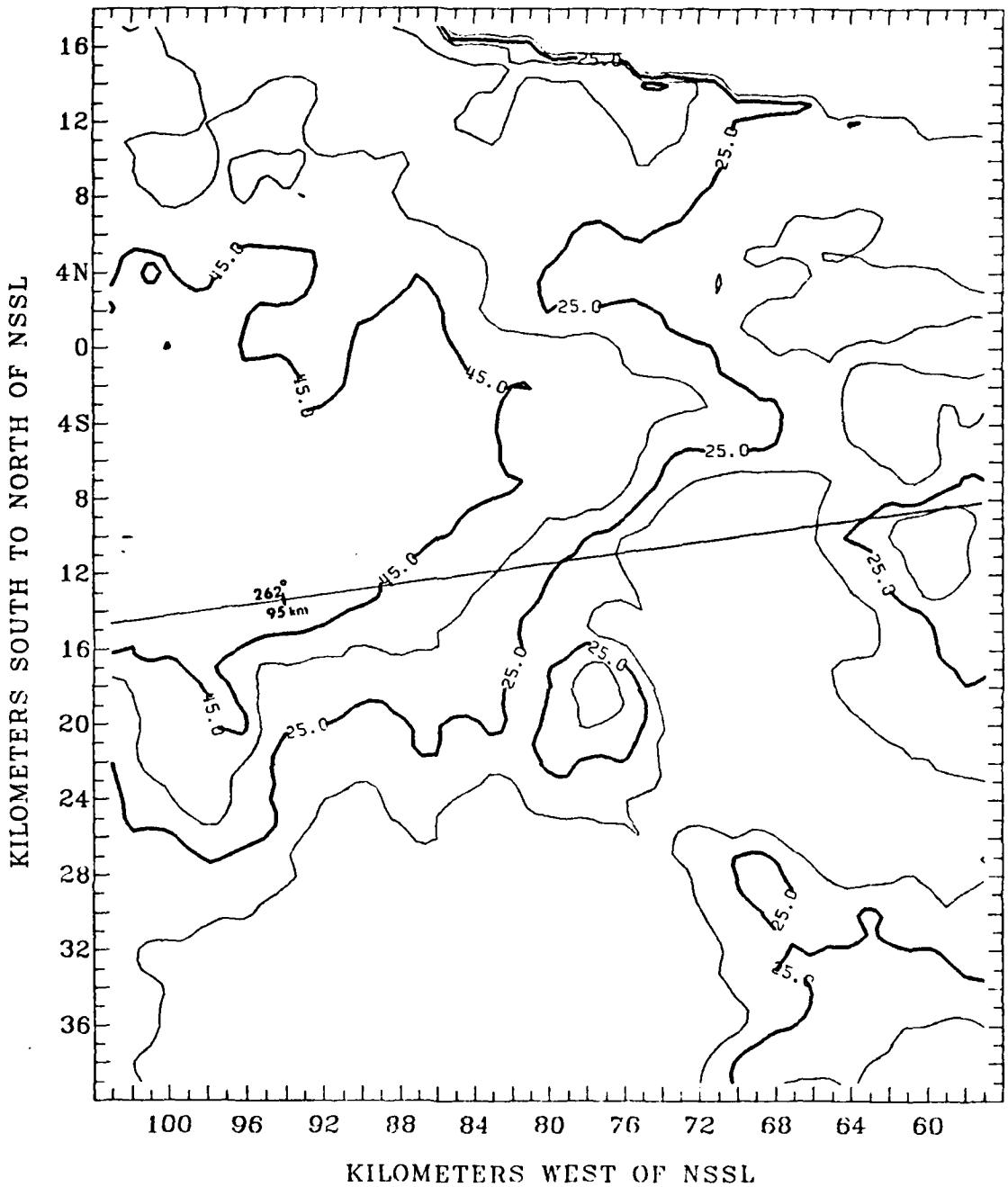

FIG. 35. 2-km CAZM, 1634-1640 CDT, 20 May 1977 (1-km grid), Doppler data.

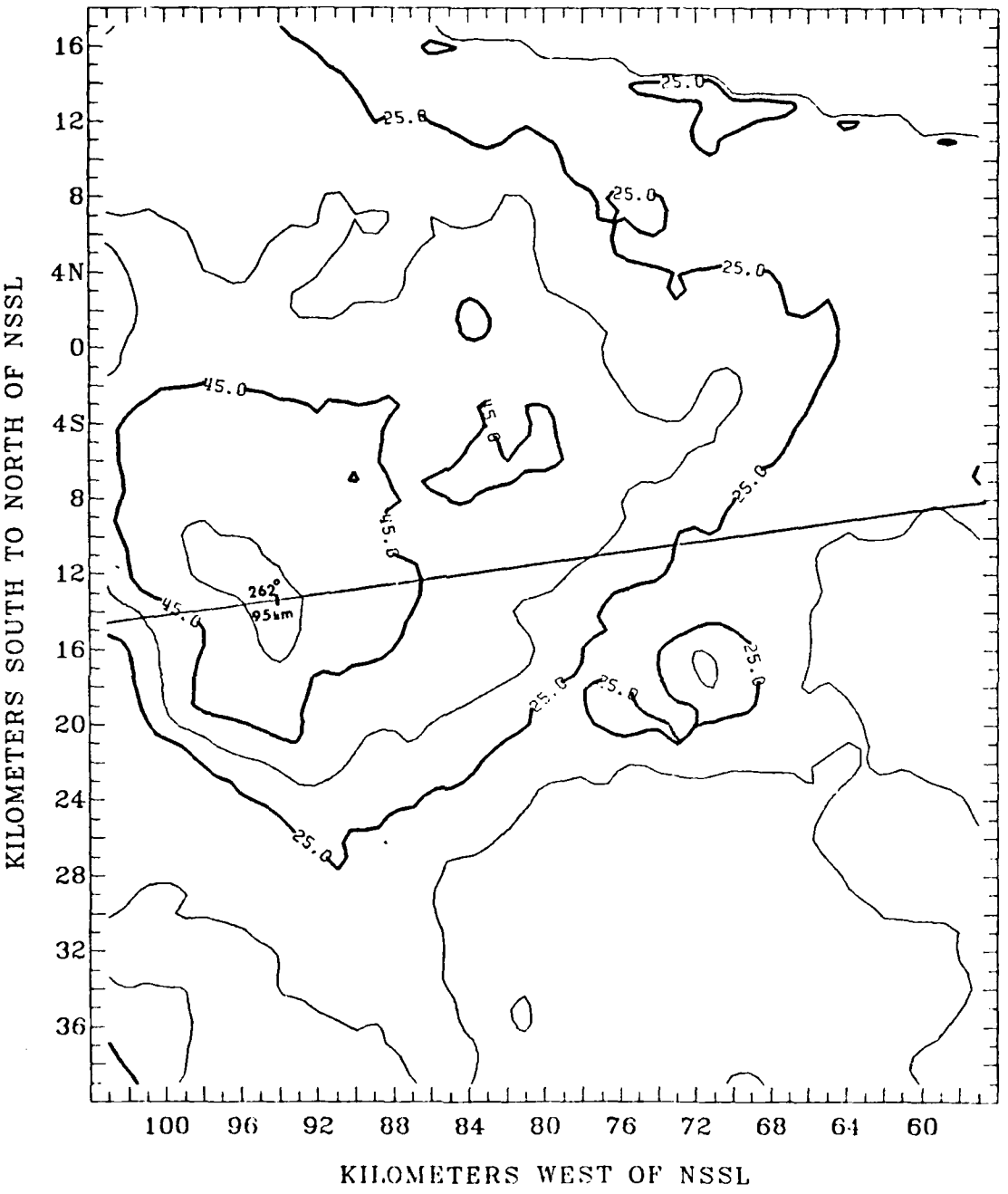

FIG. 36. 5-km CAZM, 1634-1640 CDT, 20 May 1977 (1-km grid), Doppler data.

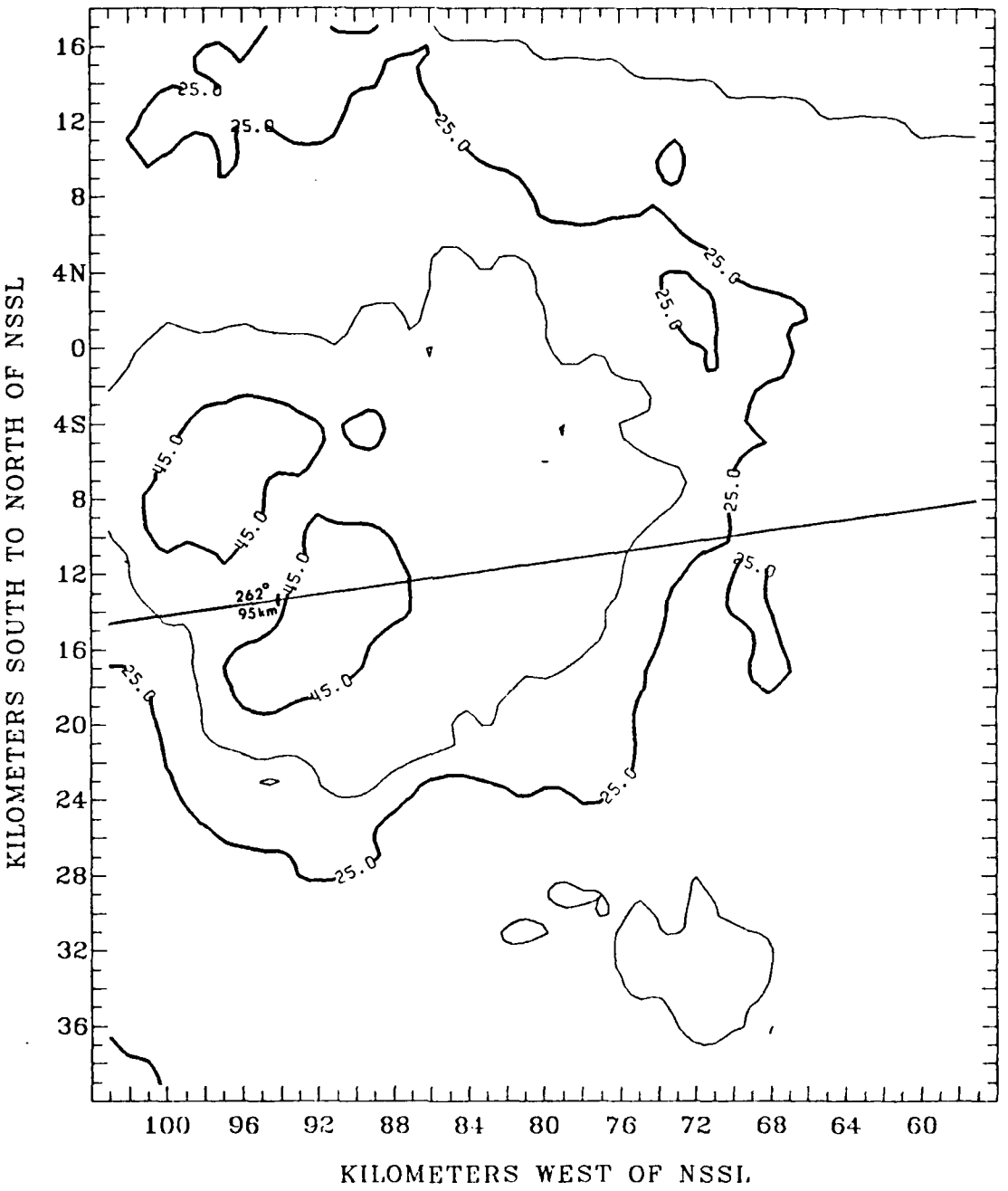

FIG. 37. 7-km CAZM, 1634-1640 CDT, 20 May 1977 (1-km grid), Doppler data.

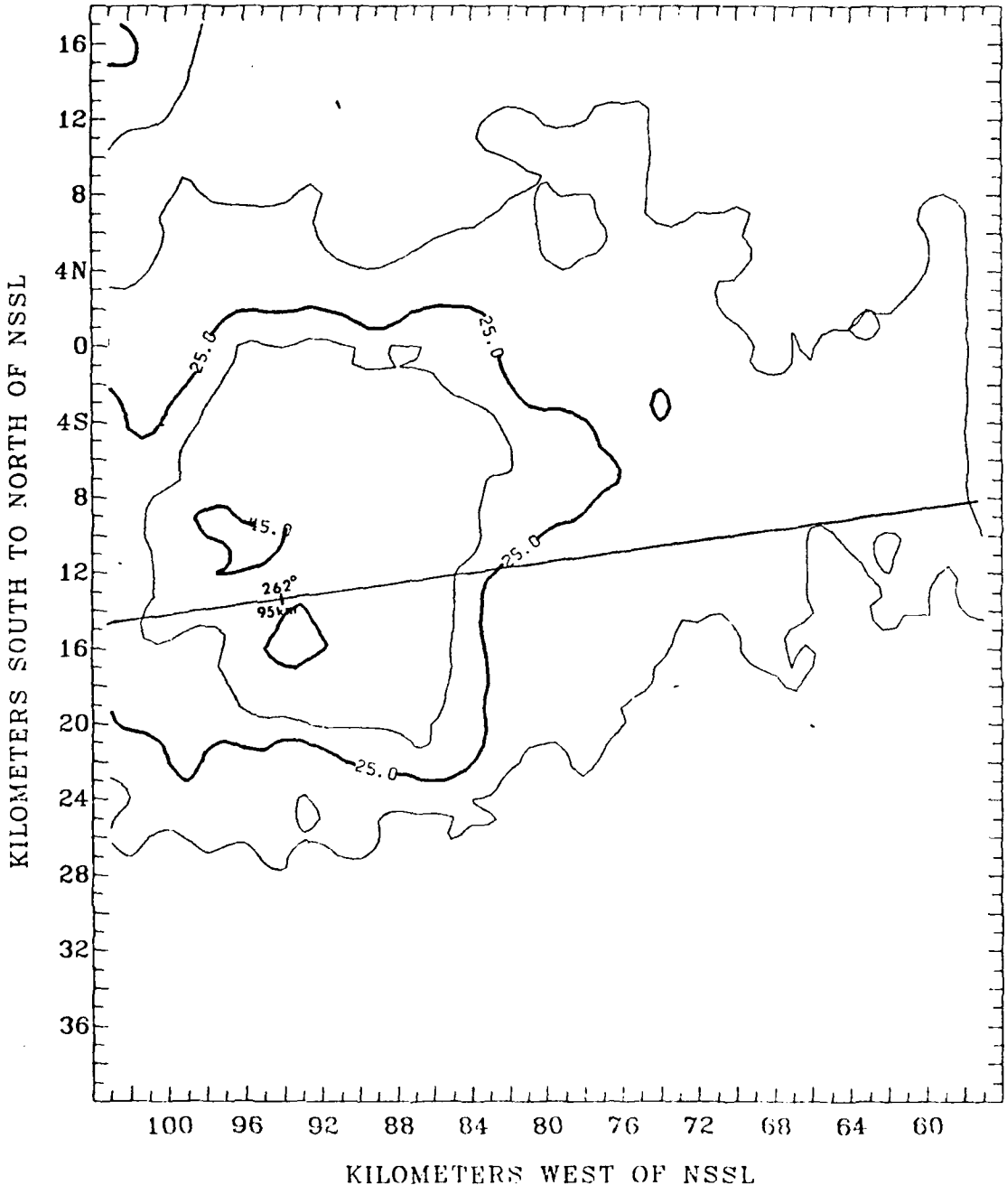

FIG. 38. 11-km CAZM, 1634-1640 CDT, 20 May 1977 (1-km grid), Doppler data.

the mesocyclone is detected. Strong cyclonic shear is indicated from 1 through 3 km with radial velocities changing as much as 40 m s^{-1} along a 1-km distance normal to the radar beam on the 1-km CAVM (Fig. 39). Donaldson et al. (1975) found that 20 m s^{-1} shear over a 1-km distance normal to the radar beam proved to be an excellent indicator for identifying severe storms. Figures 39 and 40 show the tornado vortex signature (TVS) tilted to the south at 2 km, while adding Fig. 41 shows a rapid curvature back to the north. By the 4- and 5-km CAVM heights, cyclonic rotation has broadened while the tornado still tilts northward (Figs. 42 and 43). Above 6 km, the cyclonic circulation continues to broaden and decrease in intensity with no positive isodops indicated on the 8-km CAVM. The TVS is very obvious in the low levels and readily pinpoints the tornado location. On the other hand, reflectivity data indicated a hook echo (Burgess et al., 1977). This is best identified at the 2-km CAZM as a sharp-pointed appendage of the 45-dBZ isopleth (Fig. 44). The strongest isopleth, 55 dBZ, is located about 7 km north of the TVS and extends through the 5-km CAZM.

Since this storm was so much stronger than the May 1, 1977, mesocyclone, the data also were analyzed on the 2-km grid during the TVS time sequence. Figure 45 shows that the TVS was still very obvious at 2 km; it was just as obvious on the 1- and 3-km CAVM's. Cyclonic rotation was easily detectable through the 5-km CAVM but only a 0-m s^{-1} isodop and suspected rotation was evident at 6 through 8 km. However, the sharp-pointed appendage seen on Fig. 44

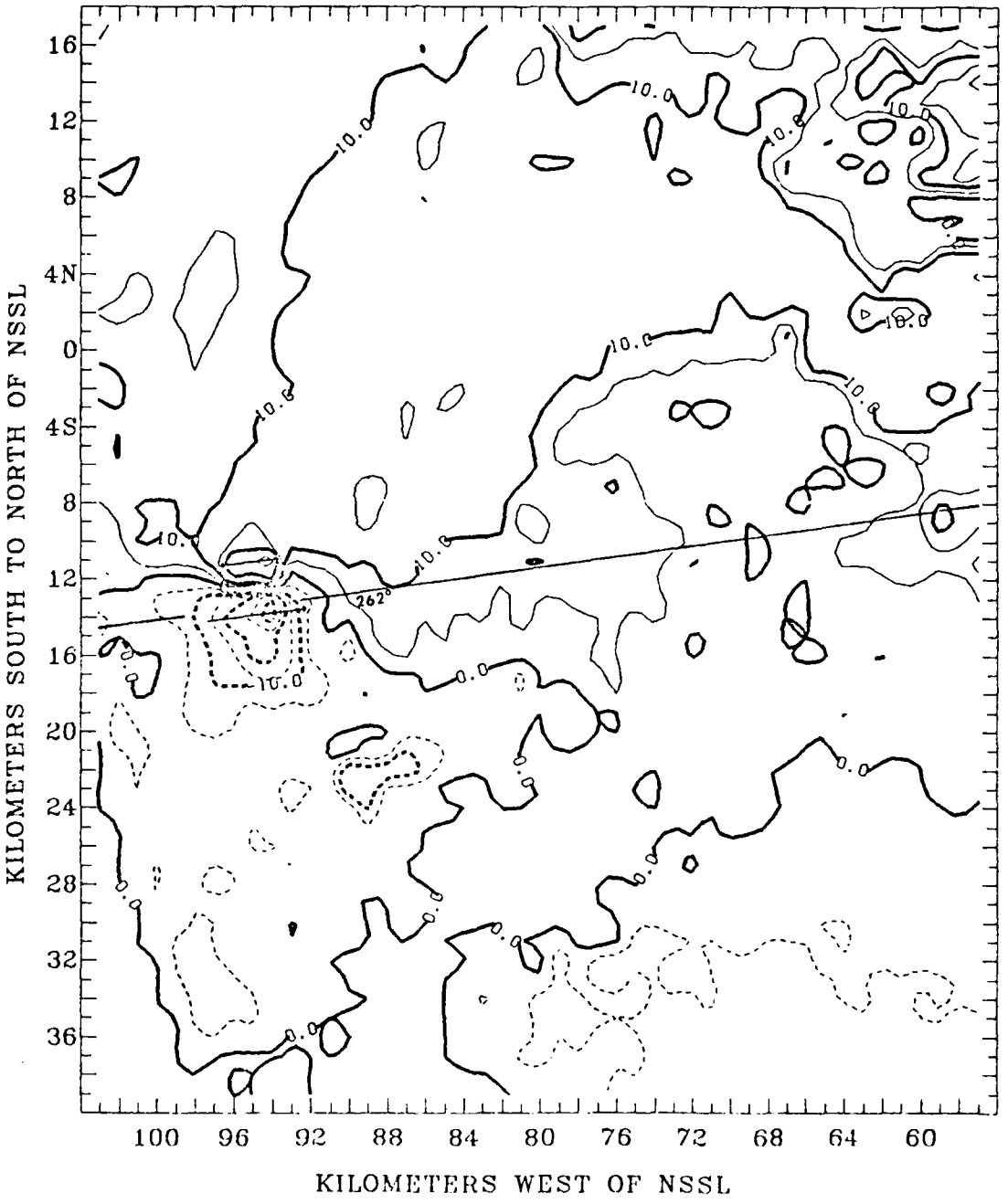

FIG. 39. 1-km CAVM, 1640-1643 CDT, 20 May 1977 (1-km grid), Doppler data.

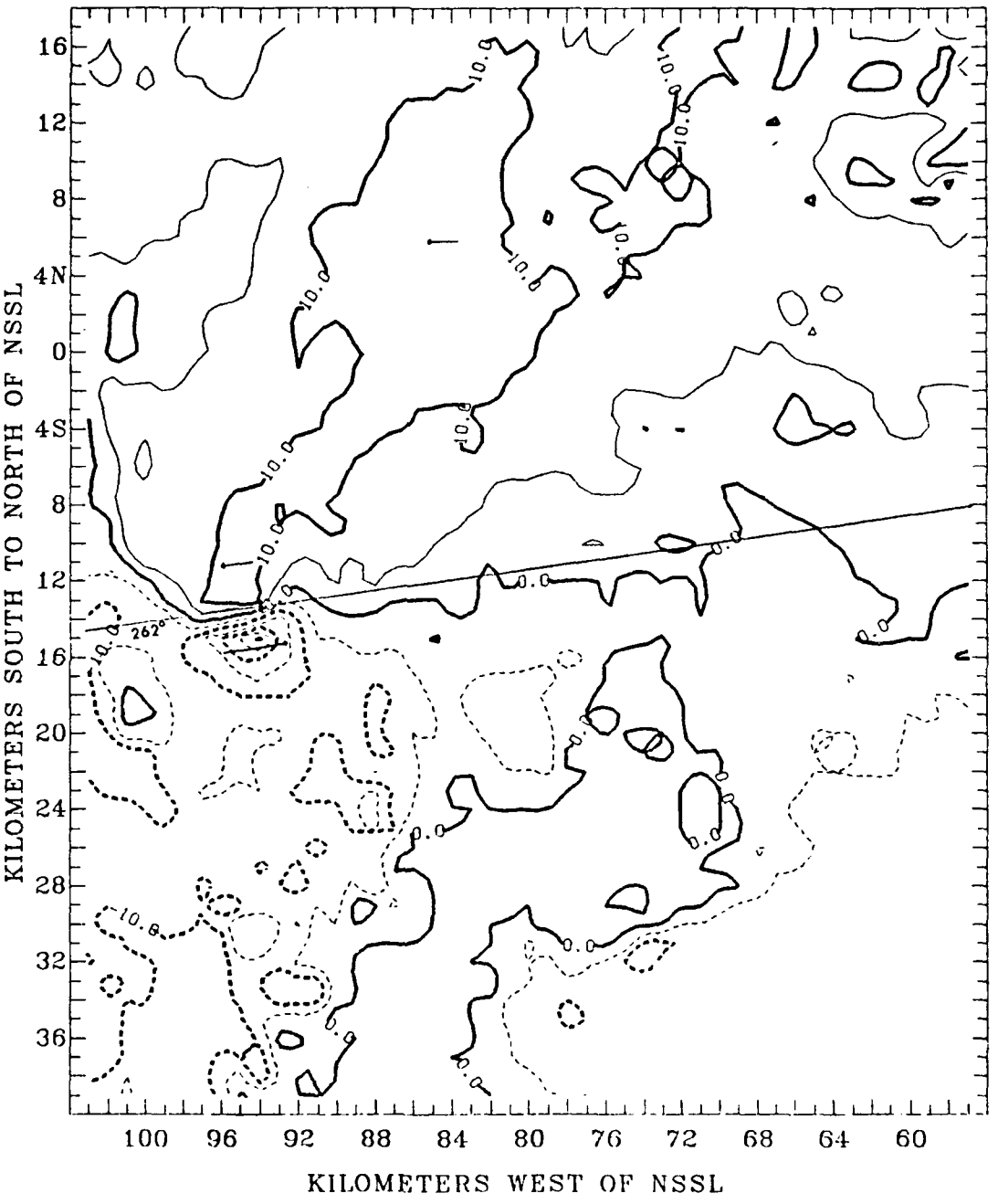

FIG. 40. 2-km CAVM, 1640-1643 CDT, 20 May 1977 (1-km grid), Doppler data.

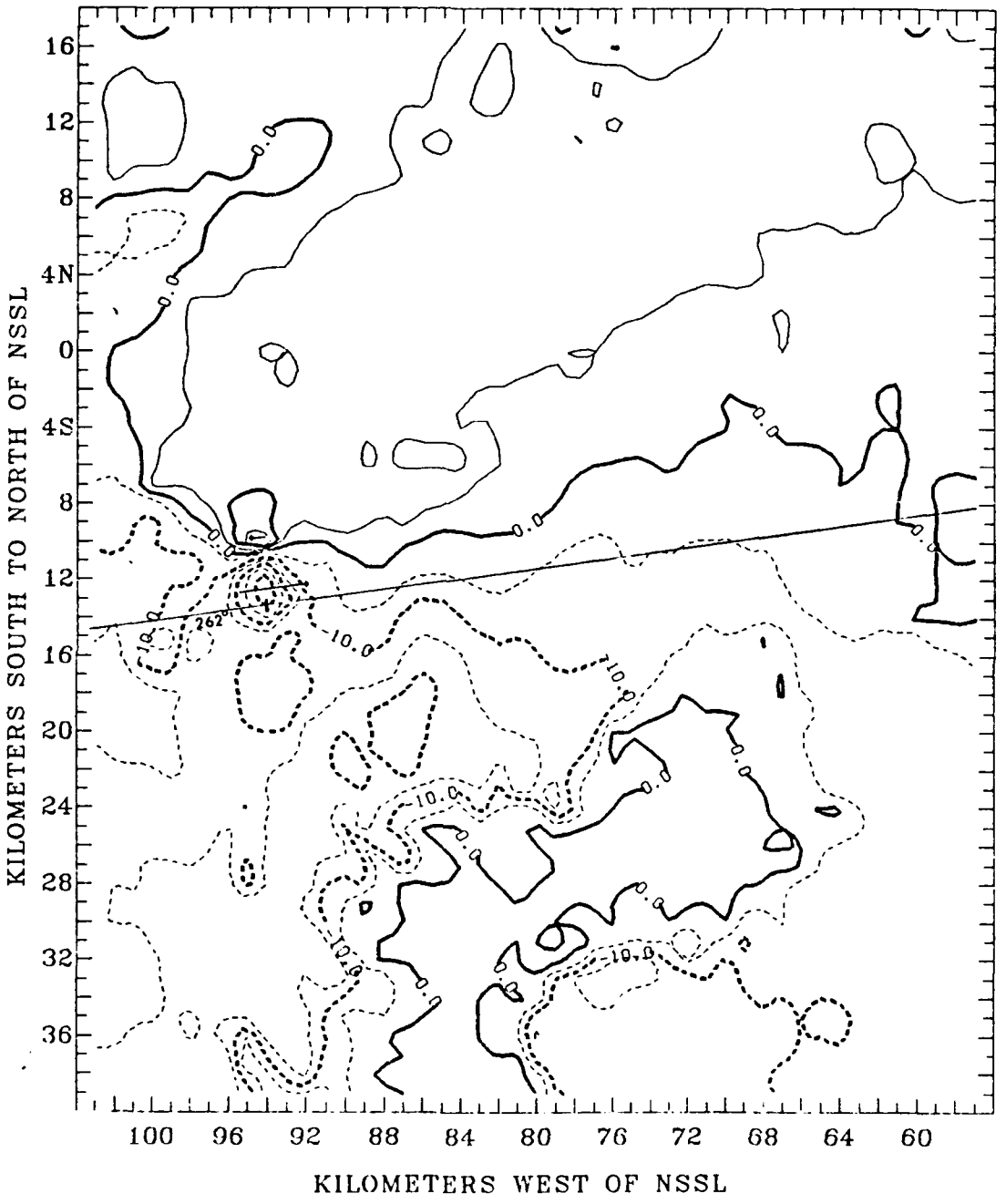

FIG. 41. 3-km CAVM, 1640-1643 CDT, 20 May 1977 (1-km grid), Doppler data.

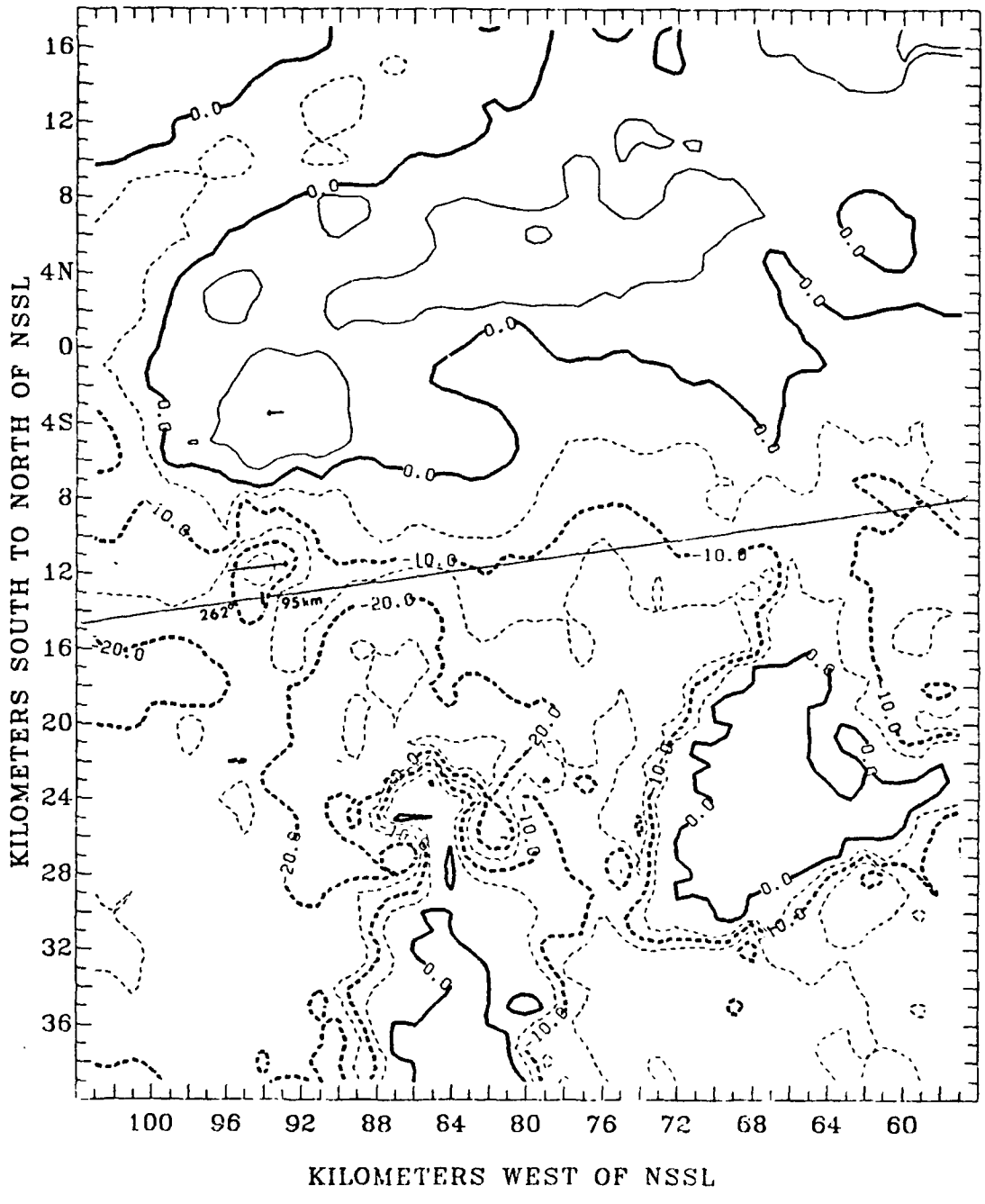

FIG. 42. 4-km CAVM, 1640-1643 CDT, 20 May 1977 (1-km grid), Doppler data.

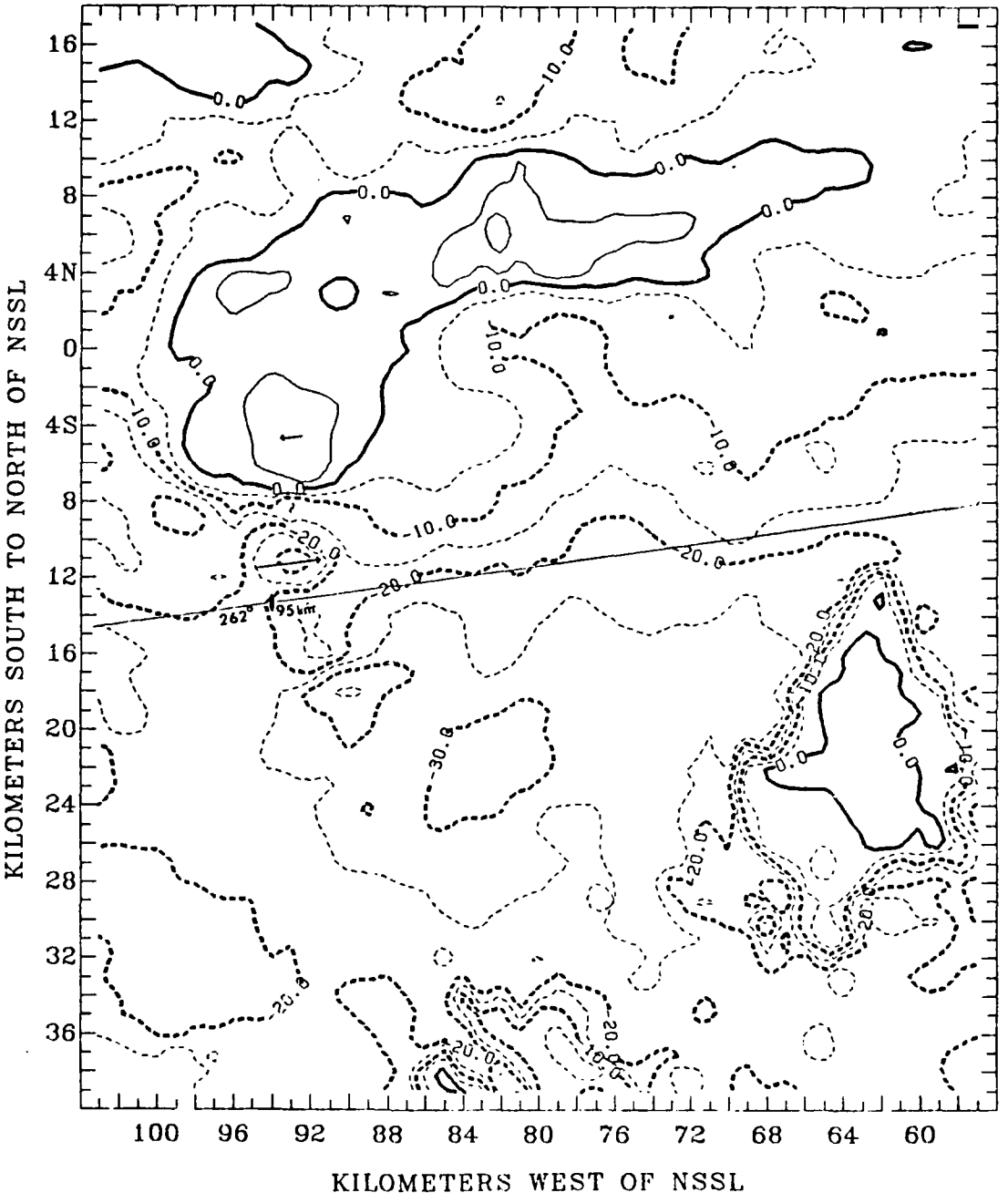

FIG. 43. 5-km CAVM, 1640-1643 CDT, 20 May 1977 (1-km grid), Doppler data.

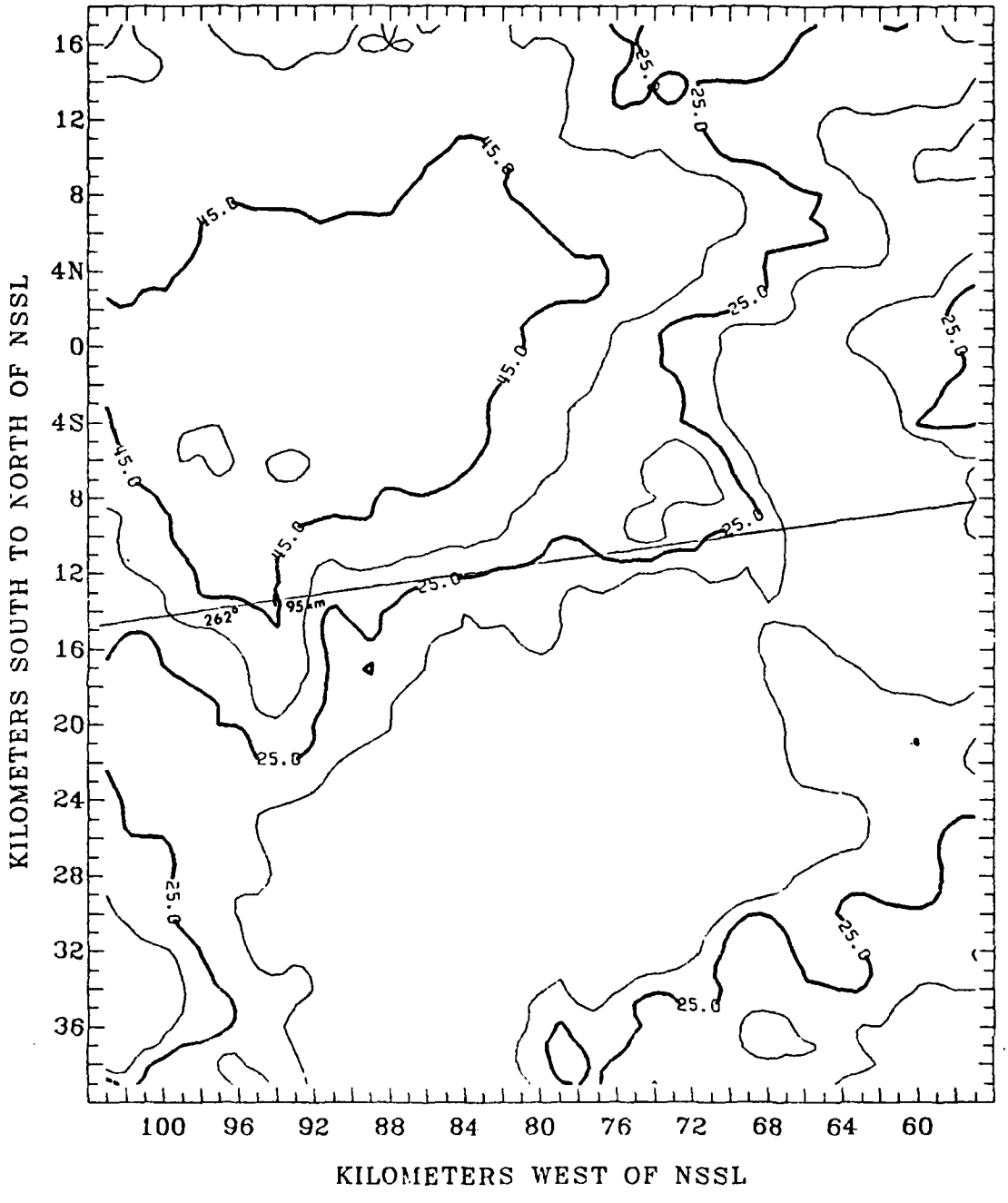

FIG. 44. 2-km CAZM, 1640-1643 CDT, 20 May 1977 (1-km grid), Doppler data.

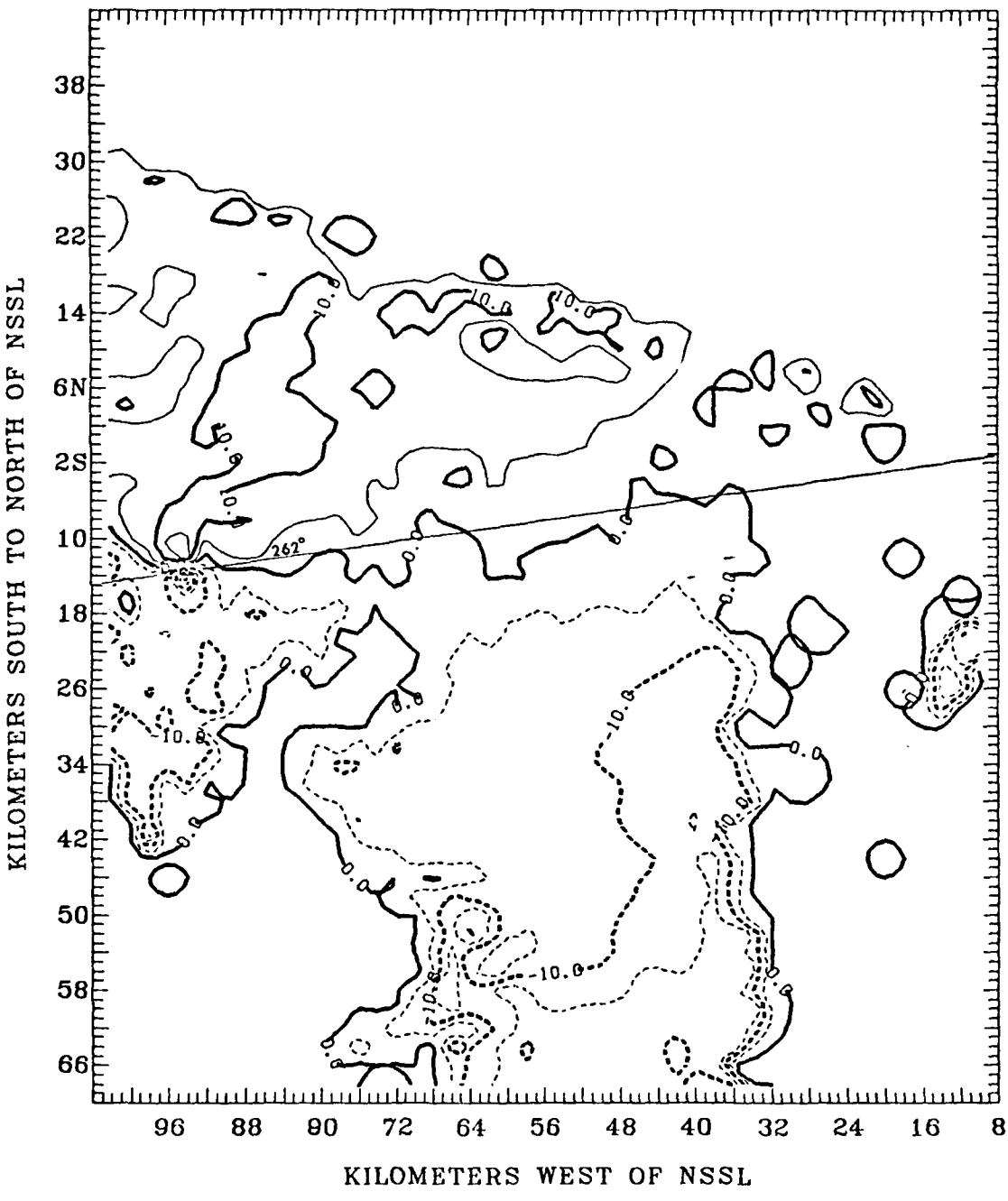

FIG. 45. 2-km CAVM, 1640-1643 CDT, 20 May 1977 (2-km grid), Doppler data.

was not nearly as evident on the 2-km CAZM with a 2-km grid scale (Fig. 46). Again, the radial velocity analysis not only readily identified the location of the severe storm but did so at more altitude levels than did the reflectivity analysis. In addition, although the 1-km grid had better resolution, the TVS was still locatable on the 2-km CAVM grid; however, the sharp reflectivity appendage was not noted on the 2-km CAZM grid.

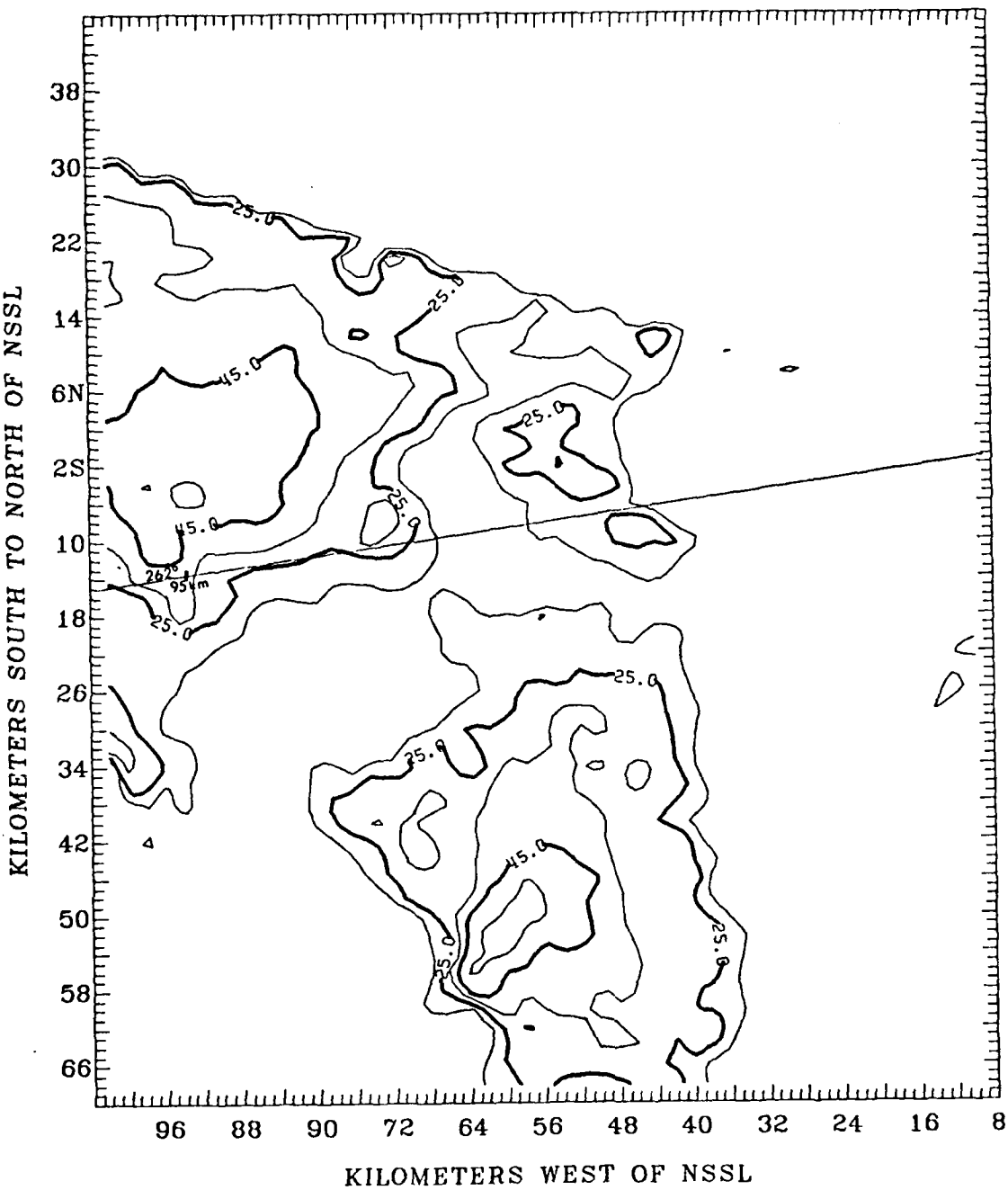

FIG. 46. 2-km CAZM, 1640-1643 CDT, 20 May 1977 (2-km grid), Doppler data.

7. CONCLUSIONS

The objectives of this research were two-fold: The first objective was to determine if it was feasible to detect mesocyclones by using constant-altitude mappings of radial velocities, and if it was feasible then to determine the 'optimum' map scales. The second objective was to compare radial velocity features with simultaneous reflectivity features of at least one severe storm. Actually two severe storms were analyzed and the following conclusions are drawn.

It was determined that mesocyclones, including both weak and tornadic mesocyclones, were, in fact, readily detectable on constant-altitude maps. These constant-altitude velocity maps (CAVM) were constructed by first correcting the folded velocity values, then finding the recorded azimuth closest to its integral value azimuth and using a 450-m radius-of-influence averaging technique along the radial to calculate values for each kilometer point. When all of the radials within the grid box were calculated in this manner for all tilt angles, the data, in spherical coordinates, were converted to cylindrical coordinates at constant heights. Finally, by use of a quadratic linear interpolating scheme (Sieland, 1977), the data in cylindrical coordinates were transferred to rectangualr coordinates and objectively analyzed by the 'Conrec' computer routine. The 'optimum' vertical interval was determined to be 1 km. A 1-km vertical interval was required since by definition a mesocyclone must have a vertical extent comparable to its horizontal diameter,

and, by using a larger increment such as 1.5 km, the vertical structure of cyclonic rotation may not be detectable for small mesocyclones.

Initially a 2-km horizontal grid scale was used and in both cases the cyclonic vortex was identified. This proved that a 2-km horizontal grid scale was adequate for the initial detection of even small mesocyclones. However the 2-km grid scale lacked the detail necessary to study the radial velocity fields. Therefore, both a 450-m and a 1-km scale were tested. While the 450-m scale was very detailed, it lacked sufficient range dimensions. Consequently, a 1-km horizontal scale was selected as 'optimum', thereby giving both detail and sufficient range dimensions, 49 km by 59 km, to locate and study velocity fields in comparison to reflectivity fields.

From a review of both reflectivity and radial velocity analyses, it was found that radial velocities located severe storms much more readily and much earlier than reflectivity analyses. Even on a 1-km CAZM grid, severe storm reflectivity features could neither be readily nor definitively pinpointed, whereas the radial velocity displays left little doubt as to the location of probable severe storms. Likewise CAVM analyses indicated convergence or cyclonic rotation at consecutive heights, while reflectivity analyses were hit-and-miss from one height to the next. Unfortunately, neither of the storms analyzed had enough continuous data from 1-km through at least 10-km heights to reach any conclusions on the relationships

of WER, BWER, etc., to convergence or cyclonic rotational areas.

The final conclusion is that radial velocities can be analyzed from constant-altitude maps, and they in fact do locate severe storms much more quickly and more precisely than constant-altitude reflectivity analyses.

8. RECOMMENDATIONS

The following recommendations are suggested which could be based upon the computer technique used in this study to analyze radial velocity and reflectivity fields from Doppler radar data.

(1) Analyses of several mesocyclones with tilt sequences capable of producing constant altitude maps from at least 1- through 10-km heights should be studied. The study should attempt to relate severe storm reflectivity features with radial velocity features for a better understanding of severe storm structure.

(2) Hail storms should be studied to determine if there are any radial velocity signatures that imply or identify hail storms and not tornadoes.

(3) Numerous cases should be studied where mesocyclones are detected at low-to mid-levels but do not propagate to the surface. This study should attempt to determine why these mesocyclones do not reach the surface.

(4) A comparison should be made between the radial velocity shear at various levels and the resultant intensity of surface wind reports.

(5) Criteria should be established for turbulence forecasts at various levels and areas of extent from CAVM analyses.

(6) Radial velocity fields should be compared with surface precipitation to determine if precipitation rates or amounts are predictable from radial velocities.

The following recommendations involve the development of more sophisticated computer programs while using the technique of this study as a starting point.

(1) Develop a computer program to calculate the maximum tangential velocity of a mesocyclone by using a Rankine combined vortex model.

(2) Develop an advanced computer program capable of locating and tracking mesocyclones, and process mesocyclone CAVM analyses for real time use.

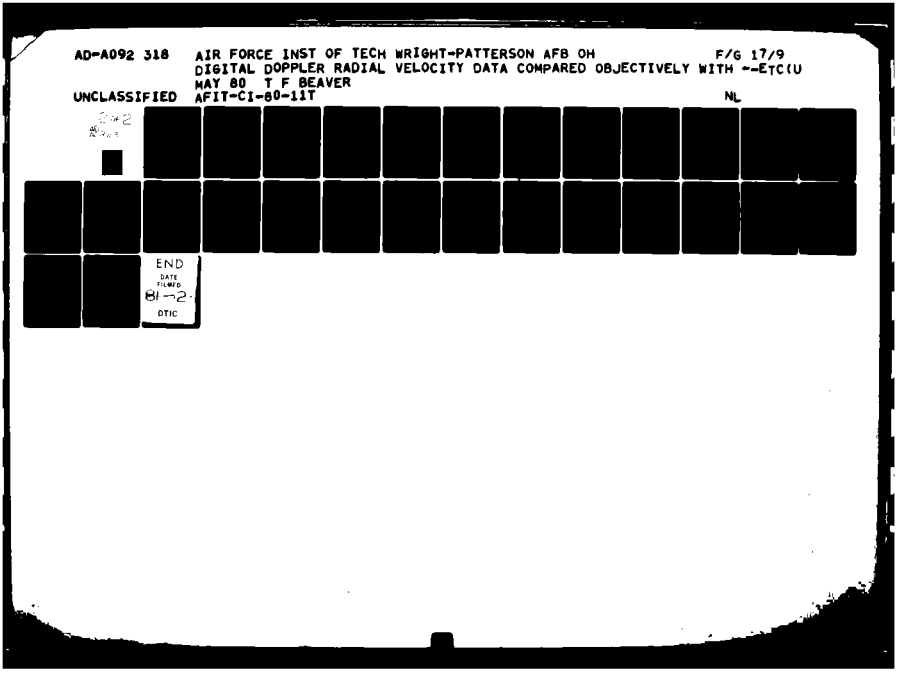
AD-A092 318
AIR FORCE INST OF TECH WRIGHT-PATTERSON AFB OH
F/G 17/9
DIGITAL DOPPLER RADIAL VELOCITY DATA COMPARED OBJECTIVELY WITH --ETC(U
MAY 80 T F BEAVER
UNCLASSIFIED
AFIT-CI-80-11T
NL
END
DATE FILMED
81-2-
DTIC

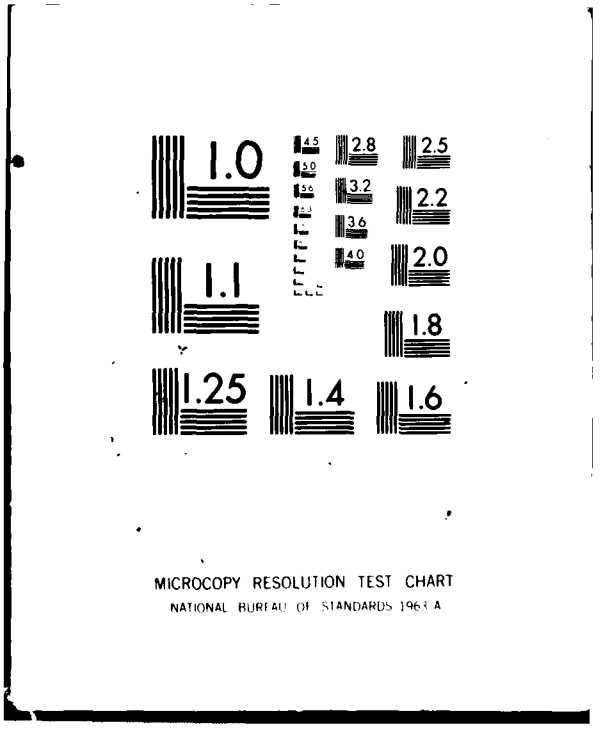

MICROCOPY RESOLUTION TEST CHART
NATIONAL BUREAU OF STANDARDS 1963 A

REFERENCES

Armstrong, G. H., and R. J. Donaldson, Jr., 1969: Plan shear indicator for real-time Doppler radar identification of hazardous storm winds. J. Appl. Meteor., 8, 376-383.

Balsterholt, W. H., 1978: An investigation of radar returns and their relationship to severe weather occurrences. M. S. Thesis, Saint Louis University, 90 pp.

Battan, L. J., 1973: Radar Observation of the Atmosphere, rev. ed. The University of Chicago Press, 324 pp.

Bluestein, H. B., and C. J. Sohl, 1979: Some observations of a splitting severe thunderstorm. Mon. Wea. Rev., 107, 861-873.

Brandes, E. A., 1972: The use of digital radar data in severe storm detection and prediction. Preprints 15th Radar Meteorology Conf., Champaign-Urbana, Amer. Meteor. Soc., 45-48.

Brown, R. A., and L. R. Lemon, 1976: Single Doppler radar vortex recognition: Part II-Tornadic vortex signatures. Preprints 17th Radar Meteorology Conf., Seattle, Amer. Meteor, Soc., 104-109.

Bumgarner, W. C., 1979: Private Communication.

Burgess, D. W., 1976: Single Doppler radar vortex recognition: Part I-Mesocyclone signatures. Preprints 17th Radar Meteorology Conf., Seattle, Amer. Meteor. Soc., 97-103.

———, J. D. Bonewitz, and D. R. Devore, 1977: Operational Doppler experiment: Results year 1. Unpublished report, National Severe Storms Laboratory, NOAA.

_____, L. D. Hennington, R. J. Doviak, and P. S. Ray, 1976: Multimoment Doppler display for severe storm identification. J. Appl. Meteor., 15, 1302-1306.

_____, L. R. Lemon, and R. A. Brown, 1975: Evolution of a tornado signature and parent circulation as revealed by single Doppler radar. Preprints 16th Radar Meteorology Conf., Houston, Amer. Meteor. Soc., 99-106.

_____, K. E. Wilk, J. D. Bonewitz, K. M. Glover, D. W. Holmes, and J. Hinklemen, 1979: Doppler radar--The Joint Doppler Operational Project. Weatherwise, 32, 72-75.

Canipe, Y. J., 1972: Temporal variability in intensity-height profiles of a severe storm using digital radar data. M. S. Thesis, Texas A&M University, 78 pp.

_____, 1973: On the structure and development of severe local storms as revealed by digital radar observations. Ph.D. Dissertation, Texas A&M University, 142 pp.

Donaldson, R. J., Jr., 1970: Vortex signature recognition by a Doppler radar. J. Appl. Meteor., 9, 661-670.

_____, 1975: History of a tornado vortex traced by plan shear indicator. Preprints 16th Radar Meteorology Conf., Houston, Amer. Meteor. Soc., 80-82.

_____, R. M. Dyer, and M. J. Kraus, 1975a: Operational benefits of meteorological Doppler radar. AFCRL-TR-75-0103, Hanscom Air Force Base, MA, 26 pp.

_____, _____, and _____, 1975b: An objective evaluator of techniques for predicting severe weather events. Preprints Ninth Conf., Severe Local Storms, Norman, Amer. Meteor. Soc., 321-326.

Elvander, R. C., 1975: The relationship between digital weather radar data and reported severe weather occurrences. Preprints 16th Radar Meteorology Conf., Houston, Amer. Meteor. Soc., 333-336.

Greene, D. R., 1971: Numerical techniques for the analysis of digital radar data with applications to meteorology and hydrology. Ph.D. Dissertation, Texas A&M University, 124 pp.

Howell, D. E., 1979-1980: Private Communication.

Knight, K. S., 1979-1980: Private Communication.

Kraus, M. J., 1973: Doppler radar investigation of flow patterns within severe thunderstorms. AFCRL-TR-73-0153, L. G. Hanscom Field, MA, 11 pp.

Lemon, L. R., 1977: New severe thunderstorm radar identification techniques and warning criteria: A preliminary report. Tech. Rept. 77-271, Air Weather Service, USAF, 60 pp.

_____, and C. A. Doswell, III, 1979: Mesocyclone and severe thunderstorm structure: A revised model. Preprints 11th Conf. on Severe Local Storms, Boston, Amer. Meteor. Soc., 458-463.

_____, R. J. Donaldson, Jr., D. W. Burgess, and R. A. Brown, 1977: Doppler radar application to severe thunderstorm study and potential real-time warning. Bull. Amer. Meteor. Soc., 58, 1187-1193.

Lhermitte, R. M., 1964: Doppler radars as severe storm sensors. Bull. Amer. Meteor. Soc., 45, 587-596.

_____, 1966: Application of pulse Doppler radar technique to meteorology. Bull. Amer. Meteor. Soc., 47, 703-710.

Marwitz, J. D., 1971: The structure and motion of severe hailstorms, Part I: Supercell storms. J. Appl. Meteor., 11, 166-179.

Muench, H. S., 1976: Use of digital radar data in severe weather forecasting. Bull. Amer. Meteor. Soc., 57, 298-303.

NOAA Technical Memorandum ERL NSSL-86, 1979: Final report on the Joint Doppler Operational Project (JDOP), National Severe Storms Laboratory, Norman, Oklahoma.

Neyland, M. A., 1978: An analysis of the data collection modes of a digital weather radar system with respect to significant severe weather features. M. S. Thesis, Texas A&M University, 143 pp.

Pittman, D. W., 1976: Tornado identification from analysis of digital radar data. M. S. Thesis, Texas A&M University, 93 pp.

Ray, P. S., J. Weaver, and NSSL Staff, 1977: NOAA technical memorandum ERL NSSL-84: 1977 Spring program summary. National Severe Storms Laboratory, Norman, Oklahoma.

_____, R. A. Brown, and C. L. Ziegler, 1979: Doppler radar-Research at the National Severe Storms Laboratory. Weatherwise, 32, 68-71.

Rinehart, R. E., D. Atlas, and P. J. Eccles, 1975: Meteorological interpretation of Doppler radar data in a hailstorm. Preprints 16th Radar Meteorology Conf., Houston, Amer. Meteor. Soc., 73-78.

Sieland, T. E., 1977: Real-time computer techniques in the detection and analysis of severe storms from digital radar data. Ph.D. Dissertation, Texas A&M University, 141 pp.

Vogel, J. E., 1973: Applications of digital radar in the analysis of severe local storms. M. S. Thesis, Texas A&M University, 95 pp.

Whiton, R. C., 1971: On the use of radar in identifying tornadoes and severe thunderstorms: A diagnostic guide for radar scope interpretation. Tech. Rept. 243, Air Weather Service, USAF, 18 pp.

Wilk, K. E., and K. C. Gray, 1970: Processing and analysis techniques used with the NSSL weather radar system. Preprints 14th Radar Meteorology Conf., Tucson, Amer. Meteor. Soc., 369-374.

Wilson, J. W., and T. T. Fujita, 1979: Vertical cross section through a rotating thunderstorm by Doppler radar. Preprints 11th Conf. on Severe Local Storms, Boston, Amer. Meteor. Soc., 447-452.

APPENDIX A

This appendix gives a brief description of the 7-track to 9-track conversion of the 'raw' Doppler tapes received from NSSL.

A computer program to 'unpack' the tapes was developed by Knight and Howell (1980) at Texas A&M University. Their program uses the calibration data, supplied by NSSL with each set of tapes, to properly calibrate the 'raw' data when processed onto 9-track tapes. In addition, the program is designed to convert both normal and expanded mode data. However, since the primary research area was over the Chickasha synoptic network (Fig. 3), only data out to the first trip (115-km) were written onto 9-track tapes. Expanded mode data are written in 150-m increments by assigning the 600-m gate values to the three previous 150-m gates. Each 'raw' data tape is loaded onto two 9-track tapes in the following format: a header consisting of the year, Julian date, beginning and ending time, beginning and ending azimuth angles, lowest and highest tilt angles, plus the number of scans (revolutions), is written at the start of each sequence of data. Each radial in the sequence consists of a time, azimuth angle, elevation angle, 762 values of reflectivity corrected to dBZ, 762 values of radial velocity in m s^{-1} (not corrected for folding), and 762 values of spectrum width in m s^{-1}. Spectrum width data were not used in this research. In addition, a pound sign (#) precedes each header to identify the start of a new tilt sequence. Further information on this program is noted

in the comments of Appendix B. A copy of this program is obtainable from either co-author, or from Dr. Glen Williams, Industrial Engineering Department, or from Dr. George Huebner, Meteorology Department, at Texas A&M University.

APPENDIX B

This appendix contains a commented copy of the computer program that was used to process the Norman Doppler digital radar data. The program is used after the raw 7-track tapes are converted to 9-track by using the program written by Dave Howell and Keith Knight.

```
//DOPLERV1 JOB (J312,0038,003,003,TB),'BEAVER  ',MSGLEVEL=(1,1)          J0B4392
/*PASSWORD      *****
/*SETUP
/*JOBPARM R=1020,TAPE9=1,K=0
/*LEVEL         0
// EXEC FORTG,REGION=1020K
//F102F001 DD UNIT=TAPE9,DISP=OLD,
// LABEL=(1,SL),VOL=SER=(ZZ8546,ZZ5500),
// DSN=RADAR.MAY0177,DCB=(RECFM=VS,LRECL=9160,BLKSIZE=9164,BUFNO=1)
//FT11F001 DD UNIT=SYSDA,DSN=&TWO,DISP=(NEW,PASS),
// DCB=(RECFM=FB,LRECL=1445,BLKSIZE=13005,BUFNO=1),
// SPACE=(TRK,(200,10))
//SOURCE DD *
C
C THIS PROGRAM USES 'RAW' NOT 'ARCHIVED' DIGITAL DOPPLER DATA FROM NSSL.
C THIS PROGRAM WAS WRITTEN BY TOM BEAVER IN 1979. DATA ARE OBTAINED ON
C 7-TRACK TAPES AND ARE CONVERTED TO 9-TRACK. IN FORTRAN BEFORE USING
C THIS PROGRAM. THE CONVERSION PROGRAM WAS WRITTEN BY DAVE HOWELL AND
C KEITH KNIGHT AT TEXAS A&M. TWO OUTPUT TAPES ARE NEEDED FOR EACH CONVERSION.
C DATA ON THE TWO 9-TRACK TAPES CONSIST OF A '#' SIGN INDICATING THE
C START OF A NEW TILT SERIES, HEADERS FOR EACH TILT SERIES, AND THREE
C 762 UNIT ARRAYS FOR EACH AZIMUTH. (REFLECTIVITY,RADIAL VELOCITY, AND
C SPECTRUM WIDTH).
C THIS PROGRAM IS DESIGNED TO INITIALIZE A 96X116KM GRID BOX BY USING A
C 49X59 ARRAY WITH A GRID SPACING OF 2KM. A SECOND OPTION USES A 49X59
C ARRAY WITH A GRID SPACING OF 1KM WHICH DOUBLES HALF THE BOX FOR MORE
C DETAIL. THE LOCATION, SIZE, &  GRID SPACING CAN EASILY BE CHANGED BY
C ADJUSTING THE INPUT DATA AND A FEW CARDS IN THE PROGRAM.
C AZIMUTHS WITHIN THE GRID BOX ARE COMPARED TO FIND THE ONE CLOSEST TO
C THE INTEGER VALUE AZIMUTH. THEN GATES ALONG EACH RADIAL ARE AVERAGED
C USING A 450M RADIUS OF INFLUENCE TO CALCULATE VALUES IN 1KM INCREMENTS
C THIS IS DONE FOR EITHER REFLECTIVITY OR RADIAL VELOCITY VALUES. NOTE:
C SPECTRUM WIDTH DATA WERE NOT USED IN THIS PROGRAM. THIS ESTABLISHES
C THE SPHERICAL ARRAY 'ZW', WHICH IS THEN CONVERTED TO CYLINDRICAL ARRAY
C 'ZZ' IN THE MAIN PROGRAM. SUBROUTINE QD2 THEN CONVERTS IT TO A
```

```
C RECTANGULAR ARRAY 'Z' AND THIS IS OBJECTIVELY ANALYZED USING 'CONREC'
C AND PLOTTED BY THE VERSATEC PLOTTER. OUTPUT ARE CONSTANT ALTITUDE MAPS
C OF REFLECTIVITY OR RADIAL VELOCITY.
C COMMENT CARDS BEGINNING WITH '***' INDICATE POSSIBLE CARDS TO CHANGE
C BETWEEN DATA PROCESSING. ******
C *** 'JCL' CHANGES: ZZ TAPE NUMBERS MUST MATCH THE TAPES BEING USED.
C *** ALSO DATE 'MAY2077' MUST MATCH DATE OF DATA.
C *** DIMENSION CARD MUST BE CHANGED WHEN CHANGING ANY DIMENSION OR
C *** WHEN SWITCHING FROM RADIAL VELOCITY TO DBZ. *****
C EXAMPLE: REMOVE 'IVLOC(762)' & 'IVELOC(762)' WHEN PROCESSING DBZ DATA
C
      DIMENSION ZW(160,108,12),ZZ(160,108),Z(49,59),IDBZ(762),AZ(160),TI
     *LT(12),IDBZ1(762),IVLOC1(762),IVELOC(762)
C
C 'ZW'- SPHERICAL ARRAY; AZIMUTH, RANGE, TILT.
C 'ZZ'- CYLINDRICAL ARRAY; AZIMUTH, RANGE.
C 'Z'-  RECTANGULAR ARRAY; EAST-WEST BY NORTH-SOUTH DIMENSIONS.
C 'IDBZ' & 'IDBZ1'- REFLECTIVITY VALUES.
C 'IVELOC' & 'IVLOC1'- RADIAL VELOCITY VALUES
C 'AZ'- AZIMUTH ARRAY.
C 'TILT'- ELEVATION ARRAY.
C
       INTEGER*4 STIME,ETIME,SIGN,POUND,ORM,LOTILT,HITILT
       DATA POUND/'#   '/
      COMMON ZZ,Z,AZ,AAZONE,AAZEND
      EQUIVALENCE(AZMTH,NAZ),(IDBZ,IVELOC)
C
C READ CARD INPUT DATA THAT IDENTIFIES THE GRID BOX.
C *** DATA CARD MUST CORRESPOND TO 'JCL' TAPES & GRID BOX SET UP.*****
C IF BOX IS CHANGED, USE THE DEFINITIONS TO DETERMINE YOUR INPUT DATA.
C DEFINITIONS FOR DATA CARD
C  ILEFT - DISTANCE EAST OR WEST OF NSSL TO THE LEFT SIDE OF THE GRID.
C  WEST IS +; EAST IS -. ALSO MUST ADD 2 IF USING A 2KM SPACING OR ADD 1
C  IF USING A 1KM SPACING.
C JDOWN - DISTANCE NORTH OR SOUTH OF NSSL TO BOTTOM OF GRID.
C  SOUTH IS +; NORTH IS -.ALSO MUST ADD 2 IF USING A 2KM SPACING OR ADD
```

```
C  1 IF USING A 1KM SPACING.
C EXAMPLE 80 WEST =082, 80 EAST =-78 AND  30 NORTH =-28, 30 SOUTH =032
C KAZ - DESIRED STARTING AZIMUTH TO LOAD GRID BOX (MOVING CLOCKWISE).
C LASTAZ - LAST DATA AZIMUTH REQUIRED TO LOAD GRID BOX.
C NOTE: MAXIMUM OF 160 DEGREES.
C NTILT - NUMBER OF TILT ANGLES TO BE READ. CHANGE 'ZW' DIMENSION IF MORE
C THAN 12 TILTS WERE RECORDED. ALSO CHANGE 'TILT( )' DIMENSION.
C KRANGE - DISTANCE, EVEN KM, TO NEAREST POINT OF GRID BOX MINUS 4 KM.
C NYEAR - YEAR OF THE DATA BEING PROCESSED.
C NTIME - APPROXIMATE TIME OF INTEREST MUST BE BETWEEN THE STARTING TIME
C   AND ENDING TIME OF A TILT SERIES. CHANGE FOR EACH SET OF DATA.
C NDATE - JULIAN DATE OF THE DATA. I.E. MAY 01 1977 WAS 121.
C
  1    READ(5,5000,END=999) ILEFT,JDOWN,KAZ,LASTAZ,KRANGE,NYEAR,NTIME,
     *NDATE
5000  FORMAT(5I3,I4,I6,I3)
      WRITE(6,5002) ILEFT,JDOWN,KAZ,LASTAZ,KRANGE,NYEAR,NTIME,NDATE
 5002 FORMAT(' ','INPUT DATA: ILEFT=',I3,' JDOWN=',I3,' KAZ=',I3,' LASTA
     *Z=',I3,' KRANGE=',I3,' NYEAR=',I4,' NTIME=',I6,' NDATE=',I3)
C 'KAZLS1' IS 1 DEGREE LESS THAN THE BEGINNING AZIMUTH OF THE BOX. IT IS
C USED TO SET UP THE 'AZ' ARRAY FOR AZIMUTHS.
      KAZLS1=KAZ-1
      WRITE(6,5555) KAZLS1
 5555 FORMAT(' ','KAZLS1=',I4)
C LIBRARY SUBROUTINE 'CLEAR' INITIALIZES THE ENTIRE ARRAY TO ZERO
      CALL CLEAR (ZW,207360)
C
C READ HEADER DATA FROM TAPE:
C  1) CHECK FOR TAPE TIME EQUAL OR AFTER DESIRED PROCESSING TIME.
C  2) THE BEGINNING OF A NEW TILT SEQUENCE IS NOTED BY '#   'I.E.POUND.
C  3) WRITE HEADER DATA
C  4) BEGINNING AZIMUTH FOR THIS BOX IS LESS THAN THE LAST AZIMUTH.
C     DON'T PROCESS DATA TILL AZIMUTH IS EQUAL OR GREATER THAN 'KAZ'.
C  5) LTILT IS THE NUMBER OF THE TILT IN THIS SEQUENCE.
C  6) 'LOTILT' IS THE CLOSEST INTEGER VALUE TO THE STARTING TILT ANGLE.
C  7) 'HITILT' IS THE CUTOFF INTEGER VALUE OF THE HIGHEST TILT ANGLE + 1
```

```
C
  3   READ(02) SIGN,IYEAR,IDATE,STIME,ETIME,SAZ,EAZ,STILT,ETILT,NSCAN
      IF(SIGN.NE.POUND) GO TO 3
      IF(STIME.LE.NTIME.AND.ETIME.LT.NTIME) GO TO 3
      WRITE(6,5005) IYEAR,IDATE,STIME,ETIME,SAZ,EAZ,STILT,ETILT,NSCAN
5005  FORMAT('0',  APE HEADER DATA ',2I6,2I8,4F6.1,I6)
      LOTILT=IFIX  (ILT+0.5)
      HITILT=IFIX(ETILT)+1
C
C LOOP TO PROCESS DATA BETWEEN 'KAZ' & 'LASTAZ' FOR EACH TILT SEQUENCE
C NOTE: 'NSCAN' IS THE NUMBER OF TILTS IN THE SEQUENCE
C RECALL WHEN 'ITIME' IS '#', A NEW TILT SEQUENCE BEGINS
C 'TI_T(LTILT)' INITIALIZED TO 0.THEREFORE IF A TILT ANGLE IS NOT FOUND
C IT IS WRITTEN AS 0.0 KEYING YOU TO A PROBLEM. GO TO THE CONVERSION PROGRAM
C OUTPUT (HOWELL & KNIGHT) TO DETERMINE WHAT EXTRA CHECKS ARE NEEDED FOR
C THIS SET OF DATA.
C AAZEND IS THE LAST AZIMUTH OF TILT 1.
C
      DO 88 LTILT=1,NSCAN
      TILT(LTILT)=0.0
      IF(LTILT.NE.2) GO TO 5
      IAZEND=IAZ-1
      AAZEND=AZ(IAZEND)
      WRITE(6,5009) IAZEND,AAZEND
 5009 FORMAT(' ','IAZEND=',I4,' AAZEND=',F5.1/)
  5   READ(02,END=85) ITIME,AZMTH,ELEV
      IF(ITIME.EQ.POUND) GO TO 101
C SPECIAL CHECK FOR A 'GLITCH' IN SOME MAY 20 DATA. HERE 235.9 WAS A BAD
C NUMBER, READ BETWEEN RADIALS OUTSIDE THE GRID BOX BUT 235.9 WAS INSIDE
      IF(AZMTH.EQ.235.9) GO TO 5
      IF(AZMTH.LT.KAZLS1.OR.AZMTH.GT.LASTAZ) GO TO 5
C 'AZ' IS THE ARRAY OF AZIMUTH ANGLES,CAN PROCESS UP TO 160 ANGLES.
C CLEAR INITIALLY SETS ALL AZIMUTHS TO ZERO BEFORE EACH TILT.
      CALL CLEAR (AZ,160)
C
C BEGIN PROCESSING  AZIMUTHS WHEN WITHIN THE GRID BOX:
```

```
C   1) USE A 450 METER RADIUS OF INFLUENCE AVERAGING TECHNIQUE ALONG EACH
C      RADIAL; DON'T USE THE FIRST 6 KILOMETERS.
C   2) DATA FOR EACH GATE IS AT 150M INTERVALS; THIS DATA IS AVERAGED TO
C      A VALUE AT EACH 'KM' UNIT  USING THE 450M RADIUS OF INFLUENCE.
C   3) DATA IS GATHERED IN 1 DEGREE INCREMENTS WHERE POSSIBLE, I.E.
C      DATA IS COMPARED TO THE NEAREST INTEGER VALUE & ONLY THE CLOSEST
C      RADIAL DATA IS USED.
C   4) EACH AZIMUTH IS THEN LABELLED BY SUBTRACTING 'KAZLS1' FROM THE
C      INTEGER VALUE OF THE RADIAL, AND IS DENOTED AS 'IAZ'.
C   5) DATA CAN THEN BE GATHERED EVEN IF THE RADAR WAS OPERATED IN A
C      COUNTER-CLOCKWISE ROTATION.
C   6) UNUSABLE RECORDS WERE LABELLED AS 999. IF 999 IS FOUND THEN READ
C      THE NEXT RECORD.
C   7) 'ITIME1','AZMTH1','ELEV1','IDBZ1',&'IVLOC1' IDENTIFY THE MOST
C      RECENT READ AZIMUTH RECORD FOR THE PROCESSING MODE.
C   8) WHEN USING RADIAL VELOCITIES, 'LASTRV' IS THE VALUE OF THE PRIOR
C      GATE & IS COMPARED TO THE CURRENT GATE. IF AN ABSOLUTE VALUE
C      GREATER THAN 34 IS FOUND, FOLDING CCCURED , A CORRECTION IS MADE
C      AND 'LASTRV' STAYS THE SAME UNTIL NO FOLDING IS FOUND.
C
       IAZ=0
C *** CHANGE READ WHEN SWITCHING FROM RADIAL VELOCITY TO DBZ. I.E.IVELOC
C *** NOT USED IF PROCESSING DBZ.I.E. REMOVE 'IVELOC(J),J=1,762)' FROM
C 'READ' AND ALL OTHER 'IVELOC' & 'IVLOC1' STATEMENTS.
   7   READ(02,END=85) ITIME,AZMTH,ELEV,(IDBZ(J),J=1,762),(IVELOC(J),J=1,
      *762)
       IF(NAZ.EQ.999) GO TO 7
 363   CONTINUE
       ITIME1=ITIME
       AZMTH1=AZMTH
       ELEV1=ELEV
       DO 400 IW=1,762
       IDBZ1(IW)=IDBZ(IW)
C *** REMOVE 'IVLOC1' IF ONLY USING DBZ VALUES. ****
       IVLOC1(IW)=IVELOC(IW)
 400   CONTINUE
```

```
C 'IAZMTH' IS THE INTEGER VALUE OF THE LATEST READ AZIMUTH.
      IAZMTH=IFIX(AZMTH1+0.49)
C *** CHANGE READ WHEN SWITCHING FROM RADIAL VELOCITY TO DBZ. ****
C I.E. REMOVE '(IVELOC(J),J=1,762)'
   9  READ(02,END=85) ITIME,AZMTH,ELEV,(IDBZ(J),J=1,762),(IVELOC(J),J=1,
     *762)
      IF(NAZ.EQ.999) GO TO 9
      AZCHK=ABS(AZMTH-AZMTH1)
C
C 'AZCHK' IS ABSOLUTE VALUE DIFFERENCE OF THE TWO READ AZIMUTHS, FROM
C STATEMENTS 7 & 9. USED TO FIND WHICH IS CLOSER TO THE INTEGRAL VALUE.
C WHEN 'AZCHK' IS LESS THAN 0.1 & 'IAZ' IS 0, THEN READ UNTIL 2 AZIMUTHS
C ARE NOT THE SAME; IF 'IAZ' IS NOT 0, THEN ASSUME THE END OF A TILT.
C WHEN 'AZCHK' IS BETWEEN 0.1 & 1.0 THE 2 AZIMUTHS HAVE THE SAME INTEGER
C VALUE. IF 'AZMTH1' IS CLOSER THAN 'AZMTH' TO 'IAZMTH' PROCESS 'AZMTH1'
C IF NOT, DISCARD 'AZMTH1', SET 'AZMTH' TO 'AZMTH1' & READ THE NEXT.
C WHEN 'AZCHK' IS GREATER THAN 1 & LESS THAN 3 PROCESS 'AZMTH1'.
C IF 'AZCHK' IS GREATER THAN 3, CHECK THE ELEVATION ANGLES,IF ELEVATION
C ANGLES ARE LESS THAN 0.3 DEGREES DIFFERENCE THEN 'AZMTH' IS A BAD
C NUMBER, OR A GROUP OF AZIMUTHS WERE NOT RECORDED. IF A GROUP OF
C AZIMUTHS WERE SKIPPED THEN IDENTIFY A NEW 'IAZ' & PROCESS LEAVING
C SKIPPED AZIMUTHS AS 0.0. IF 'AZMTH' IS ITSELF THE ONLY BAD NUMBER
C DISCARD IT. IF ELEVATION ANGLES ARE GREATER THAN 0.3 DEGREES
C DIFFERENCE, ASSUME A NEW TILT.
C
      IF(AZCHK.GT.0.1) GO TO 12
      IF(IAZ.EQ.0) GO TO 363
      GO TO 85
  12  IF(AZCHK.GT.1.0) GO TO 14
      IF(ABS(AZMTH-FLOAT(IAZMTH)).LT.(ABS(AZMTH1-FLOAT(IAZMTH)))) GO TO
     * 363
  14  IF(AZCHK.LT.3.0) GO TO 15
      IF(ABS(ELEV1-ELEV).GT.0.3) GO TO 85
      AZMTHX=AZMTH
      READ(02,END=85) ITIME,AZMTH,ELEV,(IDBZ(J),J=1,762),(IVELOC(J),J=1,
     *762)
```

```
      IF(ABS(AZMTHX-AZMTH).GE.1.5) GO TO 15
      IAZ=IFIX(AZMTH+0.49)-KAZLS1
      GO TO 363
   15 IF(IAZ.GT.0) GO TO 21
      IF(LTILT.GT.1) GO TO 16
C THE FIRST TIME THROUGH A TILT CALCULATE THE 'IAZ' VALUE, ALSO THE
C FIRST ONE OF TILT 1 IS IDENTIFIED AS 'IAZ1', & FIRST AZIMUTH IS AAZONE
C 'AAZONE' & 'AAZEND' USED AS FIRST AND LAST AZIMUTHS OF ALL TILTS.
      IAZ1=IFIX(AZMTH1+0.49)-KAZLS1
      AAZONE=AZMTH1
      WRITE(6,5007) IAZ1,AAZONE
 5007 FORMAT('0','IAZ1=',I4,' AAZONE=',F5.1)
C 'DIRCHK' DETERMINES IF THE RADAR IS ROTATING CLOCKWISE OR COUNTER-
C CLOCKWISE AND SETS 'IADD' APPROPRIATELY.
   16 DIRCHK=AZMTH-AZMTH1
      IADD=1
      IF(DIRCHK.LT.0.0) IADD=-1
      IAZ=IFIX(AZMTH1+0.49)-KAZLS1
   21 AZ(IAZ)=AZMTH1
C USE THE TILT ANGLE OF 265 OR 266 DEGREES AS THE  ELEVATION ANGLE FOR
C THIS TILT. APPROXIMATELY THE MIDDLE OF THE GRID BOX.
C ***MUST CHANGE IF THE BOX DOES NOT CONTAIN 265 OR 266 DEGREES.
   22 IF(IAZMTH.EQ.265.OR.IAZMTH.EQ.266) TILT(LTILT)=ELEV1
C
C BEGINNING HERE TO THE STATEMENT BEFORE # 40 IS THE RADIUS OF INFLUENCE
C AVERAGING ALONG EACH DETERMINED AZIMUTH. RESULTING IN 106 KM VALUES
C FOR EACH RADIAL.
C 'NKM'- DISTANCE IN KILOMETERS MINUS 6.I.E.NKM=1 IS REALLY 7KM.
C 'DXE'- RADIUS OF INFLUENCE IN KILOMETERS.
C 'AK'- DIVISOR USED TO DETERMINE THE WEIGHTING VALUE I.E.150M.
C 'IDIST'- ACTUAL KILOMETER DISTANCE FROM NSSL IN METERS.
C 'J' & 'JPLUS'- NUMBERS OF GATES FROM NSSL THAT ARE USED AS AVERAGING
C   GATES FOR KILOMETER POINTS.
C 'AW'- SUM OF THE WEIGHTED VALUES FOR EACH AVERAGING.
C 'WT'- IS THE WEIGHTED VALUE FOR EACH INDIVIDUAL POINT.
C 'SUM'- VALUE OF THE POINTS AFTER BEING WEIGHTED.
```

```
C NOTE: SINCE  150M GATE SPACING DOES NOT DIVIDE EVENLY INTO KILOMETERS
C  THIS PROCESS IS PROGRAMMED 3 TIMES TO CONVERT DATA TO KILOMETER VALUE
C
      NKM=0
      DXE=450.
      AK=DXE/3.0
      IDIST=7000
      J=44
   23 AW=0.0
      SUM=0.0
      JPLUS5=J+5
      DO 25 M=J,JPLUS5
C *** REPLACE 'IVLOC1' CARDS WITH 'IDBZ1' CARDS IF PROCESSING DBZ'S
C ALSO ADD 'IF(IDBZ1(M).LE.0) GO TO 25'; AND REMOVE ALL CARDS THRU #315
      IF(IVLOC1(M).EQ.998.OR.IVLOC1(M).EQ.999) IVLOC1(M)=0
      IF(M.EQ.44) GO TO 315
C CHECK AND CORRECT FOR FOLDING WHERE NECESSARY
      IF(IABS(LASTRV-IVLOC1(M)).LE.34) GO TO 315
      IF(IABS(IVLOC1(M)).LE.28) WRITE(6,3000) LASTRV,M,IVLOC1(M),AZ(IAZ)
 3000 FORMAT(' ',' PREVIOUS VELOCITY VALUE IS',I4,'; NEXT VELOCITY AT',I4
     *,' GATES IS',I4,' ALONG RADIAL ',F5.1)
      IF(LASTRV.LT.0) GO TO 300
      MAXV=68
      GO TO 310
  300 MAXV=-68
  310 IVLOC1(M)=MAXV+IVLOC1(M)
      IF(IABS(IVLOC1(M)).GE.40) WRITE(6,3010) IVLOC1(M)
 3010 FORMAT(' ',' CORRECTED VELOCITY VALUE IS',I4)
      GO TO 24
  315 LASTRV=IVLOC1(M)
   24 DISR=ABS(FLOAT(IDIST-(M*150)))
      WT=EXP(-DISR/AK)
      AW=AW+WT
      SUM=SUM+WT*(FLOAT(IVLOC1(M)))
   25 CONTINUE
      NKM=NKM+1
```

```
      IF(AW.EQ.0.0) AW=1.0
      ZW(IAZ,NKM,LTILT)=SUM/AW
      IF(NKM.EQ.107) GO TO 40
      IDIST=IDIST+1000
      AW=0.0
      SUM=0.0
      J=J+7
      JPLUS5=J+5
      DO 27 M=J,JPLUS5
C *** FOR DBZ'S REPLACE  'IVLOC1', ADD 'IF(IDBZ1(M).LE.0) GO TO 27'
C *** AND REMOVE ALL THRU # 335 AS PREVIOUSLY NOTED. ******
      IF(IVLOC1(M).EQ.998.OR.IVLOC1(M).EQ.999) IVLOC1(M)=0
C CHECK AND CORRECT FOR FOLDING WHERE NECESSARY
      IF(IABS(LASTRV-IVLOC1(M)).LE.34) GO TO 335
      IF(IABS(IVLOC1(M)).LE.28) WRITE(6,3000) LASTRV,M,IVLOC1(M),AZ(IAZ)
      IF(LASTRV.LT.0) GO TO 320
      MAXV=68
      GO TO 330
  320 MAXV=-68
  330 IVLOC1(M)=MAXV+IVLOC1(M)
      IF(IABS(IVLOC1(M)).GE.40) WRITE(6,3010) IVLOC1(M)
      GO TO 26
  335 LASTRV=IVLOC1(M)
  26  DISR=ABS(FLOAT(IDIST-(M*150)))
      WT=EXP(-DISR/AK)
      AW=AW+WT
      SUM=SUM+WT*(FLOAT(IVLOC1(M)))
  27  CONTINUE
      NKM=NKM+1
      IF(AW.EQ.0.0) AW=1.0
      ZW(IAZ,NKM,LTILT)=SUM/AW
      IF(NKM.EQ.107) GO TO 40
      IDIST=IDIST+1000
      AW=0.0
      SUM=0.0
      J=J+6
```

```
      JPLUS6=J+6
      DO 29 M=J,JPLUS6
C *** FOR DBZ'S REPLACE 'IVLOC1', ADD '(F(ICBZ1(M).LE.0) GO TO 29'
C *** AND REMOVE ALL THRU # 355 AS PREVIOUSLY NOTED. ******
      IF(IVLOC1(M).EQ.998.OR.IVLOC1(M).EQ.999) IVLOC1(M)=0
C CHECK AND CORRECT FOR FOLDING WHERE NECESSARY
      IF(IABS(LASTRV-IVLOC1(M)).LE.34) GO TO 355
      IF(IABS(IVLOC1(M)).LE.28) WRITE(6,3000) LASTRV,M,IVLOC1(M),AZ(IAZ)
      IF(LASTRV.LT.0) GO TO 340
      MAXV=68
      GO TO 350
  340 MAXV=-68
  350 IVLOC1(M)=MAXV+IVLOC1(M)
      IF(IABS(IVLOC1(M)).GE.40) WRITE(6,3010) IVLOC1(M)
      GO TO 28
  355 LASTRV=IVLOC1(M)
   28 DISR=ABS(FLOAT(IDIST-(M*150)))
      WT=EXP(-DISR/AK)
      AW=AW+WT
      SUM=SUM+WT*(FLOAT(IVLOC1(M)))
   29 CONTINUE
      NKM=NKM+1
      IF(AW.EQ.0.0) AW=1.0
      ZW(IAZ,NKM,LTILT)=SUM/AW
   30 IDIST=IDIST+1000
      J=J+7
      IF(NKM.LT.107) GO TO 23
C
C ADD OR SUBTRACT 1 TO 'IAZ'. THEN CHECK FOR A NEW TILT, NEXT AZIMUTH TO
C  BE PROCESSED ,&/OR A MISSING AZIMUTH.
C IF 'AZMTH' IS OUTSIDE THE GRID BOX START A NEW TILT.
C IF THE INTEGER VALUE OF 'AZMTH' IS THE SAME AS 'AZMTH1',READ TWO NEW
C  AZIMUTHS.
C IF THE DIFFERENCE IS 1, IDENTIFY 'AZMTH' AS 'AZMTH1' & READ NEXT ONE.
C IF DIFFERENCE IS GREATER THAN 1 AN AZIMUTH IS MISSING, USE THE LAST
C PROCESSED VALUES , CHANGE TO THE NEXT 'IAZ' & CONTINUE PROCESSING.
```

```
C
  40   IAZ=IAZ+IADD
       IF(AZMTH.LE.KAZLST.OR.AZMTH.GT.LASTAZ) GO TO 85
       JAZMTH=IFIX(AZMTH+0.49)
       IF(JAZMTH.NE.IAZMTH) GO TO 42
       IAZMTH=IAZMTH+IADD
       ITIME1=ITIME
       AZMTH1=AZMTH
       ELEV1=ELEV
       DO 410 IW=1,762
       IDBZ1(IW)=IDBZ(IW)
       IVLOC1(IW)=IVELOC(IW)
  410  CONTINUE
       GO TO 9
  42   IF(IABS(JAZMTH-IAZMTH).EQ.1) GO TO 363
       MISGAZ=IAZ
       AZ(MISGAZ)=AZMTH1
       LASTAZ=MISGAZ-IADD
       DO 420 NKM=1,107
  420  ZW(MISGAZ,NKM,LTILT)=ZW(LASTAZ,NKM,LTILT)
       WRITE(6,5012) MISGAZ,AZ(MISGAZ)
 5012  FORMAT(' ',' MISSING AZIMUTH NUMBER',I4,' NOW EQUAL TO ',F5.1,' DEG
      *REES')
       IAZ=MISGAZ+IADD
       GO TO 363
C
  85   WRITE(6,6005) AZ
 6005  FORMAT(' ',16F6.1)
       WRITE(6,5015) LTILT,TILT(LTILT)
 5015  FORMAT(' ',' **** END OF TILT',I3,' ELEVATION ANGLE USED IS',F4.1/)
C PROCESS REMAINING TILTS IN THIS SEQUENCE BETWEEN KAZ AND LASTAZ.
  88   CONTINUE
C
C COMPUTE CONSTANTS TO BE USED IN VERTICAL INTERPOLATION OF SPHERICAL
C DATA INTO CYLINDRICAL COORDINATES AT A CONSTANT HEIGHT
C 'ANTILT' IS THE MAXIMUM TILT ANGLE
```

```
C  RP2 - EQUALS 2R' FOR R'=4/3RE. RE BEING EARTH RADIUS IN KM.
C  TANTOP - TANGENT OF HIGHEST ELEVATION ANGLE USED
C  VERTICALLY INTERPOLATE SPHERICAL DATA OF  ZW ARRAY TO YIELD CONSTANT
C  ALTITUDE CYLINDRICAL ARRAY ZZ. COMPUTE CLOSEST DISTANCE TO NSSL THAT
C  DIGITAL DATA ARE AVAILABLE AT HEIGHT H.
C  'LOTILT' & 'HITILT' ARE USED IN DETERMINING WHICH CAZM'S CAN BE PLOTED
C  H - HEIGHT OF CAZM IN KM.
C  IF 'H=FLOAT(M-1)' WILL PLOT A 0.5KM MAP. THEN A 1KM & 1KM INCREMENTS
C  TO 'HITILT'.   IF 'H=(FLOAT(M))'  & STATEMENT 'IF(M.EQ.1) H=0.5' IS
C  REMOVED THEN WILL START AT 1KM & PLOT IN 1KM INCREMENTS TO 'HILILT'.
C  NOTE: WHEN SPECIFICALLY INTERESTED IN A SECTION OF THE BOX; LOWER &/OR
C  HIGHER MAPS MAY BE POSSIBLE, DETERMINED BY USING THE KNOWN LOWEST
C  AND/OR HIGHEST TILT ANGLES TO SOLVE EQUATION (PHIP=H/X-X/RP2).
C  XK - CLOSEST DISTANCE TO NSSL IN KM THAT DIGITAL DATA ARE AVAILABLE AT
C   HEIGHT H. FUNCTION OF MAX ANTENNA TILT USED.
C  IRM - INNER RANGE MARKER: NEAREST KILOMETER DISTANCE INSIDE 'XK'.
C  ORM - OUTER LIMIT OF DATA.
C
  101 ANTILT=ELEV1
      WRITE(6,5020) ANTILT
 5020 FORMAT('0',' ANTILT= ',F4.1)
      RP2=16990.173
      TANTOP=TAN(.0174533*ANTILT)
      IF(TANTOP.EQ.0.0) TANTOP=.0174550
      IF(LOTILT.EQ.0) LOTILT=1
      MM=1
C *** CHANGE NEXT CARD WHEN A CERTAIN SERIES OF CONSTANT ALTITUDE MAPS
C *** ARE PREFERED. MIGHT ALSO WANT TO CHANGE THE 'H= ' CARD.
C EXAMPLE: TO PROCESS ONLY THE 3, 4, & 5KM 'CAVM' USE THE FOLLOWING
C DO 168 M=3,5;   H=FLOAT(M);   & REMOVE IF(M.EQ.1) H=0.5
C *** ALSO CHECK THE HEADER WRITTEN ON THE OUTPUT, IF IT DOESN'T MATCH
C THE OUTPUT TILT ANGLES, YOU MAY WANT TO CHANGE 'DO 168'
      DO 168 M=LOTILT,HITILT
      CALL CLEAR (ZZ,17280)
      H=FLOAT(M-1)
      IF(M.EQ.1) H=0.5
```

```
      HSQ=H**2
      XK=H/TANTOP
      IRM=(IFIX(XK))-6
C *** IF A DIFFERENT GRID BOX IS USED THE 'IRM' DISTANCE CAN BE CHANGED.
C EXAMPLE: IF INNER EDGE OF A BOX IS 50KM. MAKE 'IRM' =42 WHICH RECALL
C IS REALLY 48KM SINCE THE FIRST 6KM ARE NOT USED.
      IF(IRM.LT.22) IRM=22
      ORM=107
C
C COMPUTE FOUR    POINTS IN DATA ARRAY ZW THAT BRACKET THE DESIRED POINT
C ON THE SURFACE AT HEIGHT H.
C IR - KILOMETER POINTS ALONG THE AZIMUTH (IAZ)
C X - HORIZONTAL DISTANCE TO 'IR' IN KILOMETERS
C SR - SLANT RANGE TO DESIRED ''KM'' POINT ON SURFACE AT HEIGHT 'H'.
C IR1 - RANGE COUNTER FOR ZW ARRAY
C IR2 - ALONG WITH IR1 THESE POINTS DEFINE THE NEAREST   'KM'  POINTS IN
C THE ZW ARRAY WHICH BRACKET THE DESIRED    POINT ON SURFACE AT HEIGHT H
C PHIP - PHI PRIME: ANGLE BETWEEN GROUND & DESIRED POINT ON SURFACE AT
C  HEIGHT H. CORRECTED FOR BEAM BENDING.
C
      DO 146 JAZ=IAZ1,IAZEND
      DO 145 IR=IRM,ORM
      X=FLOAT(IR)+6.0
      SR=(SQRT(HSQ+X**2))
      IR1=IFIX(SR)-6
      IF(IR1.GT.106) GO TO 146
      IR2=IR1+1
      PHIP=H/X-X/RP2
      IF(PHIP.LT.0.0) PHIP=0.0
      PHIP=57.2958*ATAN(PHIP)
      IF(PHIP.GE.ANTILT) GO TO 145
C
C COMPUTE ELEVATION ANGLES IN DATA ARRAY ZW WHICH BRACKET THE DESIRED
C POINT ON THE SURFACE AT HEIGHT H.
C
      DO 125 I=2,LTILT
```

```
      K=I-1
      IF(PHIP.LT.TILT(I)) GO TO 127
  126 CONTINUE
C
C EXTRACT DATA FROM ZW ARRAY FOR THE FOUR POINTS AT A GIVEN AZIMUTH IN
C THE SPHERICAL ARRAY WHICH BRACKET A CONSTANT LEVEL POINT ON THE SAME
C RADIAL IN THE CYLINDRICAL ARRAY ZZ. INTERPOLATE LINEARLY THE DATA TO
C FIND INTERPOLATED VALUE FOR POINT IN THE ZZ ARRAY.
C PT1 - PT4 : CONTAIN INTERPOLATED DATA FOR THE 4 POINTS SURROUNDING
C  DESIRED POINT IN ZZ ARRAY.
C
  127 PT1=ZW(JAZ,IR1,K)
      PT2=ZW(JAZ,IR1,K+1)
      PT3=ZW(JAZ,IR2,K)
      PT4=ZW(JAZ,IR2,K+1)
      IF(PT1.NE.0.0.OR.PT2.NE.0.0.OR.PT3.NE.0.0.OR.PT4.NE.0.0) GO TO 133
      GO TO 145
C
C SUBTIL - DIFFERENCE IN DEGREES BETWEEN ELEVATION ANGLES USED TO
C  BRACKET THE POINT ON THE SURFACE AT HEIGHT H.
C DS - PERCENTAGE DISTANCE BETWEEN LOWER DATA ELEVATION ANGLE USED
C  I.E. (TILT(K)) & DESIRED POINT IN ZZ ARRAY.
C DR - PERCENTAGE DISTANCE BETWEEN NEAREST DATA POINT & DESIRED POINT IN
C  ZZ ARRAY.
C EE - INTERPOLATED VALUE AT DISTANCE DS BETWEEN INNER DATA POINTS.
C FF - INTERPOLATED VALUE AT DISTANCE DS BETWEEN OUTER DATA POINTS.
C ZT - INTERPOLATED VALUE AT DISTANCE DR BETWEEN POINTS EE & FF.
C ZZ(JAZ,IR) - CYLINDRICAL DATA ARRAY
C
  133 SUBTIL=TILT(K+1)-TILT(K)
      IF(SUBTIL.EQ.0.0) SUBTIL=1.0
      DS=(PHIP-TILT(K))/SUBTIL
      IF(DS.LT.0.0) GO TO 145
      DR= SR-FLOAT((IFIX(SR)))
      EE=PT1+(PT2-PT1)*DS
      FF=PT3+(PT4-PT3)*DS
```

```
      ZT=EE+(FF-EE)*DR
      ZZ(JAZ,IR)=ZT
  145 CONTINUE
  146 CONTINUE
C CONVERT CYLINDRICAL ARRAY ZZ AT HEIGHT H, INTO RECTANGULAR ARRAY Z VIA
C SUBROUTINE CD2.
C
      CALL QD2 (ILEFT,JDOWN,KAZ)
      WRITE(11,6006)Z
 6006 FORMAT(16F5.1)
C TURN NEXT CARD AROUND IF DESIRE TO PLOT NUMERICAL VALUES ON COMPUTER
C PAPER. WILL ALSO HAVE TO ADD SUBROUTINE 'PLOTZ', SEE PITTMAN(1976).
C                                          )MM,NWODJ,TFELI,H,EMITI(ZTCLP LLAC
      WRITE(6,5050) MM,H
 5050 FORMAT(' ','*** PROCESSED DATA FOR MAP NUMBER ',I2,'; H=',F4.1,'KM
     *')
      MM=MM+1
C *** 'Z' DIMENSION WILL CHANGE WHEN A DIFFERENT 'Z' ARRAY SIZE IS USED.
C EXAMPLE: USING A 59 X 59 ARRAY , 'Z' =3481.
      CALL CLEAR (Z,2891)
  168 CONTINUE
C *** WHEN USING MORE THAN 1 SET OF TILTS AT A TIME USE 'GO TO 1'.****
      GO TO 999
C
  999 CONTINUE
      STOP
      END
      SUBROUTINE QD2 (ILEFT,JDOWN,KAZ)
C QD2 IS A QUADRATIC INTERPOLATING SUBROUTINE; GOES THRU THE RECTANGULAR
C GRID COORDINATES & COMPUTES A VALUE OF REFLECTIVITY OR RADIAL VELOCITY
C USING AN INTERPOLATION SCHEME THAT SELECTS DATA FROM THE 9 NEAREST
C CYLINDRICAL DATA POINTS OF THE 'ZP' ARRAY.
C ZP IS SAME AS ZZ OF MAIN PROGRAM.
C 'ZEE' VALUES ARE VALUES OF THE FINAL GRID POINTS ('Z' ARRAY OF MAIN).
C ***'ZEE' DIMENSIONS MUST BE THE SAME AS 'Z' DIMENSIONS.****
      REAL ZP(160,108), ZEE(49,59),AZ(160),III
```

```
      INTEGER AZONE,AZTWO,AZTHRE
      COMMON ZP,ZEE,AZ,AAZONE,AAZEND
C
      KAZLS1=KAZ-1
C *** THE 'I' & 'J' RANGE MUST EQUAL 'ZEE' DIMENSIONS.****
      DO 260 I=1,49
      DO 260 J=1,59
      ZEE(I,J)=0.0
C *** IF THE GRID SPACING CHANGES THEN 'FLOATI' & 'FLOATJ' MUST CHANGE.
C EXAMPLE: FOR A 2KM GRID SPACING USE 'FLOATI=FLOAT(2*I-ILEFT)' AND
C 'FLOATJ=FLOAT(2*J-JDOWN)' .
C   FLOATI IS DISTANCE WEST(+) OR EAST(-) OF NSSL TO GRID COORDINATE.
C   FLOATJ IS DISTANCE NORTH(+) OR SOUTH(-) OF NSSL TO GRID COORDINATE.
      FLOATI=FLOAT(I-ILEFT)
      FLOATJ=FLOAT(J-JDOWN)
C R IS DIRECT DISTANCE FROM NSSL TO GRID POINT IN KILOMETERS.
      R=SQRT(FLOATI**2+FLOATJ**2)
C *** 'R' RANGE IS DEPENDENT ON THE EAST TO WEST BOX RANGE.*****
C IF 'R' IS LESS THAN THE INNER EDGE OF THE BOX GO TO THE NEXT POINT
C LEAVE THE OUTER RANGE AS 113.0
      IF(R.LT.22.0.OR.R.GT.113.0) GO TO 260
C 'THETA' IS THE ANGLE FROM TRUE NORTH TO GRID POINT IN DEGREES.
      THETA=(ATAN2(FLOATI,FLOATJ))*57.2958
      IF(THETA.LT.0.0) THETA=THETA+360.
      IF(THETA.LT.AAZONE.OR.THETA.GT.AAZEND) GO TO 260
      ITHETA=(IFIX(THETA+0.49))-KAZLS1
      IF(ABS(THETA-AZ(ITHETA)).LE.1.0) GO TO 210
      IF((THETA-AZ(ITHETA)).LT.0.0) GO TO 200
      AZONE=ITHETA+1
      IF(ABS(THETA-AZ(AZONE)).LE.1.0) GO TO 220
      AZONE=AZONE+1
      GO TO 220
  200 AZONE=ITHETA-1
      IF(ABS(THETA-AZ(AZONE)).LE.1.0) GO TO 220
      AZONE=AZONE-1
      GO TO 220
```

```
C 'AZONE' IS NEAREST AZIMUTH TO THE GRID POINT.
C 'AZTWO' IS NEXT AZIMUTH CLOCKWISE OF 'AZONE'.
C 'AZTHRE' IS NEXT AZIMUTH COUNTER -CLOCKWISE OF 'AZONE'.
  210 AZONE=ITHETA
  220 AZTWO=AZONE+1
      AZTHRE=AZONE-1
C X IS PERCENTAGE DISTANCE FROM THETA TO ANGLE OF GRID COORDINATE.
      X=THETA-AZ(AZONE)
C WHEN 'X' IS GREATER THAN 2, AN AZIMUTH IS MISSING.
      IF(ABS(X).LE.2.0) GO TO 225
      WRITE(6,2000) AZONE,X
 2000 FORMAT(' ',*RADIAL IN AZ ARRAY AT',I4,' IS MISSING, MAKING X='F5.
     *1)
      GO TO 260
C IR1 IS CLOSEST 'KM' POINT TO 'R'.
  225 IR1=IFIX(R+0.5)-6
      IF(IR1.GE.106) GO TO 260
      IR2=IR1+1
      IR3=IR1-1
C Y IS PERCENTAGE DISTANCE FROM R TO NEAREST 'KM' POINT.
      Y=(R-6.0)-FLOAT(IR1)
C AAA TO III ARE THE 9 DATA POINTS USED IN THE INTERPOLATION SCHEME.
      AAA=ZP(AZONE,IR1)
      BBB=ZP(AZONE,IR2)
      CCC=ZP(AZONE,IR3)
      DDD=ZP(AZTWO,IR1)
      EEE=ZP(AZTWO,IR2)
      FFF=ZP(AZTWO,IR3)
      GGG=ZP(AZTHRE,IR1)
      HHH=ZP(AZTHRE,IR2)
      III=ZP(AZTHRE,IR3)
      IF(AAA.NE.0.0.OR.BBB.NE.0.0.OR.CCC.NE.0.0.OR.DDD.NE.0.0.OR.EEE.NE.
     C0.0.OR.FFF.NE.0.0.OR.GGG.NE.0.0.OR.HHH.NE.0.0.OR.III.NE.0.0) GO
     *TO 236
      GO TO 260
  236 B=(DDD-GGG)/2.0
```

```
      C=(BBB-CCC)/2.0
      D=DDD-AAA-B
      E=CCC-AAA+C
      IF(X.GE.0.0) GO TO 248
      IF(Y.GE.0.0) GO TO 245
      F=III-AAA+B+C-D-E
      FONE=III
      GO TO 254
  245 F=AAA-B+C+D+E-HHH
      FONE=HHH
      GO TO 254
  248 IF(Y.GE.0.0) GO TO 252
      F=AAA+B-C+D+E-FFF
      FONE=FFF
      GO TO 254
  252 F=EEE-AAA-B-C-D-E
      FONE=EEE
  254 ZZ=AAA+(B*X)+(C*Y)+(D*X**2)+(E*Y**2)+(F*X*Y)
C *** FOR DBZ PLOTS REMOVE THE NEXT 3 STATEMENTS *******
      IF(ZZ.GT.0) GO TO 255
      ZZ=AMIN1(ZZ,AMAX1(AAA,DDD,GGG,BBB,CCC,FONE))
      GO TO 259
  255 ZZ=AMAX1(ZZ,AMIN1(AAA,DDD,GGG,BBB,CCC,FONE))
C *** FOR DBZ ADD: IF(ZZ.LT.0.0) GO TO 260 ******
  259 ZEE(I,J)=ZZ
  260 CONTINUE
      RETURN
      END
//SYSIN DD *
03105121328403019771705001 21
//STEP2 EXEC FTNGVTEC,REGION=256K
//FORT.SYSIN DD *
C *** DIMENSION MUST MATCH 'Z' & 'ZEE' ****
      DIMENSION Z(49,59)
      COMMON/CONRE1/SIZEL,SIZEM,SIZEP,NLA,NLM,XLT,YBT,SIDE,NREP,NCRT,ILA
     *B,NULBLL,ICFFD,EXT,IOFFP,SPVAL,IOFFM,ISOLID
```

```
      CALL PLOTS(0,0,0)
C SIZEL IS THE SIZE OF LINE LABELS ON THE CONTOURED LINES. 1.31=2MM.
      SIZEL = 1.31
C NULBIL IS THE NUMBER OF UNLABELED CONTOUR LINES BETWEEN LABELED LINES.
      NULBLL =1
C INDEX IS COUNT OF HOW MANY 'SCAN SEQUENCES' ARE READ FROM THE TAPE.
      INDEX = 0
C ICOUNT IS THE MAP NUMBER. MAXIMUM OF 11 PER SCAN SEQUENCE.
      ICOUNT = 0
      INDEX = INDEX + 1
   15 CONTINUE
      READ(11,6006,END=99)Z
 6006 FORMAT(16F5.1)
      ICOUNT = ICOUNT + 1
C *** CHANGE 'SET', 'PERIM', & LABELING WHEN THE BOX IS CHANGED.***
C SEE NEYLAND, 1978 OR TOM REID 6TH FLOOR O     & M BUILDING.
      CALL SET(110.847,110.1000.0,.48,,0,,58,,1)
      CALL PERIM(24,2,29,2)
      CALL PWRX(55,28,,38H'IRU'KILOMETERS SOUTH TO NORTH OF NSSL.38,1,,1
     *,1)
      CALL PWRX(24,,50,28H'IRU'KILOMETERS WEST OF NSSL.28,1,,0,1)
      CALL PWRX(4,,90,7H'IRU'76,7,1,,0,1)
      CALL PWRX(8,,90,7H'IRU'72,7,1,,0,1)
      CALL PWRX(12,,90,7H'IRU'68,7,1,,0,1)
      CALL PWRX(16,,90,7H'IRU'64,7,1,,0,1)
      CALL PWRX(20,,90,7H'IRU'60,7,1,,0,1)
      CALL PWRX(24,,90,7H'IRU'56,7,1,,0,1)
      CALL PWRX(28,,90,7H'IRU'52,7,1,,0,1)
      CALL PWRX(32,,90,7H'IRU'48,7,1,,0,1)
      CALL PWRX(36,,90,7H'IRU'44,7,1,,0,1)
      CALL PWRX(40,,90,7H'IRU'40,7,1,,0,1)
      CALL PWRX(44,,90,7H'IRU'36,7,1,,0,1)
      CALL PWRX(100,4,,7H'IRU'46,7,1,,0,3)
      CALL PWRX(100,8,,7H'IRU'42,7,1,,0,3)
      CALL PWRX(100,12,,7H'IRU'38,7,1,,0,3)
      CALL PWRX(100,16,,7H'IRU'34,7,1,,0,3)
```

```
      CALL PWRX(100.20..7H'IRU'30.7.1..0.3)
      CALL PWRX(100.24..7H'IRU'26.7.1..0.3)
      CALL PWRX(100.28..7H'IRU'22.7.1..0.3)
      CALL PWRX(100.32..7H'IRU'18.7.1..0.3)
      CALL PWRX(100.36..7H'IRU'14.7.1..0.3)
      CALL PWRX(100.40..7H'IRU'10.7.1..0.3)
      CALL PWRX(100.44..6H'IRU'6.6.1..0.3)
      CALL PWRX(100.48..7H'IRU'2S.7.1..0.3)
      CALL PWRX(100.52..7H'IRU'2N.7.1..0.3)
      CALL PWRX(100.56..6H'IRU'6.6.1..0.3)
C *** CHANGE 'CONREC' ACCORDING TO DESIRED OUTPUT.****
C SEE NEYLAND.1978 OR TOM REID 6TH FLOOR O & M BUILDING.
      CALL CONREC(Z(2.2).49.47.57.-60..60..5..1.-1.-341)
      CALL PLOT(12..0..-999)
      GO TO 15
   99 CONTINUE
      CALL PLOT(0..0..+999)
      STOP
      END
//LKED.DDNAME DD DISP=SHR.
// DSNAME=USER.OCN.GUINASSO.JO3LIB
//LKED.SYSIN DD *
 INCLUDE DDNAME(PLOTVTEC.CNRCSMTH.PWRX)
//GO.PLOTPARM DD *
 &PLOT MSGLVL=1.XMAX=10. &END
//GO.FT11F001 DD DSN=&TWO.DISP=(OLD.DELETE)
//GO.SYSIN DD *
```

VITA

Thomas F. Beaver was born on August 20, 1948, in Lewisburg, Pennsylvania to Bernard F. and Anna M. Beaver. He attended grade school and high school in Milton, Pennsylvania. After graduating from Milton Area Joint Senior High School in 1966, he attended Grove City College, Grove City, Pennsylvania. In 1970 he graduated from Grove City with a Bachelor of Science degree in Mathematics and was commissioned a Second Lieutenant in the United States Air Force.

His first assignment was to the University of Texas, where he received his basic meteorological training. The next two assignments were to Shaw AFB, South Carolina, and Kadena AB, Okinawa, where he held the position of duty forecaster, and while at Kadena also held position of Wing Weather Officer, Radar Officer, Chief Forecaster, and Assistant Detachment Commander. From Kadena he attended Squadron Officer School and was then assigned to Laughlin AFB, Texas, as a Weather Instructor and also performed duties as Squadron Scheduler and Assistant Branch Chief.

The author entered Texas A&M University in August 1978, to pursue the degree of Master of Science in Meteorology under the auspices of the United States Air Force Institute of Technology.

He is married to the former Roxanna Lynn Murray, and they have three children, daughters, Tara and Amy, and son, Broc. His permanent mailing address is P.O. Box 146, Rt. 3, Milton, Pennsylvania 17847.

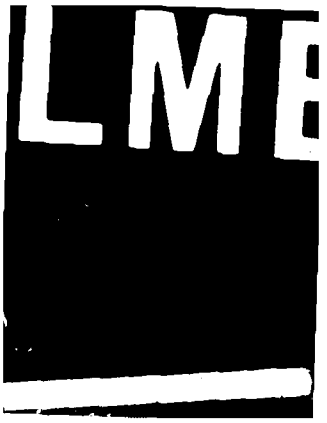
LME